The Dissertation Committee for Jena Renee Campbell Certifies that this is the approved version of the following dissertation:

THE ROLE OF PROTOZOAN GRAZERS IN HARMFUL ALGAL BLOOM DYNAMICS: TOOLS FOR COMMUNITY AND GRAZING ANALYSES

Committee:

Edward J. Buskey, Supervisor

Lisa Campbell

Deana Erdner

Jim McClelland

Tracy Villareal

THE ROLE OF PROTOZOAN GRAZERS IN HARMFUL ALGAL BLOOM DYNAMICS: TOOLS FOR COMMUNITY AND GRAZING ANALYSES

by

Jena Renee Campbell, B.S.

Dissertation

Presented to the Faculty of the Graduate School of

The University of Texas at Austin

in Partial Fulfillment

of the Requirements

for the Degree of

Doctor of Philosophy

The University of Texas at Austin

December 2012

Dedication

This dissertation is dedicated to my family without whom I would not be here. Your constant encouragement to follow my dreams and never give up no matter what the challenge has made me the person I am today. For that I thank you.

Acknowledgements

Thank you to the many individuals who made this dissertation possible. Thanks to my advisor, Edward Buskey, for his guidance and supervision. Thank you to my dissertation committee: Edward Buskey, Lisa Campbell, Deana Erdner, Jim McClelland, and Tracy Villareal for their guidance, comments, and insight throughout the course of this project. Thank you to Cammie Hyatt for instructions on proper algal culturing technique and taxonomic identification of microalgae and protozoans. Thank you to Lindsay Scheef for writing the R programming for the multivariate regressions. Thank you to the Buskey Lab and SMWP technicians for their support, encouragement, dedication to fieldwork, and the procurement of water samples. Thank you to the Erdner Lab for sharing of lab space and equipment. Thank you to former undergraduate research students for their lab assistance. Thank you to the administrative and facilities staff for helping to keep this institute running. This project was funded through the NOAA National Estuarine Research Reserve Graduate Research Fellowship (NA09NOS4200027), NSF OCE-0825009, and the University of Texas Marine Science Institute E.J. Lund Endowed Fellowship.

THE ROLE OF PROTOZOAN GRAZERS IN HARMFUL ALGAL BLOOM DYNAMICS: TOOLS FOR COMMUNITY AND GRAZING ANALYSES

Jena Renee Campbell, Ph.D.

The University of Texas at Austin, 2012

Supervisor: Edward J. Buskey

Harmful algal blooms (HABs) are becoming more prevalent throughout the world's aquatic systems. These blooms have been the subjects of numerous studies because they can cause human health issues and economic impact through fish kills, contaminated shellfish and decreased tourism. Much research has focused on the "bottom-up" aspect of these blooms; namely, the potential role of increased nutrient input into coastal waters from anthropogenic sources causing increased growth in harmful algal species. However, there are also potential "top-down" controls affecting the rate at which harmful algal species are consumed by grazers. The aim of this project was to determine protozoan grazer population fluctuations and their grazing impact on HAB species through field monitoring and laboratory grazing experiments. Protozoan grazers were chosen because their growth rates could potentially keep up with those of HAB species. Declines in grazer populations before the onset of a bloom could be indicative of a release of the HAB from a "top-down" grazing control. Field samples taken during bloom and non-bloom events helped elucidate any microplankton community changes. After establishing that there appear to be changes to the grazer population before and after a bloom, ingestion experiments including direct epifluorescence microscopy and DNA

analyses were conducted to determine if it is possible that a chosen protozoan grazer can ingest a HAB species. Finally, experiments were conducted to determine whether the HAB species was a favorable food source for the grazer. Population growth experiments in which grazers are fed a HAB species, 50:50 mixture, or normal culture food source were used to determine the survival and growth rate of the grazer. Although certain ciliates and heterotrophic dinoflagellates were found to feed on HAB species in the lab and in natural bloom samples, the HAB species as a food source produces lower grazer growth rates than on control food. Protozoan grazers may be a more effective control during bloom initiation than after the bloom has been established.

Table of Contents

List of Tables

List of Figures

Chapter 1: Patterns of microplankton and ciliate abundance in the Mission-Aransas National Estuarine Research Reserve

ABSTRACT

Microplankton abundance and community composition were recorded in the Mission-Aransas National Estuarine Research Reserve (MANERR) from June 2009 – December 2010. Located on the south Texas coast of the Gulf of Mexico, the MANERR is subjected to large fluctuations in salinity and temperature as well as harmful algal blooms (HABs). The System Wide Monitoring Program (SWMP) in the MANERR allows characterization of how these environmental processes, including physical and chemical water parameters such as temperature, salinity, and nutrients, interact to influence ciliate abundance and population patterns. Protozoan grazers, such as ciliates, are of interest because they may be able to impose a grazing control on HAB species because of their rapid growth rates compared to mesozooplankton grazers such as copepods. Broad microplankton group and ciliate characterization was carried out on live microplankton (20 μm – 200 μm organism size) in whole seawater samples using the FlowCAM, a semi-automated system for quantifying plankton populations, which has provided a less time consuming characterization of the ciliate communities at each of the reserve's SWMP sites. During this monitoring, ciliate abundance patterns related to possible drought-driven conditions were observed at all SWMP sites except the Port Aransas ship channel. FlowCAM enumeration indicated that the *Strombidium/Strobilidium* group drove the total ciliate population. The other ciliate taxonomic groups present were not reliably enumerated by the FlowCAM because of low occurrence of those ciliates in samples or underestimation by the FlowCAM due to ciliate escape responses to the sampling tube. Multivariate linear regressions indicated a

significant relationship between *Strombidium*/*Strobilidium* abundance and salinity. Significant overall regressions were also found when considering size fractionated chlorophyll, phosphate (PO_4^{3-}) and silicate (SiO_2); however, the nutrient and chlorophyll measurements individually did not significantly explain the variance in *Strombidium*/*Strobilidium* abundance. More nutrient, chlorophyll, and zooplankton measurements over dynamic environmental periods were needed to create more robust multivariate linear regressions.

INTRODUCTION

The Mission-Aransas National Estuarine Research Reserve (MANERR) includes portions of Aransas, Mission, Copano, St. Charles, Ayers, and Mesquite Bays on the south Texas coast (Figure 1.1). A salinity gradient is normally present within the MANERR with lowest salinities occurring in West Copano Bay at the mouth of the Aransas River and highest at the Port Aransas ship channel where exchange with the Gulf of Mexico occurs. The general circulation pattern within the MANERR is a northward movement of water from the Laguna Madre through Aransas and Mesquite Bays (Chandler *et al*. 1981). Copano Bay is dominated by internal circulation that is influenced by the presence of oyster reefs (Chandler *et al*. 1981, NOAA 1993). Circulation and water exchange within the MANERR is also governed by astronomical and wind tidal exchange. Of these two types, the wind tides, which occur over long periods of time and can account for a large portion of water transport between the Gulf of Mexico and the MANERR, appear to be the most important for water exchange (Morton and McGowen 1980, Armstrong 1987). Astronomical tidal effects are mainly restricted to the Port Aransas ship channel and other inlets along the Texas coast because of the relatively small inlet sizes (Morton and McGowen 1980). This area is home to many commercial

and recreational fish (Simmons and Bruer 1967), crab (Leary 1964), oyster (Hofstetter 1965), and shrimp (Zimmerman 1983, Moffett 1990) fisheries and to the endangered whooping crane (Hunt and Slack 1989). Because of these fisheries and the endangered whooping crane habitat, environmental assessments of harmful algal blooms (HABs) and their potential grazer community in the MANERR are of utmost importance.

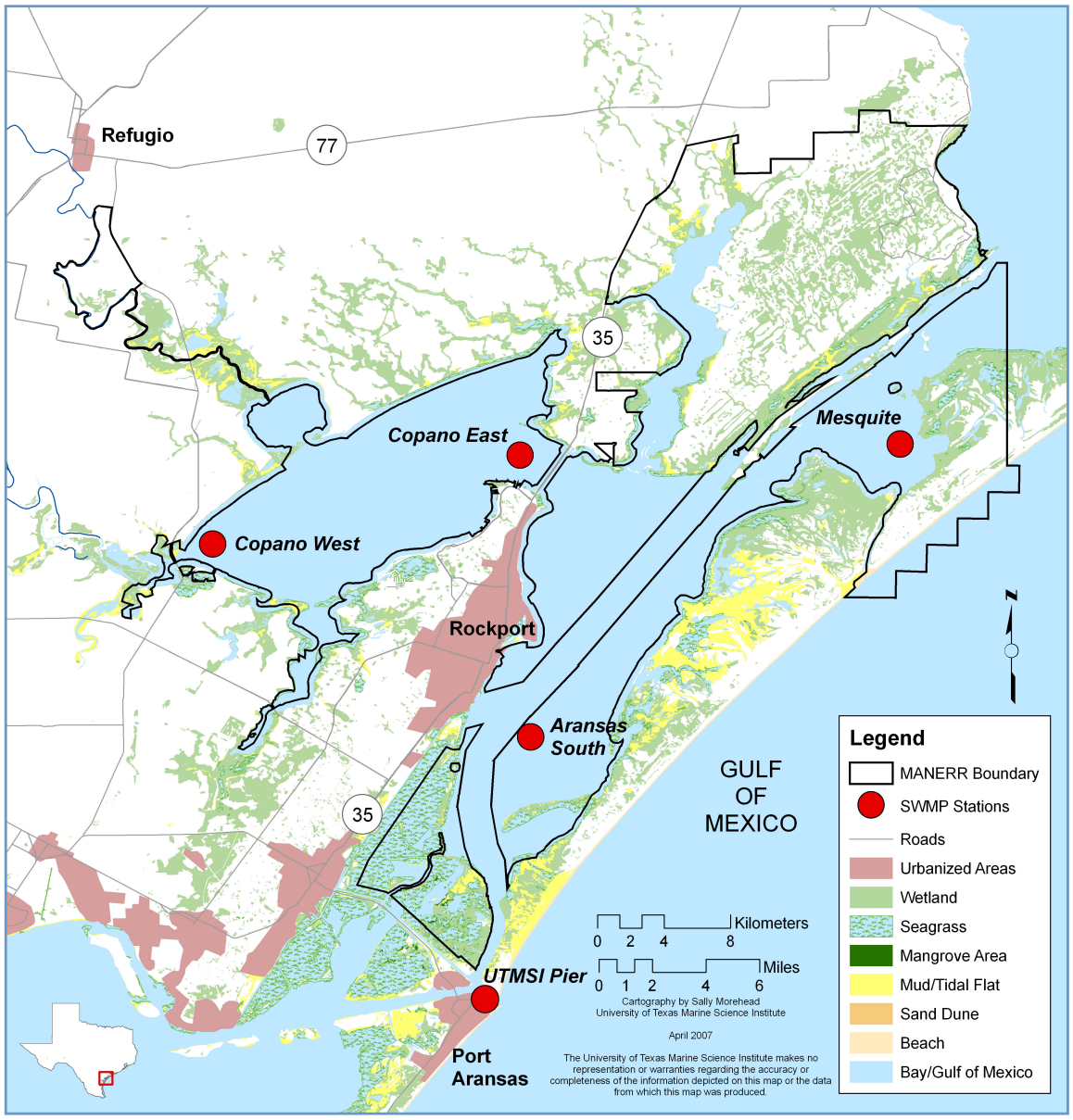

Figure 1.1: Map of the MANERR. Red dots indicate SWMP sampling stations in the Port Aransas ship channel, Aransas Bay, east and west Copano Bay, and Mesquite Bay.

It has been hypothesized that protozoan grazers such as heterotrophic dinoflagellates and ciliates can provide a more effective "top down" control on HAB species than can mesozooplankton because of faster protozoan growth rates (Admiraal and Venekamp 1986, Strom and Morello 1998). The protozoan grazer community in the MANERR has yet to be described. Ciliate population abundance in relation to temperature, salinity, wind speed, nutrients, mesozooplankton (200-2,000 μm organism size) and chlorophyll, a proxy for overall phytoplankton biomass, may allow for better predictive modeling to determine how ciliate abundances will change in response to different physical, chemical, and biological changes.

Temperate North Atlantic coastal waters experience strong seasonal changes in phytoplankton and zooplankton populations (Davis 1987). In contrast, subtropical environments, such as the South Texas coast, do not experience seasonal dynamics at the same magnitude as temperate environments (Cushing 1959, Beers *et al*. 1982, Buskey 1993). In recent decades, the Laguna Madre on the South Texas coast has experienced an unusual persistent brown tide caused by a combination of a freeze event and a long period of hypersalinity (Buskey *et al*. 1997), drastically decreasing micro- and mesozooplankton grazers. However, characterization of microplankton communities and factors affecting those populations within the MANERR during longer scale seasonal cycles are not well understood.

Microscope counting techniques can be time consuming and require taxonomic expertise to accurately identify and calculate abundances of ciliates. In order to build a database of ciliate identifications and abundances, a FlowCAM (Fluid Imaging Technologies, Inc.) was used to characterize MANERR water samples from June 2009 through December 2010. The FlowCAM allows for faster sample processing and analysis than microscope counts. The FlowCAM also has the potential advantage of being able to

enumerate living plankton samples. Preservation of ciliates with formaldehyde causes extensive destruction of ciliates, and preservation with Lugol's iodine causes less cell loss, but masks chlorophyll autofluorescence (Stoecker *et al*. 1994). For this study approximately 5.4 ml volumes of water were analyzed through the FlowCAM for 20 minutes with an added 30-60 minutes of manual image classification or correction as opposed to 24 hours of sample settling of the same volume in an Utermöhl counting chamber before microscopic analysis can begin, plus 60-180 minutes of enumeration via manual microscopy (Reid 1983, Park and Marshall 2000). The FlowCAM also provides for an image archive of organisms present in the plankton. However, the accuracy of counting ciliates in natural plankton assemblages with the FlowCAM compared to manual microscopic enumeration is unknown.

Using data from 2009-2010, the aims of this study were to determine the validity of using the FlowCAM to enumerate broad microplankton (20 μm – 200 μm organism size) categories, to characterize the ciliate communities present in the MANERR, and to determine any relationships with physical (*e.g*. temperature, salinity, wind speed), chemical (*e.g.* dissolved inorganic nutrients) and biological (*e.g*. phytoplankton biomass, copepod abundance) factors that could affect ciliate populations within the MANERR over multiple seasons. Of the total ciliate community, the *Strombidium*/*Strobilidium* taxonomic group is the most abundant throughout the MANERR (see below) and was used as the representative protozoan grazer for further analyses. This study tested the hypotheses that: 1) The FlowCAM can be used to enumerate broad microplankton (20 μm – 200 μm organism size) categories as well as *Strombidium*/*Strobilidium* ciliate abundances and 2) protozoan grazer abundances, represented by the major ciliate group *Strombidium/Strobilidium*, are significantly related to changes in phytoplankton biomass, mesozooplankton, and salinity and other environmental variables that are associated with

drought and wet cycles within the MANERR rather than seasonal environmental fluctuations that are associated with temperate coastal waters.

MATERIALS AND METHODS

Sample Sites

The sampling sites were located at the five System Wide Monitoring Program (SWMP) stations within the MANERR. These stations include the Port Aransas ship channel, Aransas Bay, East Copano Bay, West Copano Bay, and Mesquite Bay (Figure 1.1). Aransas Bay has a surface area of 232 km^2 with a volume of 526 x 10^6 m^3 and average depth of 2.4 m (Ward 1997). Copano Bay covers an area of approximately 196 km^2 with a volume of 429 x 10^6 m^3 and average depth of 2.2 m (Ward 1997). Mesquite Bay, including Ayres and Carlos Bays, has a surface area of 71 km^2 with a volume of 74 x 10^6 m^3 and an average depth of 1.2 m (Ward 1997). The Port Aransas ship channel, which has been stabilized with jetties and is the main connection of the MANERR with the Gulf of Mexico, is approximately 19 km^2 and 45 feet deep (NOAA 1993, Ward 1997).

Field Data Collection

Water samples from SWMP stations were collected during twice monthly small boat sampling trips from June 2009 through December 2010. Water samples were taken with a Van Dorn sampler 0.5 m from the bottom at all SWMP stations except the Port Aransas ship channel. Due to a deeper water column, samples were taken approximately 1 m from the bottom at the Port Aransas ship channel site. These depths corresponded to the sampling depth of the data sondes in accordance with protocols set forth by the Central Data Management Office and the National Oceanic and Atmospheric Administration. Water samples were stored in opaque brown 500-ml Nalgene bottles and

incubated in ambient temperature seawater during transport back to the laboratory. Upon return to the laboratory a 100-150 ml aliquot of each whole water sample was preserved in 1% acid Lugol's iodine for later microscopic analysis and archival. Live aliquots of each of the water samples were analyzed on the FlowCAM. Small data gaps occurred throughout the sampling period because microplankton cell density in the water samples was too low (<200 classifiable images) to obtain an accurate cell count.

The FlowCAM is an imaging in flow system, which records images, florescence, and light scatter for particles such as microplankton in a water sample (Sieracki *et al*. 1998). Water samples flowed through the instrument at a rate of ~0.27 ml min^{-1} (~5.4 total volume per sample) powered by a downstream peristaltic pump. A 10x objective paired with a 100 μm deep by 2000 μm wide glass flow cell was used to analyze all water samples on the FlowCAM. Cell size thresholds were set to a minimum of 10 and a maximum of 200 μm. A 532-nm laser was used to excite fluorescence of chlorophyll-containing particles present in a water sample as they pass through the flattened glass capillary flow cell. Trigger mode rather than autoimage mode was used to analyze the water samples because trigger mode is more suitable for water samples which contain a lower density of cells and images particles based on both fluorescence and light scatter. Autoimage mode is more suitable for use in enumerating dense cultures of cells and does not record fluorescence measurements. Using both fluorescence and light scatter parameters should allow for more accurate sampling of heterotrophic protozoa, since not all protozoa contain chlorophyll or food vacuoles containing chlorophyll. In this mode, cell concentrations are calculated based on the width of the flow cell, width of the field of view, number of particle images, and volume of sample analyzed. An image of the camera field of view is taken and areas with particles (region of interest) are selected and recorded once a predetermined fluorescence and light scatter threshold is reached

(Sieracki *et al*. 1998). The FlowCAM, unlike true flow cytometers, does not use sheath fluid, which allows for cell-by-cell counting through the center of the field of view where a majority of cell images are in focus (Olson and Sosik 2007), so multiple images may appear in the field of view at one time. Final cell concentrations of the microplanktonic organisms present in the sample were calculated with Visual Spreadsheet^{TM} software. Using this software, images were manually classified into user created categories for ciliates, which included (listed from most to least abundant): *Strombidium*/*Strobilidium*, *Myrionecta*, other ciliates, agglutinated tintinnids, *Tontonia*, hypotrichs, hyalinated tintinnids, *Laboea*, and *Strombidinopsis*. *Strombidium*/*Strobilidium* ciliates were grouped into one taxonomic category because of the difficulty in distinguishing differences in morphology from the FlowCAM images.

The SWMP station's data sondes (YSI Model 6600 V2) recorded temperature, salinity, turbidity, pH, chlorophyll, and dissolved oxygen at 15-min intervals. Dissolved inorganic nutrient (PO_4^{3-}, NH_4^+, $NO_{2,3}^-$, and SiO_2) and extracted chlorophyll samples (total and size fractionated) were analyzed once per month. Water for dissolved inorganic nutrient and chlorophyll analyses were collected via duplicate Van Dorn bottle grabs at 0.5 m from the bottom at each of the SWMP stations except the Port Aransas ship channel. Bottle grabs occurred at a depth of 1 m from the bottom in the Port Aransas ship channel. These depths corresponded to the sampling depth of the data sondes. Water samples (15 ml) for nutrient analysis were prefiltered on the boat with 0.45 μm pore filters (Millipore) and stored on ice during transport back to the laboratory. Samples were then frozen (-4 ^oC) until analysis occurred. Water samples were analyzed for nutrients using the Lachat Quikchem 8000 (Lachat Instruments) and associated protocols. Water samples for total and size fractionated chlorophyll analyses were stored in opaque brown 500-ml Nalgene bottles and incubated in ambient temperature seawater during transport

to the laboratory. Extracted chlorophyll samples were not acidified and followed the protocol in Welschmeyer (1994). Samples for total chlorophyll were filtered (15 ml – 50 ml depending on field Secchi disk reading) under low light conditions onto 25 mm diameter 0.7 μm pore GF/F glass fiber filters (Whatman), extracted overnight with 10 ml of 90% acetone, and the extract was analyzed under low light with a fluorometer (Trilogy® Laboratory Fluorometer, Turner Designs). Blanks for the fluorometer were 10 ml of 90% acetone. Samples for size fractionated chlorophyll (>20 μm, 5-20 μm, and <5 μm) were filtered (15 ml – 50 ml depending on field Secchi disk reading) under low light conditions onto 25 mm diameter 20 μm pore (>20 μm fraction) and 5 μm pore nylon filters, extracted, and analyzed as with the total chlorophyll. The 5-20 μm chlorophyll fraction was calculated by subtracting the 20-μm pore nylon filter extraction fluorometer readings from those of the 5-μm pore nylon filter extraction. The <5 μm chlorophyll fraction was calculated by subtracting the 5 μm pore nylon filter extraction fluorometer readings from those of the 0.7 μm pore GF/F glass fiber filter extraction.

Zooplankton samples were collected at each SWMP station using a 153 μm, 20 cm diameter mesh bongo net (Research Nets) equipped with a flow meter (General Oceanics). The net was deployed just below the surface and towed slowly behind the boat for 2 minutes. The net was rinsed with additional seawater and the samples preserved with 5% buffered formalin. Samples were concentrated to 100 ml (or 200 ml if sample was dense) upon return to the lab. Before enumeration, samples were stirred to ensure they were well-mixed, and a 1 or 2 ml aliquot was taken using a Hensen Stempel pipet (Wildlife Supply Company). The samples were then enumerated for identification of mesozooplankton and meroplankton using a Wild dissecting microscope. Copepods are important predators of ciliates and other microplankton (Gifford and Dagg 1988, Stoecker and Capuzzo 1990) and their total abundance is reported. Meroplankton

included barnacle nauplii, barnacle cyprids, polychaete larvae, gastropod larvae, mollusk veligers, echinoderm larvae, fish eggs, larval fish, and crab zoea.

Wind speed measurements were collected from the meteorological station located in East Copano Bay. Wind speed (m s^{-1}) was recorded at 15-minute intervals over the entire study period. A combined average wind speed for the entire day before water sampling plus the morning hours prior to water sampling was used as the wind speed variable in the data analyses. This was done to account for any possible lag effects of wind speed on the ciliate community.

FlowCAM Validation – Natural Microplankton and Ciliate Assemblages

Single subsamples of microplankton in acid Lugol's iodine-preserved whole water samples collected from August 2009 through November 2010 (n = 14) from the UTMSI pier were counted in a Sedgewick-Rafter counting chamber using a compound microscope (Olympus BX60). The entire Sedgewick-Rafter chamber was counted (1 ml volume) and the same taxonomic groups of ciliates and broad microplankton groups used for the FlowCAM analyses were recorded. These counts were compared to FlowCAM images and counts performed on those same live water samples from which the preserved aliquots originated. FlowCAM analysis of the live water samples was performed as described above. A 1:1 agreement between manual microscopy might be expected if the outflow of the FlowCAM was counted via manual microscopy and compared to those counts obtained by the FlowCAM; however, the sample outflow first travels through the peristaltic pump before deposition in a waste beaker. The passage of the sample through the peristaltic pump could damage cells within the sample, making an accurate microscopic comparison to the same water sample not possible. For this validation two subsamples (one via FlowCAM and one via manual microscopy) from a well-mixed

water sample were compared with the caveat that proportions of microplankton could vary between samples.

Data Analysis

Log transformed whole water counts for the broad microplankton groups (e.g. diatoms, dinoflagellates, and ciliates) and ciliate taxonomic groups from the microscope and FlowCAM analyses were compared using a linear regression model using the R software (Version 2.15.0). If the comparison of microscope and FlowCAM counts resulted in a slope significantly different from zero, log transformed counts from the microscope and FlowCAM for each microplankton and ciliate taxonomic group were further analyzed with an offset linear model to determine whether the slope was significantly different from one. The offset was obtained by subtracting the x-values from the y-values, essentially bringing a slope of one down to a slope of zero. The offset model then compared the offset slope of the log transformed count data to the new offset slope of zero. Microscope and FlowCAM comparisons with slope significantly different from zero but not significantly different from one would indicate good agreement between FlowCAM and microscope cell counts. Single linear regression models were also used to compare log transformed cell counts among the broad microplankton groups at each of the SWMP stations to determine any possible biological relationships.

Following the linear regression analyses comparing the FlowCAM and microscope counts, it was decided to continue on with multivariate linear regression analyses using the *Strombidium*/*Strobilidium* group of ciliates only. This group is the most common and abundant throughout the MANERR and resulted in the most accurate FlowCAM counts (see below). Multivariate linear regression models were used to compare log transformed *Strombidium*/*Strobilidium* counts combined across all five

SWMP stations in order to allow for more statistical power with more measurements. Sample location was included as a factor in the regressions to account for any differences between sample sites. Multivariate linear regressions were first used to compare *Strombidium*/*Strobilidium* abundances to salinity and sample location with and without the added variables of temperature and wind speed. The most robust multivariate regression was used as the model to cycle in one of each of the nutrient or chlorophyll measurements collected at each site. When accounting for sample location, the model chose Aransas Bay as the baseline and made adjustments by adding coefficients for the other sample sites. There were too few nutrient and chlorophyll measurements to use the multivariate linear regressions on all measurements simultaneously. The most robust multivariate regression was also used as the model to compare *Strombidium*/*Strobilidium* abundances to copepod and total meroplankton abundances.

RESULTS

FlowCAM Validation – Natural Microplankton and Ciliate Assemblages

Linear regressions of the broad microplankton category counts collected by the two methods showed significant relationships between the microscope and FlowCAM counts across all microplankton categories (Table 1.1). Comparisons between log transformed microscope and FlowCAM counts were significantly different from a slope of zero for diatoms ($R^2 = 0.52$, $p<0.01$; Figure 1.2), dinoflagellates ($R^2 = 0.51$, $p<0.01$; Figure 1.3), and ciliates ($R^2 = 0.63$, $p<0.001$; Figure 1.4). Comparisons between log transformed microscope and FlowCAM counts of diatoms, dinoflagellates, ciliates and total microplankton were not significantly different from a slope of one (Table 1.1). In general, microscope counts were higher than FlowCAM counts for dinoflagellates (Figure 1.3) and ciliates (Figure 1.4).

Type	R^2	*p-value*
Comparison to slope = 0		
Diatoms	0.52	**<0.01**
Dinoflagellates	0.51	**<0.01**
Ciliates	0.63	**<0.001**
Total	0.26	**0.035**
Comparison to slope = 1		
Diatoms	-0.082	0.90
Dinoflagellates	0.12	0.12
Ciliates	-0.066	0.66
Total	0.20	0.064

Table 1.1: Summary of *p-values* and R^2 for the linear model comparing microscope and FlowCAM counts of microplankton. Bolded values indicate $p<0.05$. Those taxonomic groups with a slope significantly different from zero were then compared to a slope of one.

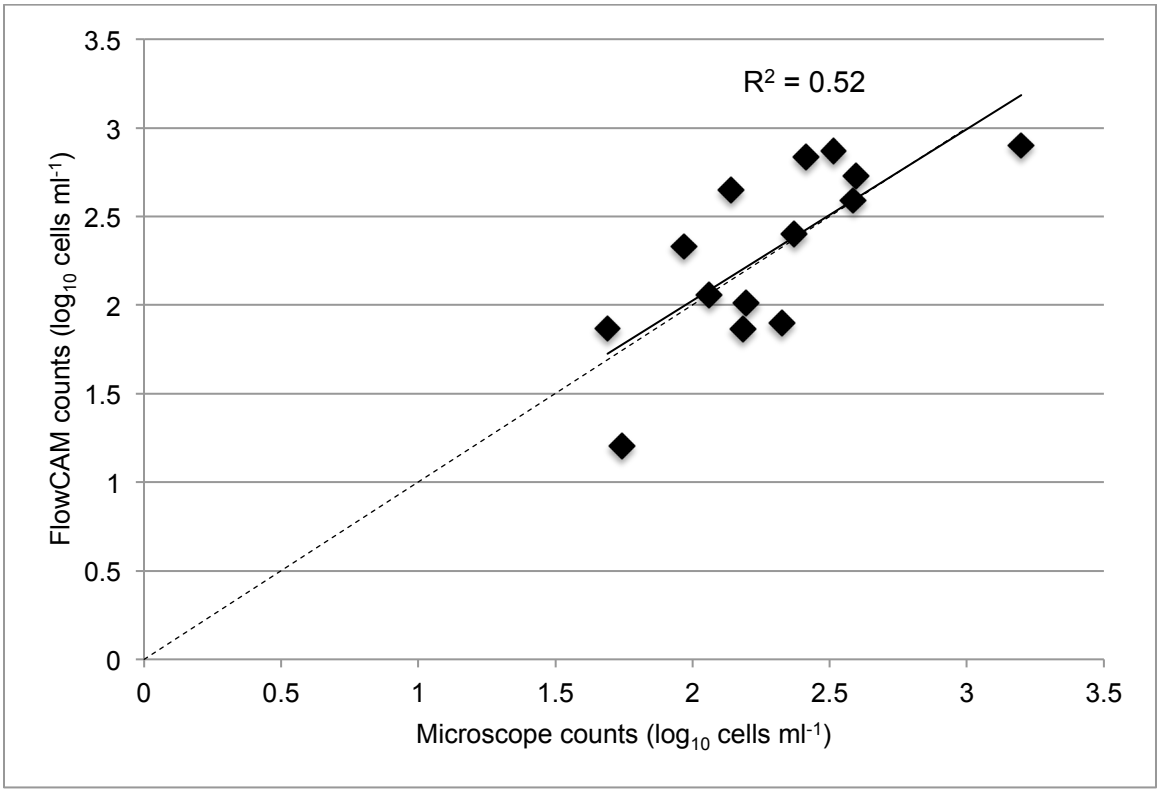

Figure 1.2: Comparison of log transformed FlowCAM and microscope counts of total diatoms (log_{10} cells ml^{-1}). Dashed line indicates a 1:1 relationship. Solid line indicates linear regression. The R^2 of the regression is posted on the graph.

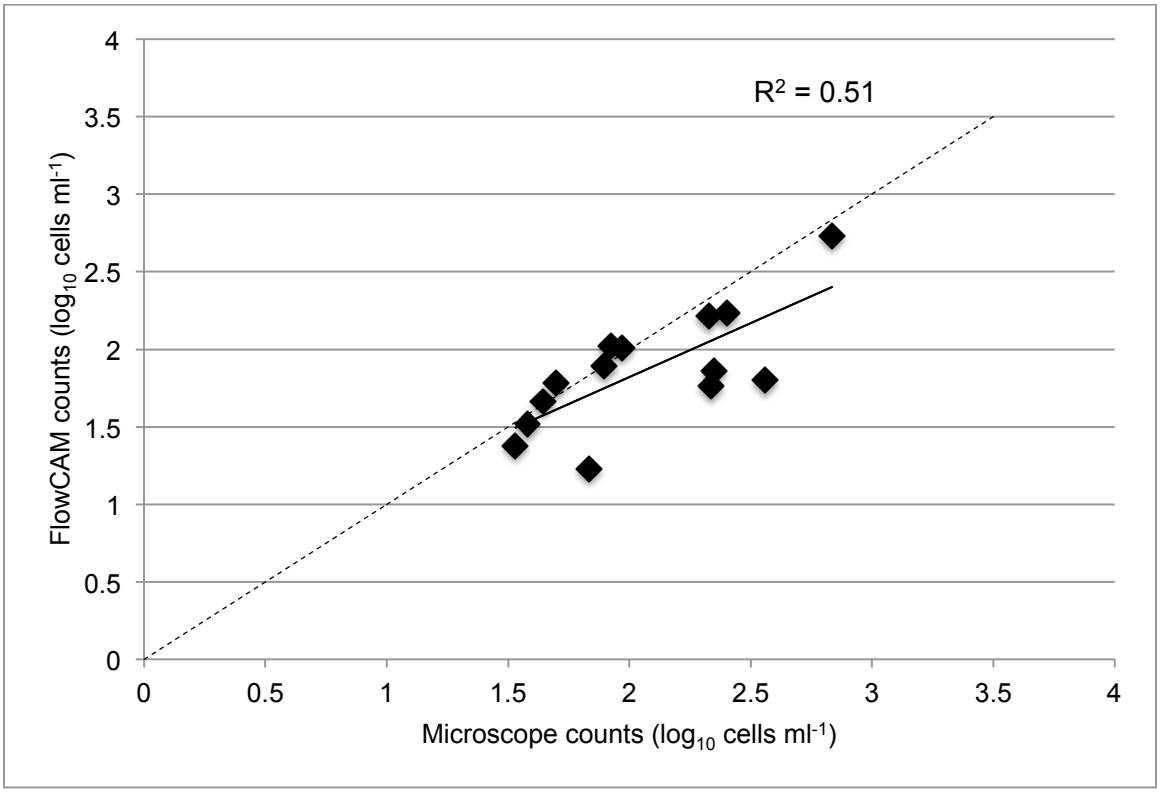

Figure 1.3: Comparison of log transformed FlowCAM and microscope counts of total dinoflagellates (log_{10} cells ml^{-1}). Dashed line indicates a 1:1 relationship. Solid line indicates linear regression. The R^2 of the regression is posted on the graph.

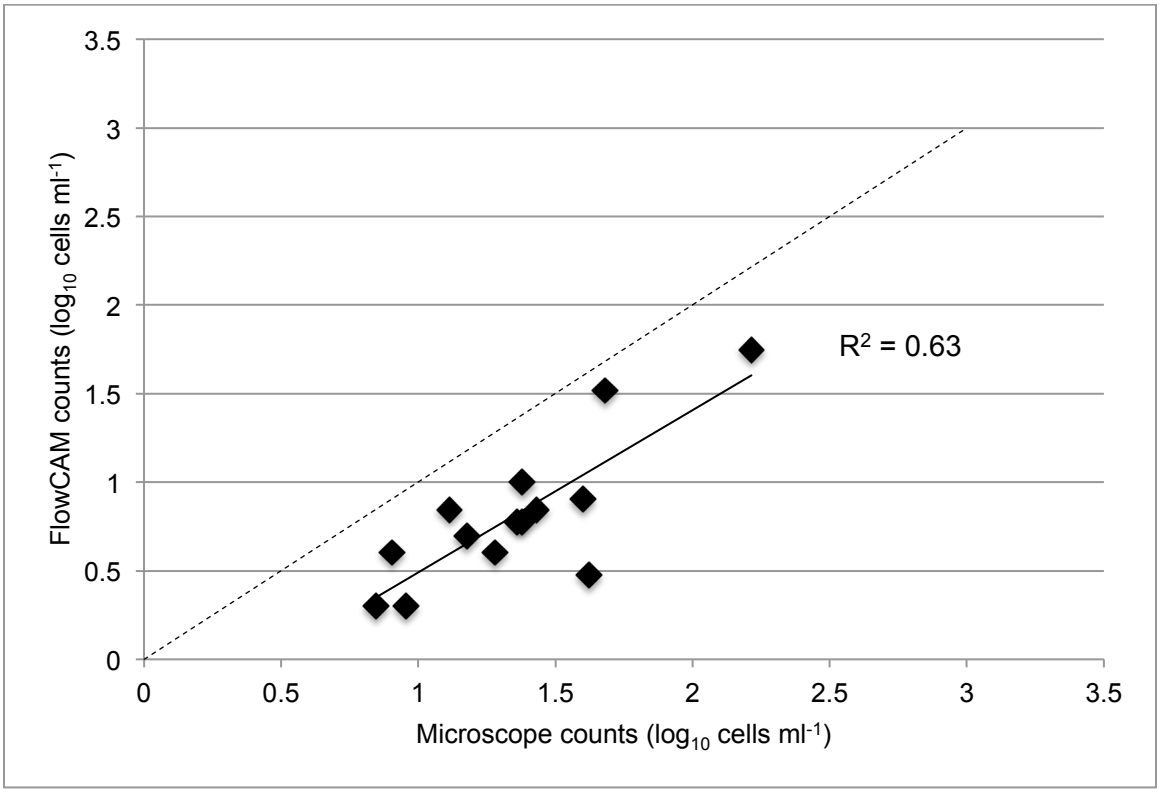

Figure 1.4: Comparison of log transformed FlowCAM and microscope counts of total ciliates (log_{10} cells ml^{-1}). Dashed line indicates a 1:1 relationship. Solid line indicates linear regression. The R^2 of the regression is posted on the graph.

Linear regressions of the ciliate taxonomic counts collected by the two methods showed significant relationships between the log transformed microscope and FlowCAM counts for *Strombidinopsis* sp. (R^2 = 0.35, p = 0.014), *Strombidium*/*Strobilidium* (R^2 = 0.57, p<0.01), agglutinated tintinnids (R^2 = 0.30, p = 0.025), and total ciliates (R^2 = 0.63, p<0.001) (Table 1.2). There were too few non-zero measurements for the hypotrichs and *Laboea* sp. to result in a linear regression. *Myrionecta* sp. (Figure 1.5), *Tontonia* sp. (Figure 1.6), and agglutinated tintinnid (Figure 1.7) counts were underestimated by the FlowCAM when compared to microscope counts. Although *Strombidinopsis* sp., *Strombidium*/*Strobilidium*, agglutinated tintinnids, and total ciliates resulted in significant

regressions, only the *Strombidium*/*Strobilidium* group was used for further data analyses because it is the most abundant group, resulting in the fewest non-zero FlowCAM counts during the validation experiment and field sampling, and drives the total ciliate population (Tables 1.3 – 1.4; Figure 1.8). The *Strombidium*/*Strobilidium* counts were still underestimated by the FlowCAM and resulted in a slope significantly different from one ($R^2 = 0.37$, $p = 0.013$); however, the significance of the regression compared to a slope of zero ($R^2 = 0.57$, $p<0.01$) allowed for a transformation of the FlowCAM *Strombidium*/*Strobilidium* data to adjust for the difference from a slope of one. The regression equation used to transform the log FlowCAM counts was $FC = \frac{(FC_{log10} - b)}{m}$ where FC is the recalculated FlowCAM *Strombidium*/*Strobilidium* counts based on the linear regression of the initial log transformed counts, FC_{log10} is the initial log transformed FlowCAM *Strombidium*/*Strobilidium* counts, b is the intercept of the linear regression (0.1023), and m is the slope of the linear regression (0.6358). A new linear regression comparing the recalculated log transformed FlowCAM *Strombidium*/*Strobilidium* counts to those from the microscope resulted in a significant regression with a slope near one (slope = 0.99, $R^2 = 0.57$, $p<0.01$). These recalculated log transformed counts were used for further data analyses.

Type	R^2	*p-value*	Percent of Total
Total ciliates	0.63	**<0.001**	100%
Strombidium/Strobilidium	0.57	**<0.01**	81.70%
Other ciliates	-0.047	0.53	9.15%
Agglutinated tintinnids	0.30	**0.025**	3.92%
Tontonia	0.095	0.15	2.61%
Myrionecta	-0.055	0.58	1.31%
Hyalinated tintinnids	-0.062	0.63	0.65%
Strombidinopsis	0.35	**0.014**	0.65%
Hypotrich	N/A	N/A	0.00%
Laboea	N/A	N/A	0.00%

Table 1.2: Summary of R^2 and *p-values* for the linear model comparing log transformed microscope and FlowCAM counts of ciliate taxonomic groups. Ciliate groups are listed in descending order based on abundance. Bolded values indicate $p<0.05$ when compared to a slope of zero. N/A values indicate groups with too few non-zero measurements to result in a linear regression. Percent of total ciliates (153 cells) counted by the FlowCAM are also presented.

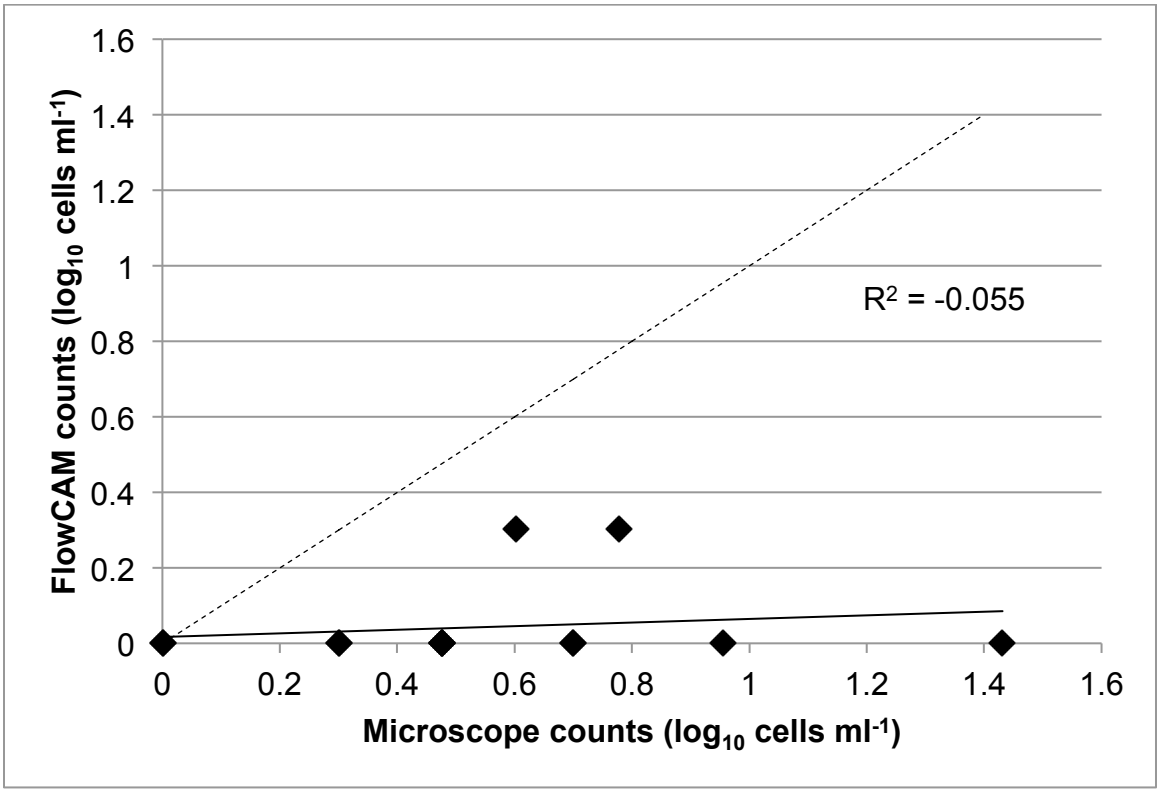

Figure 1.5: Comparison of log transformed FlowCAM and microscope counts of *Myrionecta* sp. (log_{10} cells ml^{-1}). Dashed line indicates a 1:1 relationship. Solid line indicates linear regression. The R^2 of the regression is posted on the graph.

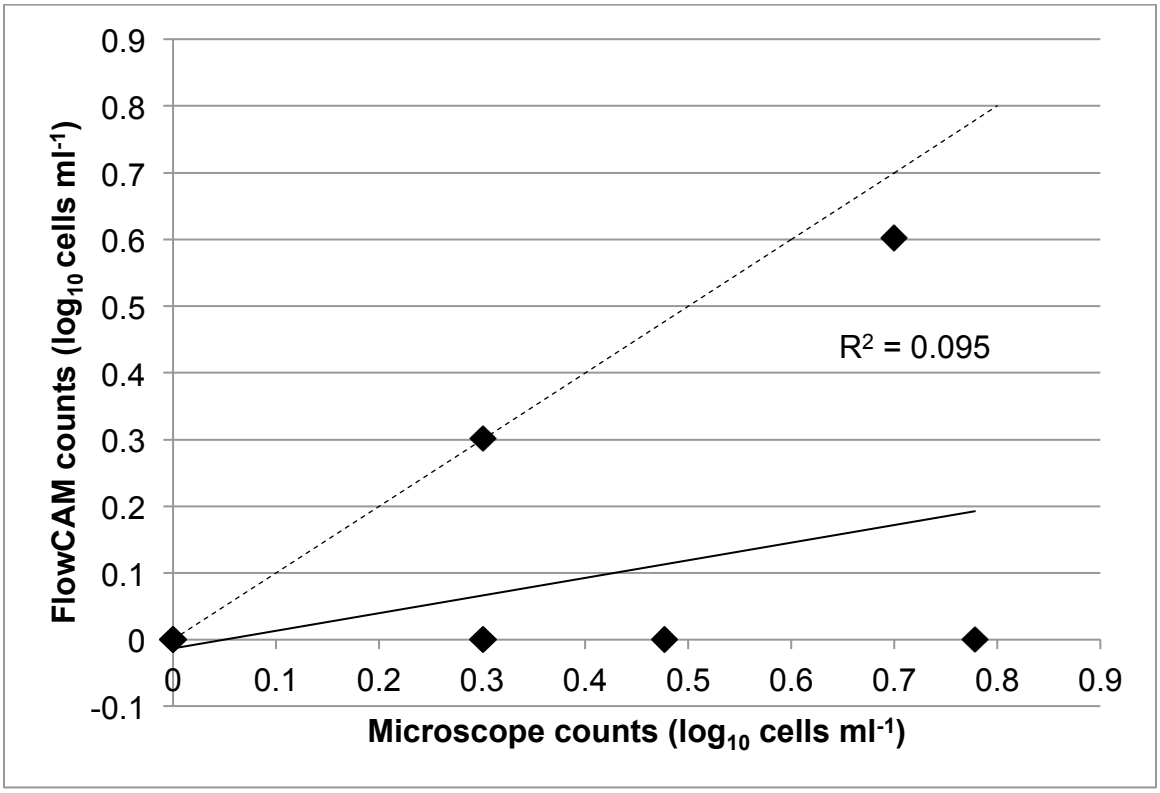

Figure 1.6: Comparison of log transformed FlowCAM and microscope counts of *Tontonia* sp. (log_{10} cells ml^{-1}). Dashed line indicates a 1:1 relationship. Solid line indicates linear regression. The R^2 of the regression is posted on the graph.

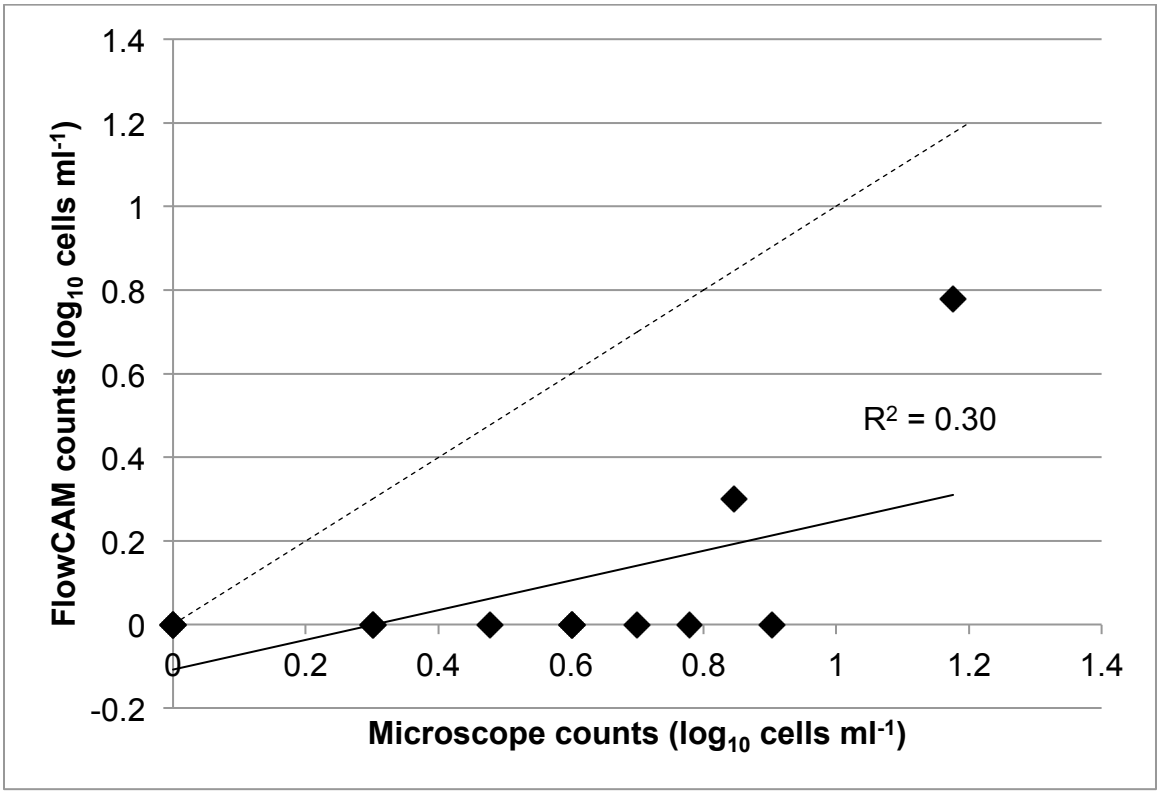

Figure 1.7: Comparison of log transformed FlowCAM and microscope counts of agglutinated tintinnids (log_{10} cells ml^{-1}). Dashed line indicates a 1:1 relationship. Solid line indicates linear regression. The R^2 of the regression is posted on the graph.

Type	Non-Zero
Strombidium/Strobilidium	14
Other ciliates	7
Agglutinated tintinnids	2
Myrionecta	2
Tontonia	2
Hyalinated tintinnids	1
Strombidinopsis	1
Hypotrich	0
Laboea	0

Table 1.3: Number of non-zero FlowCAM counts of ciliate taxonomic groups during the validation experiments. Sample size: n=14

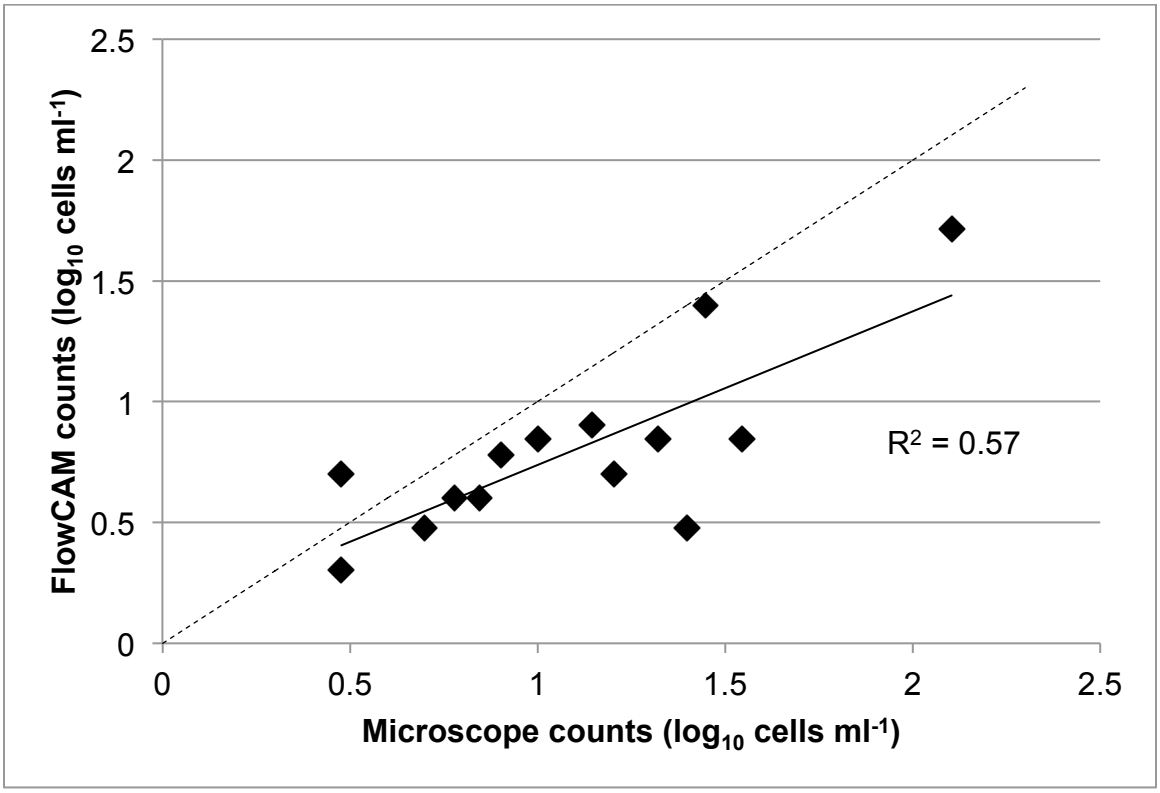

Figure 1.8: Comparison of log transformed FlowCAM and microscope counts of *Strombidium*/*Strobilidium* (log_{10} cells ml^{-1}). Dashed line indicates a 1:1 relationship. Solid line indicates linear regression. The R^2 of the regression is posted on the graph.

Type	Non-Zero	Percent of Total
Strombidium/Strobilidium	121	67.70%
Other ciliates	32	15.56%
Myrionecta	31	7.03%
Tontonia	28	5.19%
Agglutinated tintinnids	13	3.60%
Hypotrich	4	0.33%
Hyalinated tintinnids	3	0.25%
Laboea	3	0.25%
Strombidinopsis	1	0.08%

Table 1.4: Number of non-zero FlowCAM counts of ciliate taxonomic groups for the entire sampling period. Ciliate taxonomic groups are listed in descending order based on abundance. Percent of total ciliates (1195 cells) counted by the FlowCAM are also presented. Sample size: n=155

Linear Regressions – Microplankton Categories

Ciliate abundance had a significant positive relationship to dinoflagellate abundance at each sample site except Mesquite Bay (Table 1.5). Ciliate abundance was not significantly related to diatom abundance at any of the sampling sites (Table 1.5). Diatom abundance had a significant negative relationship with dinoflagellate abundance East Copano Bay (Table 1.5). In contrast, diatom abundance had a significant positive relationship with dinoflagellate abundance in Mesquite Bay (Table 1.5).

		Diatoms			Dinoflagellates			Ciliates		
		Coefficient		R^2	Coefficient		R^2	Coefficient		R^2
Aransas Bay	**Diatoms**	-		-	-0.35		0.033	-0.19		-0.014
	Dinoflagellates	-0.35		0.033	-		-	0.68	***	0.44
	Ciliates	-0.19		-0.014	0.68	***	0.44	-		-
West Copano Bay	**Diatoms**	-		-	-0.15		-0.014	-0.15		-0.007
	Dinoflagellates	-0.15		-0.014	-		-	0.48	**	0.26
	Ciliates	-0.15		-0.007	0.48	**	0.26	-		-
East Copano Bay	**Diatoms**	-		-	-0.91	**	0.22	-0.12		-0.027
	Dinoflagellates	-0.91	**	0.22	-		-	0.35	*	0.15
	Ciliates	-0.12		-0.027	0.35	*	0.15	-		-
Mesquite Bay	**Diatoms**	-		-	0.57	*	0.14	0.18		-0.014
	Dinoflagellates	0.57	*	0.14	-		-	0.32		0.084
	Ciliates	0.18		-0.014	0.32		0.084	-		-
Port Aransas Ship Channel	**Diatoms**	-		-	0.39		0.041	-0.20		-5E-04
	Dinoflagellates	0.39		0.041	-		-	0.42	**	0.27
	Ciliates	-0.20		-5E-04	0.42	**	0.27	-		-

Table 1.5: Summary of coefficients, *p-values*, and R^2 for individual linear regressions comparing log transformed total diatom, dinoflagellate, and ciliate abundances at each site. * = $p<0.05$, ** = $p<0.01$, *** = $p<0.001$ for each coefficient. Sample size for each site: n = 32

Multivariate Linear Regressions – *Strombidium*/*Strobilidium*

Of the three environmental variables tested, only salinity had a significant coefficient (Table 1.6). A multivariate linear regression (5 independent predictors) was then used to compare *Strombidium*/*Strobilidium* abundances to salinity and sample location. This regression resulted in more significant coefficients for each of variables and a more significant model overall ($R^2 = 0.11$, $p<0.001$; Table 1.7).

	Coefficient	*p-value*
(Intercept)	0.90	**0.0055**
East Copano Bay	0.082	0.60
West Copano Bay	-0.012	0.94
Mesquite Bay	0.50	**0.0020**
Port Aransas Ship Channel	0.35	**0.033**
Temperature	-0.0014	0.87
Salinity	-0.015	**0.0084**
Wind Speed	0.0054	0.89
	R^2	***p-value***
Total Model	0.10	**0.0024**

Table 1.6: Summary of coefficients and *p-values* for those coefficients for the multivariate linear regression comparing log transformed FlowCAM counts of *Strombidium*/*Strobilidium* to sample location, temperature, salinity, and wind speed. The intercept is based on the base model using Aransas Bay. The R^2 and *p-value* for the entire regression are also listed. Bolded values indicate $p<0.05$. Sample size: n=151

	Coefficient	*p-value*
(Intercept)	0.90	**<0.001**
East Copano Bay	0.082	0.60
West Copano Bay	-0.012	0.94
Mesquite Bay	0.50	**0.0018**
Port Aransas Ship Channel	0.36	**0.025**
Salinity	-0.015	**0.0022**
	R^2	***p-value***
Total Model	0.11	**<0.001**

Table 1.7: Summary of coefficients and *p-values* for those coefficients for the multivariate linear regression comparing log transformed FlowCAM counts of *Strombidium*/*Strobilidium* to sample location. The intercept is based on the base model using Aransas Bay. The R^2 and *p-value* for the entire regression are also listed. Bolded values indicate $p<0.05$. Sample size: n=151

Salinity and the sample location of Mesquite Bay were significant variables of the multivariate linear regressions in almost every regression (Table 1.8). Mesquite Bay had the highest average abundance (Figure 1.9), the highest number of non-zero counts (Table 1.9), and the most temporally dynamic abundance (Figure 1.10) of *Strombidium*/*Strobilidium*, which could account for the significant Mesquite Bay coefficients in the regressions. The higher average with larger standard deviation for West Copano Bay (Figure 1.9) can be accounted for by one bloom sample of *Strombidium*/*Strobilidium* of 150 cells ml^{-1}. Total ciliate counts (driven by *Strombidium/Strobilidium* abundance) indicated a possible pattern relating to drought and wet periods within the MANERR (Figure 1.10). Lower ciliate abundances were enumerated in 2009 during a period of extended drought (salinity >35 psu), while an increase in ciliate abundances occurred in 2010 during a period of lower salinity (Figure 1.10; Table 1.10). This pattern illustrates the significant negative relationship between salinity and *Strombidium*/*Strobilidium* abundance for each of the multivariate linear regression. Although significant regressions resulted from those models including phosphate (PO_4^{3-}), silicate (SiO_2), and each of the size fractionated chlorophyll measurements, none of the nutrients or chlorophyll measurements had significant coefficients in the model. The lack of significant coefficients indicated that the nutrient and chlorophyll measurements did not explain the variance in *Strombidium*/*Strobilidium* abundance individually. Copepod and total meroplankton abundance also did not significantly explain the variance in *Strombidium*/*Strobilidium* abundance individually (Table 1.11). The inclusion of copepod and total meroplankton variables also did not result in a significant overall regression (Table 1.11).

	PO_4^{3-} Coefficient		NH_4^+ Coefficient		$NO_{2,3}^-$ Coefficient		SiO_2 Coefficient		Total Chl *a* Coefficient		>20 µm Chl *a* Coefficient		5-20 µm Chl *a* Coefficient		<5 µm Chl *a* Coefficient	
East Copano Bay	-0.02		0.18		0.15		-0.32		-0.04		0.06		0.01		0.02	
West Copano Bay	-0.22		0.11		-0.15		-0.51		-0.29		-0.33		-0.37		-0.37	
Mesquite Bay	0.47	*	0.63	*	0.44		0.28		0.42	*	0.62	**	0.59	**	0.61	**
Port Aransas Ship Channel	0.23		0.26		0.26		0.35		0.2		0.37		0.34		0.34	
Salinity	-0.01	*	-0.01	*	-0.01		-0.02	*	-0.01		-0.02	**	-0.02	**	-0.02	**
Cycled Variable	-0.06		-0.01		0.06		0		0.01		0.01		-0.02		0	
	R^2	*p*	R^2	*p*	R^2	*p*	R^2	*p*	R^2	*p*	R^2	*p*	R^2	*p*	R^2	*p*
Entire Model	0.098	**0.024**	0.055	0.20	-0.007	0.47	0.10	**0.027**	0.08	0.055	0.19	**<0.01**	0.19	**<0.01**	0.18	**<0.01**

Table 1.8: Summary of coefficients and *p-values* for those coefficients for the multivariate linear regression comparing log transformed FlowCAM counts of *Strombidium*/*Strobilidium* to sample location, salinity, and each "cycled variable." The "cycled variable" is based on the nutrient or chlorophyll measurement listed in each column heading. Aransas Bay is not included individually because the model used Aransas Bay as the baseline. The R^2 and *p-value* for the entire regression are also listed. * = $p<0.05$, ** = $p<0.01$, *** = $p<0.001$ for each coefficient. Bolded values indicate $p<0.05$ for the entire model. Sample size for each cycled variable: PO_4^{3-} n=89, NH_4^+ n=52, $NO_{2,3}^-$ n=50, SiO_2 n=84, total chl *a* n=87, >20 µm chl *a* n=80, 5-20 µm chl *a* n=80, <5 µm chl *a* n=80.

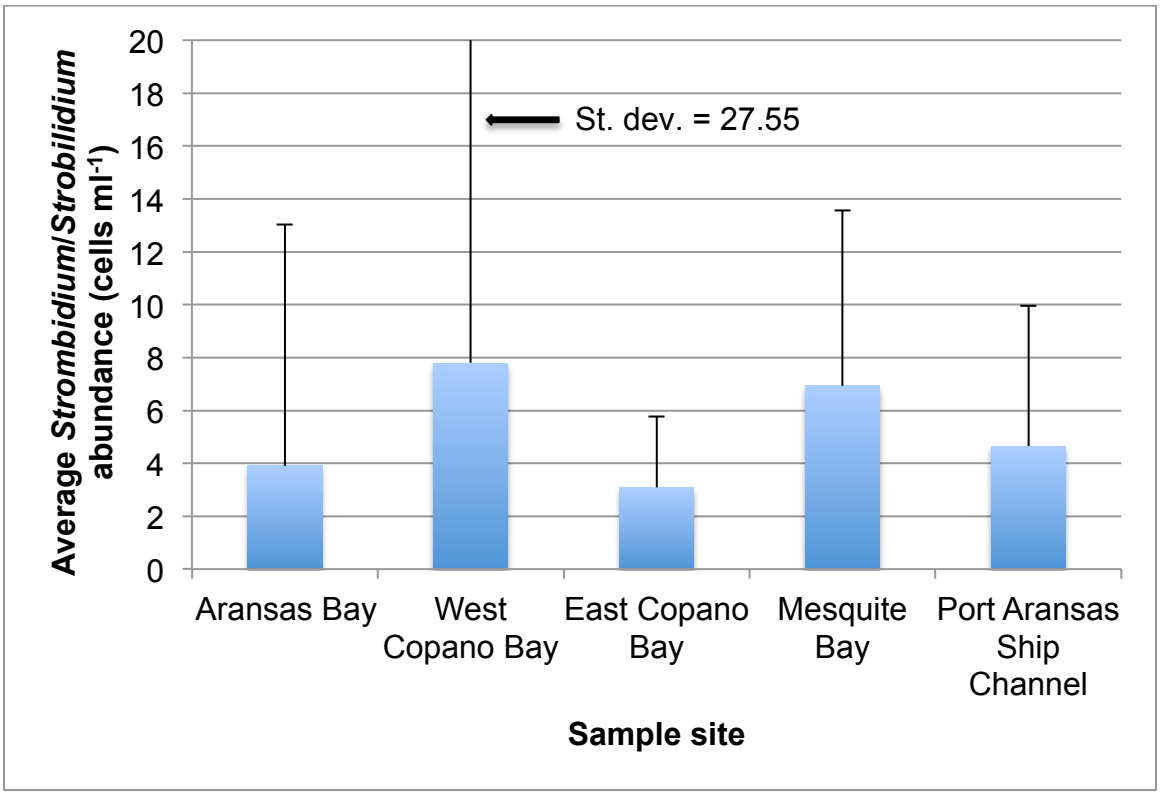

Figure 1.9: Average *Strombidium*/*Strobilidium* abundances (cells ml^{-1}) for each sample site. Error bars indicate standard deviation. Sample size: n = 32

Sample Site	Non-Zero
Aransas Bay	19
West Copano Bay	20
East Copano Bay	27
Mesquite Bay	28
Port Aransas Ship Channel	27

Table 1.9: Number of non-zero FlowCAM counts of *Strombidium*/*Strobilidium* for each sample site. Sample size: n = 32

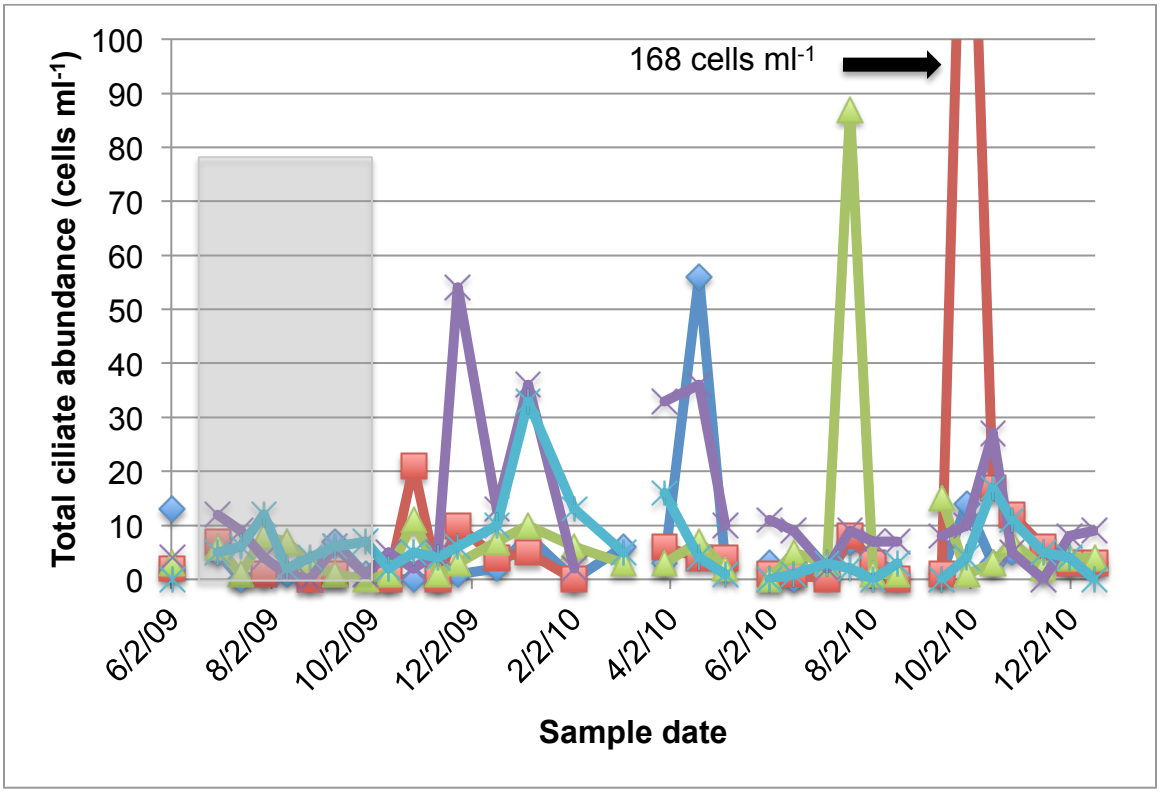

Figure 1.10: Total ciliate abundance (cells ml^{-1}) in Aransas Bay (blue), West Copano Bay (red), East Copano Bay (green), Mesquite Bay (purple), and the Port Aransas ship channel (turquoise) for June 2009 – December 2010. Gray box indicates the period of hypersalinity (>35 psu).

	Average	St. Dev.
Aransas Bay	21.4	5.4
West Copano Bay	8.0	3.5
East Copano Bay	13.2	2.6
Mesquite Bay	17.0	3.0
Port Aransas Ship Channel	30.6	4.5

Table 1.10: Summary of average salinity (psu) plus standard deviation for each sample site in the MANERR during 2010. Sample size: n = 19

	Coefficient	
Intercept	0.53	
East Copano Bay	0.093	
West Copano Bay	0.082	
Mesquite Bay	0.31	*
Port Aransas Ship Channel	0.34	*
Salinity	-0.013	**
Copepods	0.039	
Meroplankton	0.035	
	R^2	***p-value***
Entire Model	0.092	0.0502

Table 1.11: Summary of coefficients and *p-values* for those coefficients for the multivariate linear regression comparing log transformed FlowCAM counts of *Strombidium*/*Strobilidium* to sample location, salinity, and log transformed counts of copepods and total meroplankton. Aransas Bay is not included individually because the model used Aransas Bay as the baseline. The R^2 and *p-value* for the entire regression are also listed. * = $p<0.05$, ** = $p<0.01$ for each coefficient. Sample size: n = 83

DISCUSSION

Microplankton communities are very diverse, and identification of species abundance often requires taxonomic expertise and tedious, time-consuming analysis using microscopy. A FlowCAM was used to more rapidly provide cell counts and characterize broad microplankton group abundances and ciliate assemblages throughout the MANERR. The linear regressions comparing FlowCAM and microscope counts resulted in near 1:1 relationships between the two methods for counts of diatoms, dinoflagellates, and ciliates indicating that the FlowCAM, using the 10X optic, is suitable for enumerating natural microplankton populations. The slope of the dinoflagellate comparison (Figure 1.3) indicated that the FlowCAM underestimated dinoflagellate

abundance at higher cell concentrations. It has been shown that the FlowCAM is poor at counting dense cultures when operating in trigger mode (Chapter 2). Similar to underestimated counts for dense cultures, the FlowCAM operating in trigger mode may not be capable of accurate cell counts for dense natural plankton assemblages without first diluting the sample (optimal concentrations 100-200 cells ml^{-1}).

The slope of many of the ciliate taxonomic comparisons indicated that the FlowCAM underestimated ciliate abundances (Figures 1.5 – 1.8). Ciliate counts in general were higher when using traditional microscopy than on the FlowCAM. Ciliates are fragile organisms and cell losses could potentially occur during sample passage through the tubing and flow cell of the FlowCAM. Damaged ciliates can be seen when sampling with a similar instrument, the Imaging FlowCytobot (see Chapter 2). Although few to no damaged ciliates were seen in FlowCAM images, cell losses could have occurred during sample pumping through instrument tubing or during sample mixing with a stir bar near the instrument intake tube. The underestimate of agglutinated tintinnids by the FlowCAM when compared to microscope counts could be an effect of cell sinking response near the intake (due to their heavy lorica, Broglio *et al*. 2001) even though the sample was slowly mixed with a stir bar. Ciliate escape responses could also be responsible for the lower FlowCAM counts. Jakobsen (2001) found that water deformation created by a siphon elicited non-random escape responses in three species of ciliates, *Balanion comatum*, *Strobilidium* sp., and *Mesodinium pulex*. *Tontonia* sp. is also capable of fast swimming bursts (Crawford 1992), which may also enable the ciliate to escape the FlowCAM siphon. *Strobilidium* sp., *Tontonia* sp., and *M. pulex*, as well as *Myrionecta rubra* can make up a large proportion of the ciliate community in the MANERR so it is reasonable that the ciliate population is underestimated because of ciliate escape responses caused by the flow field created by the FlowCAM peristaltic

pump. This underestimate may be true only of the current FlowCAM configuration using the peristaltic pump with siphon. Other FlowCAM models feature a funnel system paired with peristaltic pump or syringe pump, which would help prevent a ciliate escape response; however, recent ciliate studies using the FlowCAM are validating the use of software classifiers and biovolume calculations rather than validating the count accuracy (Álvarez *et al*. 2012).

There appears to be a tradeoff in using the FlowCAM to analyze live microplankton as opposed to preserved samples. Studies on ciliate preservation and enumeration found that the use of different types of preservation solutions can cause cell losses, shrinkage, and malformation (Choi and Stoecker 1989, Jerome *et al*. 1993, Stoecker *et al*. 1994). Preservation with acid Lugol's results in higher ciliate counts than preservation in 2% buffered formalin; however, the use of higher concentrations of acid Lugol's also results in cell shrinkage, which will cause underestimates of ciliate biomass (Stoecker *et al*. 1994). Buffered formalin causes highest amount of cell losses and least amount of cell shrinkage (Choi and Stoecker 1989). Protargol staining is preferred for describing morphological characteristics of ciliates (Lynn and Gilron 1993); however, this method still results in significant cell shrinkage (Jerome *et al*. 1993). Analyzing live samples on the FlowCAM would ensure more distinguishable morphological characteristics than images of preserved ciliates, which may be malformed or lost due to preservation; however, significant live cell losses can occur through the ciliate escape response from the sample tube, sinking, or cell damage.

In general, microplankton communities (20 μm – 200 μm organism size) in estuarine systems can be influenced by many factors. Physical, chemical, and biological properties of an area can influence microplankton community structure, organism interactions, and the potential for algal blooms. Temperature and salinity can be

important factors driving microplankton community structure (Verity 1987; McQuoid 2005). These can be especially important in the MANERR, which experiences periodic freeze events and extended periods of drought punctuated by storm events, causing large fluctuations in temperature and salinity. Nutrients can also play an important role in shaping microplankton community structure (Örnólfsdóttir *et al*. 2004). Within the MANERR, freshwater inflows from the Aransas River can provide large nutrient inputs into West Copano Bay following storm events (Mooney and McClelland in press). Hydrological properties of bay and coastal systems, such as water circulation (Crespo and Figueiras 2007), turbulence (Guadayol *et al*. 2009), and residence times (Butrón *et al*. 2009), influence the microplankton community. Circulation patterns and water residence times within the MANERR could contribute to harmful algal bloom transport and entrainment within the bays; while turbulence and flushing from wind or storm events could dilute or transport the microplankton community from the area. Finally, biological interactions between primary producers, grazers, and predators also shape microplankton community structure (Burkill *et al*. 1987, Miller *et al*. 1995). Of particular interest are protozoan grazers because they may provide "top down" controls through potential feeding on harmful algal bloom (HAB) species and faster growth rates that can potentially keep up with HAB species growth rates (Admiraal and Venekamp 1986). The identification and characterization of these factors affecting ciliate populations would provide important insight into protozoan grazer dynamics within the MANERR.

Linear regressions comparing dinoflagellate and ciliate abundances resulted in positive significant relationships at all MANERR sampling sites except Mesquite Bay (Table 1.5). This positive relationship could indicate a grazer and food interaction between ciliates and dinoflagellates. There was also a significant negative relationship between diatom and dinoflagellate abundances in East Copano Bay, which could indicate

competition between diatoms and dinoflagellates. In general, diatoms have a higher nutrient uptake affinity than dinoflagellates (Smayda 1997). Average concentrations of dissolved phosphate (PO_4^{3-}), ammonium (NH_4^+), and nitrite/nitrate ($NO_{2,3}^-$) were 1.3±0.97 µM, 1.5±1.6 µM, and 1.6±3.1 µM, respectively, for East Copano Bay for the study period. There was a peak $NO_{2,3}^-$ concentration of 9.7 µM in April 2010. Half saturation constants for nitrate uptake by the diatoms *Skeletonema costatum*, *Ditylum brightwellii*, and *Asterionella japonica* range from 0.4-1.3 µM (Eppley *et al*. 1969). Half saturation constants for ammonium uptake for these same diatoms range from 0.6-1.1 µM (Eppley *et al*. 1969). In contrast, half saturation constants for nitrate and ammonium uptake by the dinoflagellates *Gonyaulax polyedra* and *Akashiwo sanguinea* range from 3.8-10.3 µM and 1.1-5.7 µM, respectively (Eppley *et al*. 1969). Ammonium and nitrite/nitrate concentrations in East Copano Bay would be more suitable for diatom growth.

Long-term studies of other estuaries and freshwater systems have revealed plankton community composition shifts during drought periods. An extended drought, causing hypersaline conditions, followed by a freeze event in the Laguna Madre, Texas caused a decline in the planktonic grazer populations, which may have contributed to a long-term bloom of the brown tide alga, *Aureoumbra lagunensis* (Buskey *et al*. 1997). In an oligotrophic estuary in the Adriatic, summer drought conditions resulted in a community shift from chain-forming diatoms in the winter to a nanoplankton-dominated community (Viličic *et al*. 2008). Similarly, salinity differences between drought and non-drought years may be related to *Strombidium*/*Strobilidium* and total ciliate abundance changes within the MANERR. During the 2009 drought, lower total ciliate abundances, made of the *Strombidium*/*Strobilidium* group, were enumerated across all of the NERR sampling sites (Figure 1.10). There were significant negative relationships between

Strombidium/*Strobilidium* and salinity for each multivariate linear regression analysis (Table 1.8). During 2010, when average salinities were lower across each of the sampling sites (Table 1.10), ciliate abundances were higher than the previous year (Figure 1.10). Barría de Cao *et al*. (2005) found that tintinnid ciliate density and biomass was not significantly correlated with salinity. Temperature individually also did not correlate with ciliate abundances at any of the sample sites and thus cannot be used to predict possible changes in ciliate abundance (Table 1.6). In contrast, other studies have found tintinnid ciliate density to correlate significantly with temperature (Sanders 1987, Barría de Cao *et al*. 2005).

Salinity and sample site in combination with various nutrients and chlorophyll in a multivariate linear regression analysis produced significant models for *Strombidium*/*Strobilidium* abundance within the MANERR. Regressions including phosphate (PO_4^{3-}), silicate (SiO_2), and each of the size fractionated chlorophyll measurements resulted in significant regressions for the entire model; however, the coefficients for each nutrient and chlorophyll measurement individually did not significantly explain any of the variance seen in *Strombidium*/*Strobilidium* abundance (Table 1.8). Biologically, the overall linear regression analyses of *Strombidium*/*Strobilidium* abundance throughout the MANERR were significantly related to the size fractionated chlorophyll concentrations (Table 1.8). This significant relationship could be indicative of a grazer and food relationship. Epstein *et al*. (1992) found that food vacuoles of various benthic ciliates were dominated by small dinoflagellates (~11 μm diameter) as well as bacteria. *Strobilidium* sp. (40 μm diameter) as well as other ciliates have also been found to prefer and have higher ingestion rates on food particles just under 10 μm (Anderson and Sorensen 1986, Kivi and Setälä 1995).

The low dynamic range in *Strombidium*/*Strobilidium* abundances as well as nutrient and chlorophyll concentrations likely contributed to non-significant relationships in the multivariate models. In general, *Strombidium*/*Strobilidium* abundances spanned one order of magnitude (5-20 cells ml^{-1}) punctuated by a few bloom periods (Figure 1.10). There were also many instances where ammonium (NH_4^+) and nitrite/nitrate ($NO_{2,3}^-$) concentrations were below the detection limit of the analyzer or low (<0.5 μM). Nutrient and chlorophyll measurements are also only taken once per month within the MANERR, which decreases the number of observations that can be included in the regression analysis, making the model weaker. Field sampling also does not take place during inclement weather when wind, increased precipitation, and increased freshwater inflow could cause drastic changes in nutrient inputs, mixing, flushing, salinity, and plankton community changes. If microplankton, salinity, nutrient, and chlorophyll measurements were taken on a more frequent basis, including storm events, these multivariate linear regressions may change with the added information. A longer time period of study to include at least 2 wet years is needed to see if this study's pattern of higher ciliate abundance during periods of lower salinity continues.

Abundance of copepods and total meroplankton did not significantly explain the variance in *Strombidium*/*Strobilidium*. Mesocosm experiments have shown that mesozooplankton can have a significant feeding pressure on microzooplankton populations, especially in the presence of an unpalatable phytoplankton bloom food source (Buskey *et al*. 2003). However, the low dynamic range in *Strombidium*/*Strobilidium* abundances discussed above did not allow for significant relationships between mesozooplankton and *Strombidium*/*Strobilidium* abundance.

In summary, the FlowCAM allowed for more rapid sample processing and microplankton and ciliate enumeration. However, the FlowCAM operating with a

peristaltic pump and siphon underestimates ciliate abundances through possible ciliate escape behavior and cell sinkage even with manual sample mixing. Modifications to the FlowCAM sampling procedure would be needed for more accurate ciliate enumeration. The *Strombidium*/*Strobilidium* ciliate group was the most abundant throughout the MANERR samples and most accurately counted by the FlowCAM. This group of ciliates has been shown to provide possible strong grazing pressure on the harmful dinoflagellate *P. piscicida* (Setälä *et al*. 2005), and their high abundance in the MANERR could result strong grazing effects on other organisms of the microplankton. Currently, the only relationship resulting from the multivariate linear regression analyses is a consistent significant negative relationship between *Strombidium*/*Strobilidium* abundance and salinity. Further microplankton community composition (*e.g.* diatom and dinoflagellate taxonomic groups) in comparison with the *Strombidium*/*Strobilidium* group would provide more possible insight into community interactions. An increase in nutrient, chlorophyll, and zooplankton measurements during dynamic periods will also help to make these regression analyses more robust.

Chapter 2: The utility of using imaging and inflow cytometry in observing protozoan grazer populations during harmful algal blooms

ABSTRACT

The increasing occurrence of harmful algal blooms worldwide and their associated economic costs and human health effects, makes it more essential to have early warning monitoring programs in place. Water sample analysis of phytoplankton by microscope can be time consuming and requires a high level of taxonomic expertise, which makes this approach a costly and inefficient early warning system. Advances in phytoplankton identification technology, such as the development of the Imaging FlowCytobot, make frequent continuous sampling and automated classification of taxonomic groups within the plankton possible. This allows for faster identification and earlier warning for the presence of harmful algal bloom species. One factor in harmful algal bloom development may be the disruption of grazer populations, such as ciliates or copepods, resulting in a release from a "top down" control by the grazer. The utility of using the Imaging FlowCytobot in observing and enumerating protozoan grazer populations was investigated. The Imaging FlowCytobot underestimated ciliate and heterotrophic dinoflagellate abundance. These underestimates could have resulted from protozoan damage by the instrument during sampling and the instrument triggering on chlorophyll fluorescence, which most heterotrophic protozoa do not contain. Counts for the ciliate *Myrionecta rubra*, which retains chlorophyll from its food, were accurate which supported the assumption that protozoan grazer underestimates were the result of the absence of chlorophyll fluorescence.

INTRODUCTION

Harmful algal bloom (HAB) events worldwide have been increasing over recent decades (Hallegraeff 1993, Van Dolah 2000). The high economic costs and human health effects that are associated with HABs, have stimulated the development of monitoring programs and instruments to aid in the early warning of these events. Analysis of water samples for the presence of HABs is usually performed via microscope, and the tedious nature, needed taxonomic expertise, and effort involved in analyzing numerous water samples, have made monitoring via microscopy less efficient as an early warning system. Early detection of red tide-causing organisms is especially important because in many cases we do not see symptoms of a bloom until the damage has already occurred. In the case of *Karenia brevis*, a red tide species responsible for fish kills, human respiratory distress, and neurotoxic shellfish poisoning, blooms are not typically noticed until dead fish are observed. This usually happens around 100 cells ml^{-1}; however, shellfish beds must be closed to harvesting at 5 cells ml^{-1} (Steidinger and Garccés 2006). Another red tide organism, *Dinophysis* sp., does not cause fish kills, but it is responsible for diarrhetic shellfish poisoning and the closure of shellfish beds (Hallegraeff 1995). The only way to detect the presence of *Dinophysis* sp. before people become ill is analyzing water samples taken from the areas where shellfish are harvested.

With advances in water monitoring technology and the installation of the Imaging FlowCytobot (IFCB) in the pier laboratory at the University of Texas Marine Science Institute (UTMSI), it is now possible to determine phytoplankton community structure before, during, and after a HAB event. The IFCB has helped to provide an early detection system for potential bloom conditions (Campbell *et al*. 2010) and has also allowed for the discovery of one dinoflagellate not previously seen in the Gulf of Mexico, *Brachydinium* sp., (Henrichs *et al*. 2011). The IFCB is an instrument that combines flow cytometry and

digital imaging to determine abundances and record images of phytoplankton within water samples (Olson and Sosik 2007). Similar to other flow cytometers, IFCB uses sheath fluid, which allows for single cells to pass in focus through the camera field of view (Olson and Sosik 2007). Along with morphological and optical properties of the imaged particles, IFCB also measures chlorophyll fluorescence of each cell, which is also used as the main trigger for image capture (Olson and Sosik 2007). Manually created taxonomic training sets use particle image properties such as shape, texture, orientation, and size to create automated taxonomic classification algorithms to identify microplankton species of interest. Although some human taxonomic expertise is needed to verify the classifications, the automated classification algorithm accuracy ranges from 68% to 99% across the across the different taxonomic categories, greatly reducing sample processing time (Sosik and Olson 2007).

Although the IFCB was developed for phytoplankton analysis, many image files include protozoan grazers (*e.g.* heterotrophic dinoflagellates and ciliates). It has been hypothesized that the disappearance or grazing inhibition of potential protozoan grazers and subsequent release from "top down" controls may allow a HAB species to proliferate and cause a bloom (Turner and Tester 1997). The fine spatial scale of samples analyzed by the IFCB (5 ml every 20 min.), makes it possible to observe changes within the grazer populations over time. During the time of its deployment from September 2007 through March 2012, the IFCB has recorded multiple *Dinophysis* spp. and *K. brevis* bloom events. This study aimed to validate the use of the IFCB in monitoring ciliate populations within the Port Aransas ship channel during bloom and non-bloom years.

MATERIALS AND METHODS

Sample Site

The sampling site is located on the UTMSI research pier in the Port Aransas ship channel. The channel has been modified over the years through dredging and the building of rock jetties to provide a deeper navigation channel as well as to prevent channel migration (Morton and McGowen 1980). The pass, which is the main inlet to the Corpus Christi Bay system and the Mission-Aransas National Estuarine Research Reserve (MANERR), is approximately 19 km^2, 45 feet deep, and has been stabilized with jetties (NOAA 1993, Ward 1997). Fast flowing currents, driven by tidal movement, are present in the channel for approximately half of each month (Freese 1952). This sampling location allows analysis of microplankton in water samples entering the bay system from offshore on incoming tides and exiting the bay system on outgoing tides.

Field Data Collection

The Imaging FlowCytobot (IFCB) recorded data at 20-minute intervals from the pier laboratory (UTMSI, Port Aransas, TX) in the Port Aransas ship channel at the entrance to the Mission-Aransas estuary (operated by Lisa Campbell of Texas A&M University in College Station, TX). IFCB was used to monitor for the presence of HABs and provide a continuous archive of microplankton present in the water throughout the year. IFCB was deployed from the UTMSI pier from September 2007 through March 2012. Water from a depth of approximately 3 m was pumped up to IFCB via a peristaltic pump located at the outflow end of the instrument (Campbell *et al*. 2010). A 5-ml water sample, pre-filtered through a153-µm mesh Nitex screen, was collected in a glass syringe and analyzed every 20 minutes. The sample was injected into a sheath fluid and through a thin glass flow cell where single cells were excited with a red (635 nm) diode laser and

images taken when a predetermined chlorophyll fluorescence threshold was reached (Olson and Sosik 2007). Once this threshold was reached, a xenon flash bulb illuminates the flow cell and an image of the camera field of view (300 μm by 400 μm) was taken. As the image was taken, a concurrently running "blob" analysis algorithm was used to save only those image areas with a cell present (Olson and Sosik 2007). These cell images were later classified into different taxonomic categories.

To determine the detection accuracy of the IFCB for natural populations of ciliates, whole water samples were taken at depth (~1 m from the bottom) with a Van Dorn bottle sampler during at twice monthly intervals from the UTMSI research pier. Sampling at this depth followed the protocols of the Central Data Management Office and the National Oceanic and Atmospheric Administration. Although whole water samples were collected approximately 2 m deeper than samples collected by the IFCB, water stratification was not thought to cause major changes to the water samples between the two depths. Stratification in the Port Aransas ship channel will usually occur in the first 1 m of the water column and during large freshwater inflow events (Dong-Ha Min, pers. comm.). Water samples were contained in 500 ml opaque brown polycarbonate Nalgene bottles while being transported to the laboratory. An aliquot from each sample was preserved in 1% acid Lugol's iodine until microscopic analysis could be performed.

Culture Conditions

Validation of the IFCB's ability to detect heterotrophic protozoa was tested using fed and unfed cultures of the ciliate *Strombidium stylifer* (50-60 μm length; obtained from George McManus, University of Connecticut) and the dinoflagellate *Gyrodinium spirale* (45-50 μm length). *G. spirale* cultures were obtained by isolation from phytoplankton tows in the ship channel using a 20-μm mesh net (Model 9100 Student

Net, Sea-Gear Corporation). *S. stylifer* cultures were maintained in 50 ml tissue culture flasks of 32 psu filtered seawater at 20º C on a 12:12 light:dark cycle. Seawater was collected from the UTMSI pier in the Port Aransas ship channel. Light was provided by cool white fluorescent bulbs (12.4 µmol photons m^{-2} s^{-1}), and flasks were shaded with 500 µm black mesh screening material to prevent overgrowth of food. *S. stylifer* were fed approximately 1 ml aliquots of dense cultures of *Tetraselmis suecica* twice per week. *G. spirale* cultures were maintained in 250 ml polycarbonate bottles of 32 psu filtered seawater at room temperature of approximately 27º C. Cultures were placed in bottle rollers rotating at approximately 2 rpm to keep the grazers and their food suspended. Overhead lighting in the laboratory (6.6 µmol photons m^{-2} s^{-1}) was on for approximately 8 hours per day and cultures were in complete darkness over the weekends. *G. spirale* were fed approximately 15 ml aliquots of dense cultures of *Peridinium foliaceum* once per week.

Peridinium foliaceum cultures were maintained in 1 L polycarbonate bottles of 32 psu F/2 seawater media (Guillard 1975) at 20º C on a 12:12 light:dark cycle. Cultures were transferred and diluted by 75% once a month. *Tetraselmis suecica* cultures were maintained in 250 ml polycarbonate Erlenmeyer flasks in 100-ml volumes of 32 psu F/2 seawater media at 20º C on a 12:12 light:dark cycle. Cultures were transferred and diluted by 50% once a month.

IFCB Validation – Cultures

Dense cultures of food depleted *G. spirale* and *S. stylifer* were transferred to duplicate 50-ml tissue culture flasks. One flask of each of the grazers was kept food depleted. The other flask was inoculated with approximately 250 µg C L^{-1} of *P. foliaceum* (275 cells ml^{-1}) or *T. suecica* (5,724 cells ml^{-1}) for *G. spirale* and *S. stylifer*,

respectively. Cell carbon content was calculated using Strathmann's (1967) equation for non-diatoms: $logC = -0.46 + 0.866(logV)$ where C is the carbon content in pg C cell^{-1} and V is the cell volume in μm^3. Cultures of *P. foliaceum* and *T. suecica* were subsampled and counted as a 30-grid estimate (cells ml^{-1}) on a gridded Sedgewick-Rafter cell (1,000 grids, 1 ml volume). Aliquots of *P. foliaceum* and *T. suecica* cultures were added to experimental tissue culture flasks to a final concentration of 250 μg C L^{-1} based on carbon content per cell and initial culture cell concentration. Tissue culture flasks were left under overhead lighting (6.6 μmol photons m^{-2} s^{-1}) for one hour to allow grazers ample time to feed.

After one hour, 50 ml of each test culture was diluted to a final volume of 100 ml. These dilutions were tested using three different counting techniques – IFCB, FlowCAM (Fluid Imaging Technologies, Inc.), and traditional microscopy. Triplicate samples of each dilution taken from the fed and food depleted grazer cultures were run through the IFCB (5 ml volume each sample) and FlowCAM (~5.4 ml volume each sample). Triplicate samples of each dilution were preserved in 1% acid Lugol's and counted on a compound microscope (Olympus BX60) using a gridded Sedgewick-Rafter counting chamber (1 ml volume). The entire chamber was counted.

The FlowCAM is another instrument that combines flow cytometry with particle imaging to analyze and record images of particles in water samples. Like the IFCB, the FlowCAM uses a laser (532 nm) to excite fluorescence of chlorophyll in particles passing through a thin glass flow cell. Once a predetermined fluorescence threshold is reached, an image of the field of view of the camera is taken and those areas with cells present are cut from the image and recorded (Sieracki *et al*. 1998). Unlike the IFCB and many other flow cytometers, the FlowCAM does not use sheath fluid. Sheath fluid allows for cell-by-cell counting through the center of the field of view and cell images that are a majority in

focus (Olson and Sosik 2007). The FlowCAM produces sample flow through the instrument via a downstream peristaltic pump, sampling ~0.27 ml min^{-1} (~5.4 ml total volume over a period of 20 minutes). A 100 μm deep by 2000 μm wide glass flow cell was used with a 10x objective to analyze all water samples. The cell size threshold was 10-200 μm. The FlowCAM was operated in trigger mode, which allows the user to image based on both fluorescence and light scatter, which may allow for more accurate sampling of heterotrophic protozoa. Trigger mode calculates cell concentrations based on the number of particle images, field of view width, volume of sample analyzed, and width of the flow cell. A calibration factor of 0.5556 was used to determine the field of view, which was 571 μm (29%) of the 2,000 μm total width of flow cell. The final cell concentration of the target grazers was calculated with Visual Spreadsheet™ software where images were classified into user created taxonomic categories.

IFCB classifies images into 30 taxonomic categories based on 131 different image features, including size, shape, and texture (Sosik and Olson 2007, Campbell *et al*. 2010). These classifications built on those described in Sosik and Olson (2007), which used 22 taxonomic categories. Other categories can be added to the list provided that an image training set and script has been made for that taxonomic group or the user manually classifies a new group without an automated script. Training sets consist of at least 200 manually classified images of the target organism. The different features of these known images are used to sort unclassified images. For the purposes of the validation experiment using monocultures of *S. stylifer* and *G. spirale*, classification with scripts for all available taxonomic categories was unnecessary. Images were simply counted and cell concentrations per ml were calculated based on the sample volume passed through IFCB.

IFCB Validation – Whole Water Samples

Ciliates in acid Lugol's-preserved whole water samples collected from July 2008 through October 2009 (n = 16) from the UTMSI pier were counted on a Sedgewick-Rafter slide using a compound microscope (Olympus BX60). The entire Sedgewick-Rafter was counted and taxonomic groups of ciliates were recorded. These counts were compared to 2-hour bins of image files from the IFCB. These bins coincided with the approximate whole water sampling time.

IFCB ciliate classifiers were used to analyze the 2-hour bins of images. Classifiers included those for *Myrionecta rubra*, *Strombidium*/*Strobilidium*, agglutinated tintinnids, hyalinated tintinnids, *Strombidinopsis*, *Tontonia*, *Strombidium pulchram*, *Laboea*, *Hypotrichs*, and "other" ciliates. Images were manually corrected and classified into each of the ciliate categories. Cell concentrations were calculated in cells per ml for each taxonomic group in each sample image file and averaged over the 2-hour period.

Data Analysis

A one-way ANOVA paired with a Holm-Sidak test (SigmaPlot 11.0) was used to compare starved and fed grazer counts among the three different counting techniques. A linear regression model in the R software (Version 2.15.0) was used to compare the microscope counts of ciliates in the whole water samples to the 2-hour bins of images captured by the IFCB. All count data were log transformed before regression analysis. Log transformed counts for *Myrionecta rubra* and *Strombidium/Strobilidium* were further analyzed with an offset linear model to determine whether the slope was significantly different from one. The offset was achieved by plotting the x-variable versus the y- minus x-variable, bringing a slope of one down to a slope of zero. A significant relationship between the IFCB and microscope counts could point to a predictable error in grazer sampling by the IFCB.

RESULTS

IFCB Validation – Cultures

Microscope counts differed significantly from IFCB and FlowCAM counts for all starved and fed treatments of *G. spirale* and *S. stylifer*. Mean cell concentrations for fed *S. stylifer* were 223±9 cells ml^{-1}, 34±9 cells ml^{-1}, and 8±3 cells ml^{-1} for microscope, FlowCAM, and IFCB counting techniques, respectively. Mean cell concentrations for starved *S. stylifer* were 299±18 cells ml^{-1}, 58±13 cells ml^{-1}, and 36±36 cells ml^{-1} for microscope, FlowCAM, and IFCB counting techniques, respectively. FlowCAM counts were significantly lower than microscope counts for fed (Figure 2.1; $p<0.001$) and starved (Figure 2.2; $p<0.001$) *S. stylifer*. IFCB counts were also significantly lower than microscope counts for fed (Figure 2.1; $p<0.001$) and starved (Figure 2.2; $p<0.001$) *S. stylifer*. IFCB counts were significantly lower than FlowCAM counts for fed *S. stylifer* (Figure 2.1; $p<0.01$); however, they did not significantly differ during the starved treatment (Figure 2.2; $p=0.310$). Many of the *S. stylifer* cells that passed through the IFCB were damaged during sampling as can be seen in images of burst cells (Figure 2.3). There were no damaged *S. stylifer* in the FlowCAM samples

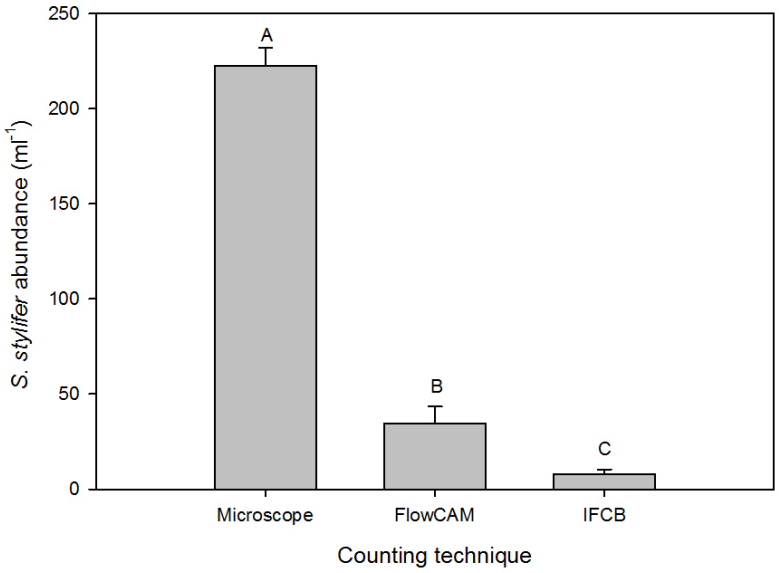

Figure 2.1: Comparison of counting techniques for fed *S. stylifer*. Means of triplicate counts (cells ml^{-1}) are graphed with error bars indicating standard deviations. Letters above graph bars indicate treatments that are significantly different (ANOVA; $p<0.05$).

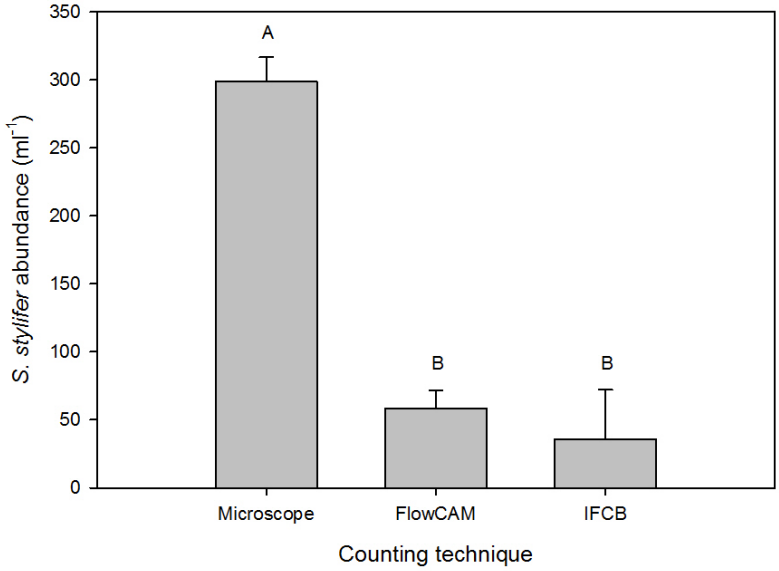

Figure 2.2: Comparison of counting techniques for starved *S. stylifer*. Means of triplicate counts (cells ml^{-1}) are graphed with error bars indicating standard deviations. Letters above graph bars indicate treatments that are significantly different (ANOVA; $p<0.05$).

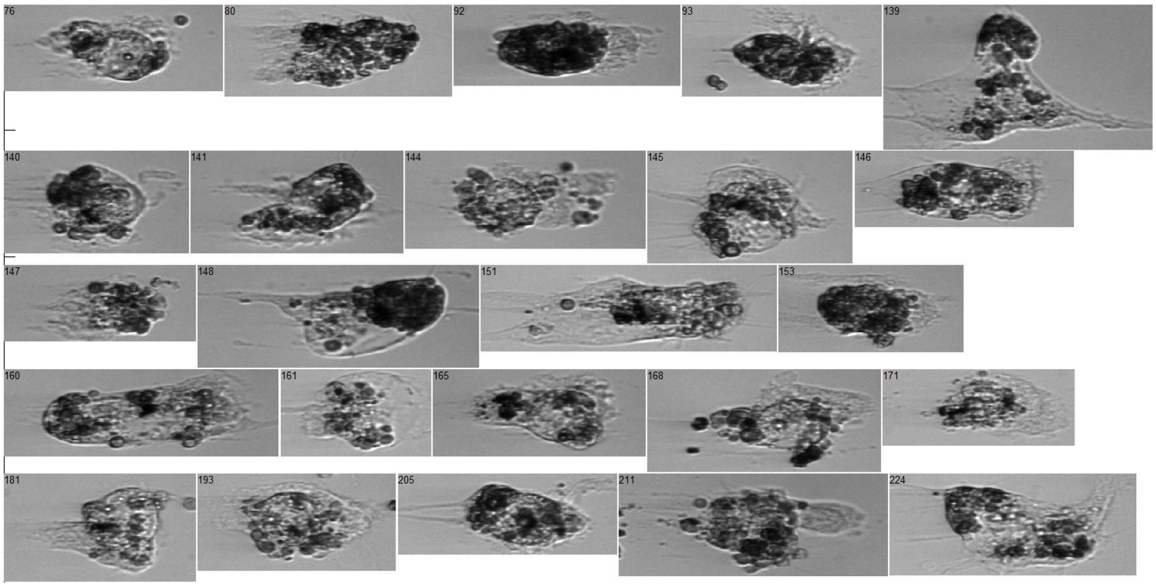

Figure 2.3: Images of burst *S. stylifer* cells taken by the IFCB. Ciliate cell structure can be seen as well as food particles of *T. suecica*.

Mean cell concentrations for fed *G. spirale* were 166±14 cells ml^{-1}, 122±16 cells ml^{-1}, and 20±6 cells ml^{-1} for microscope, FlowCAM, and IFCB counting techniques, respectively. Mean cell concentrations for starved *G. spirale* were 177±11 cells ml^{-1}, 125±13 cells ml^{-1}, and 0±0 cells ml^{-1} for microscope, FlowCAM, and IFCB counting techniques, respectively. FlowCAM counts were significantly lower than microscope counts for fed (Figure 2.4; $p<0.01$) and starved (Figure 2.5; $p<0.001$) *G. spirale*. IFCB counts were also significantly lower than microscope counts for fed (Figure 2.4; $p<0.001$) and starved (Figure 2.5; $p<0.001$) *G. spirale*. IFCB counts were significantly lower than FlowCAM counts for fed (Figure 2.4; $p<0.001$) and starved (Figure 2.5; $p<0.001$) *G. spirale*. For those fed *G. spirale* that were detected by the IFCB, every image showed a food particle within *G. spirale* (Figure 2.6). There were no instances where the *G. spirale* cell was empty.

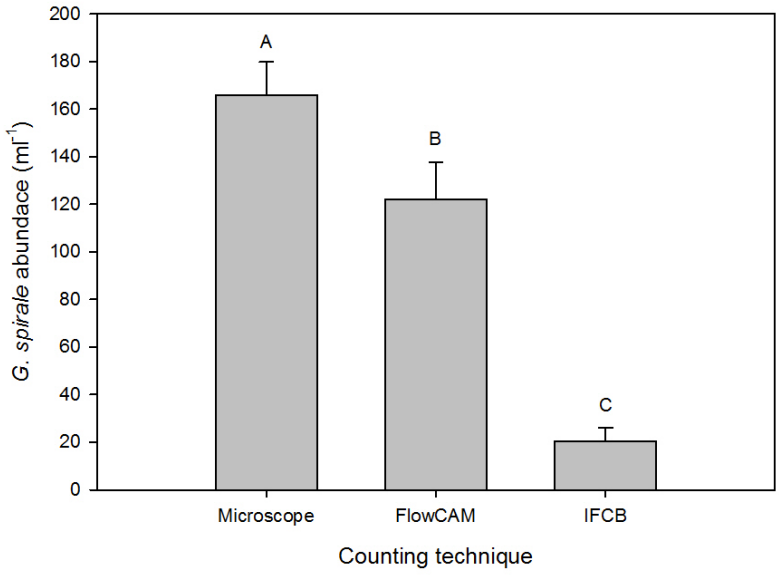

Figure 2.4: Comparison of counting techniques for fed *G. spirale*. Means of triplicate counts (cells ml^{-1}) are graphed with error bars indicating standard deviations. Letters above graph bars indicate treatments that are significantly different (ANOVA; $p<0.05$).

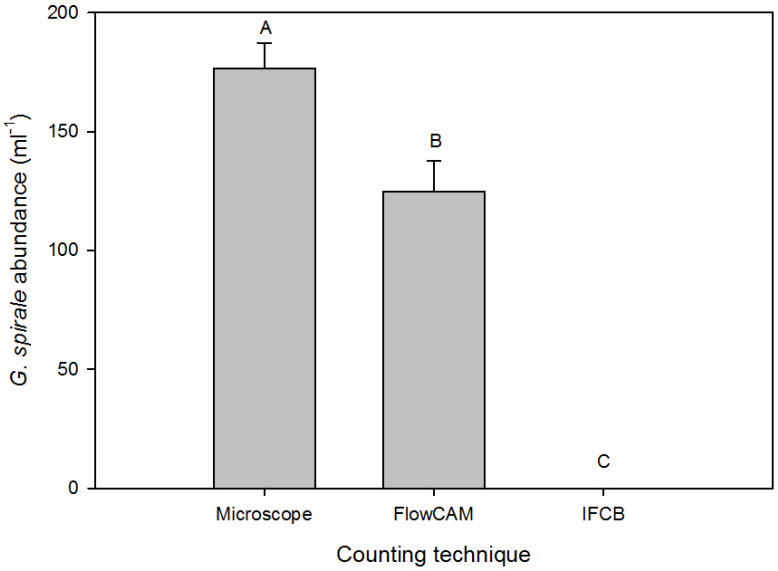

Figure 2.5: Comparison of counting techniques for starved *G. spirale*. Means of triplicate counts (cells ml^{-1}) are graphed with error bars indicating standard deviations. Letters above graph bars indicate treatments that are significantly different (ANOVA; $p<0.05$).

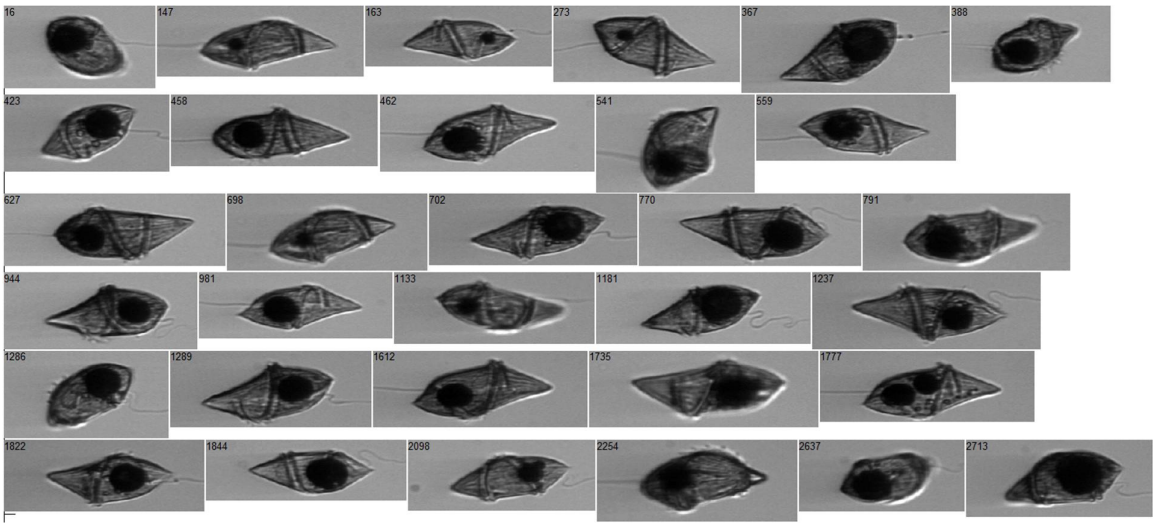

Figure 2.6: Images of fed *G. spirale* taken by the IFCB. Each *G. spirale* cell has a food particle of *P. foliaceum* present inside.

IFCB Validation – Whole Water Samples

Linear regressions of the two methods for ciliate counts showed poor agreement between the microscope and IFCB counts across all ciliate categories except *Myrionecta rubra* (Table 2.1). Only the *M. rubra* and *Strombidium/Strobilidium* regressions were significantly different from a slope of zero, and the *M. rubra* regression was not significantly different from a slope of one (Table 2.1). For all other ciliate categories the linear regressions were not significantly difference from zero, and the R-squared was never higher than 10 percent (Table 2.1). In cases where the ciliate is "rare", the IFCB counts are higher than the microscope counts. For example, hyalinated tintinnids were detected more often in the IFCB counts than by manual microscopy (Figure 2.7; $R^2 = 2.5E^{-5}$). However, for the *Strombidium/Strobilidium*, which are the most consistently abundant in water samples, microscope counts tended to be higher than those from the IFCB (Figure 2.8; $R^2 = 0.20$). *Myrionecta rubra*, which fell closest to a 1:1 ratio between the IFCB and microscope counts, was detected at similar rates on the IFCB than the microscope (Figure 2.9; $R^2 = 0.38$). Finally, for ciliates as a whole the IFCB detected fewer ciliates than microscope counting (Figure 2.10; $R^2 = 0.0031$).

Ciliate Type	*p-value*	R^2
**Myrionecta rubra*	**<0.01**	0.38
# *Myrionecta rubra*	0.32	0.38
Hypotrich	0.69	-0.059
Laboea	0.52	-0.039
Other ciliates	0.28	0.018
Strombidinopsis	0.67	-0.057
Strombidium pulchram	0.42	-0.021
**Strombidium/Strobilidium*	**0.046**	0.20
# *Strombidium/Strobilidium*	**<0.01**	0.20
Tintinnid (agglutinated)	0.82	-0.068
Tintinnid (hyalinated)	0.33	$2.5E^{-5}$
Tontonia	0.97	-0.071
Total ciliates	0.33	0.0031

Table 2.1: Summary of *p-values* and R^2 for the linear model comparing microscope and IFCB counts of ciliates. Bolded values indicate $p<0.05$. * = comparison to slope of zero. # = comparison to slope of one.

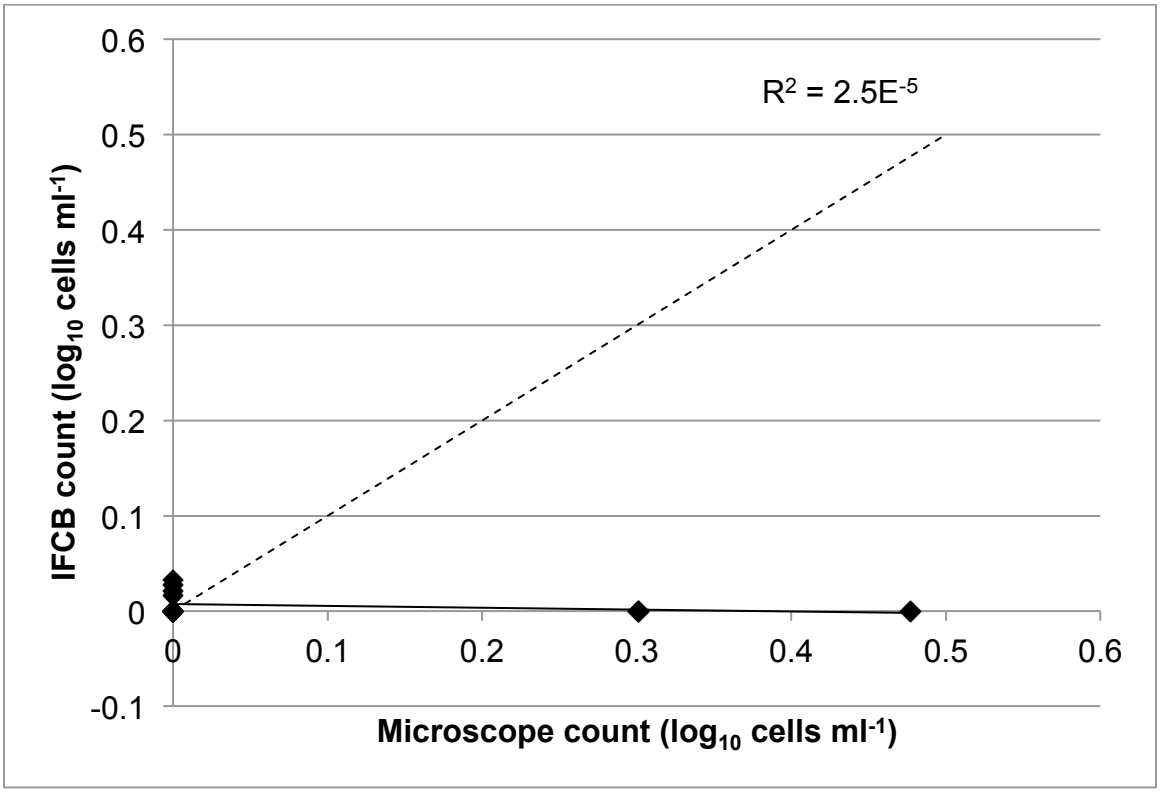

Figure 2.7: Comparison of IFCB and microscope counts of hyalinated tintinnids (log_{10} cells ml^{-1}). Dashed line indicates a 1:1 relationship. Solid line indicates linear regression. The R^2 of the regression is posted on the graph.

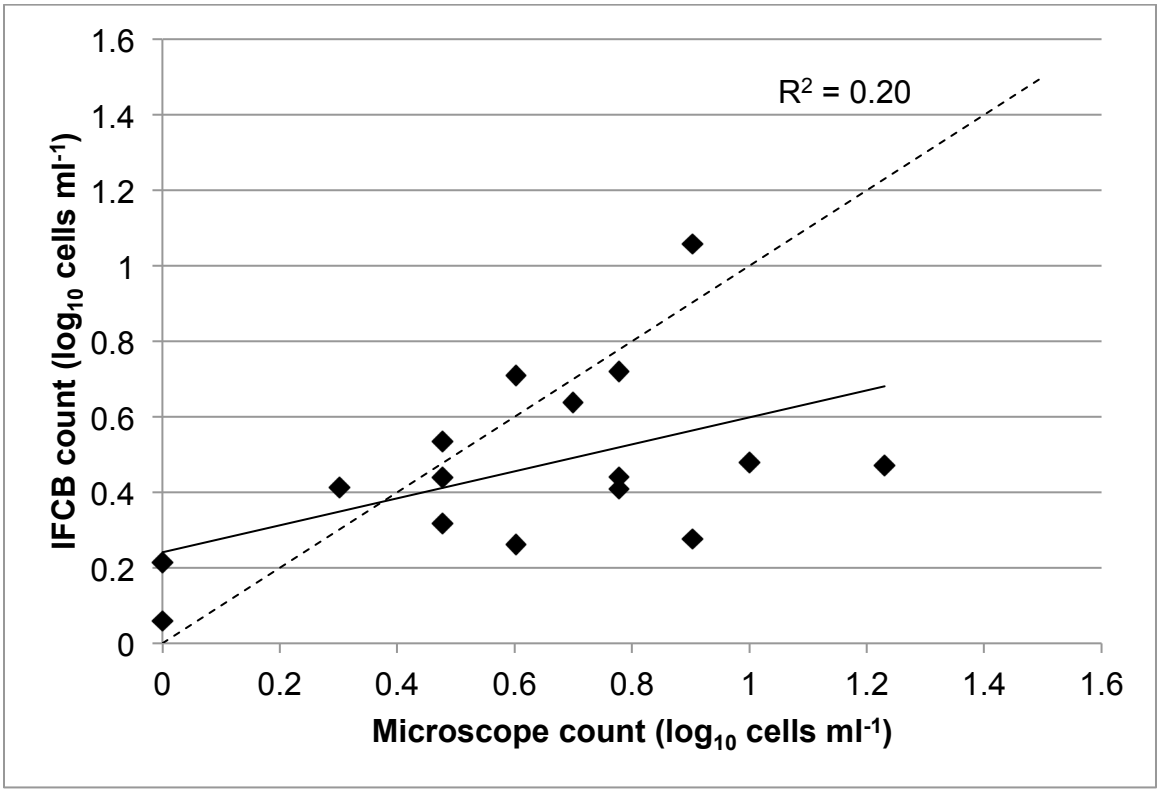

Figure 2.8: Comparison of IFCB and microscope counts of *Strombidium*/*Strobilidium* (log_{10} cells ml^{-1}). Dashed line indicates a 1:1 relationship. Solid line indicates linear regression. The R^2 of the regression is posted on the graph.

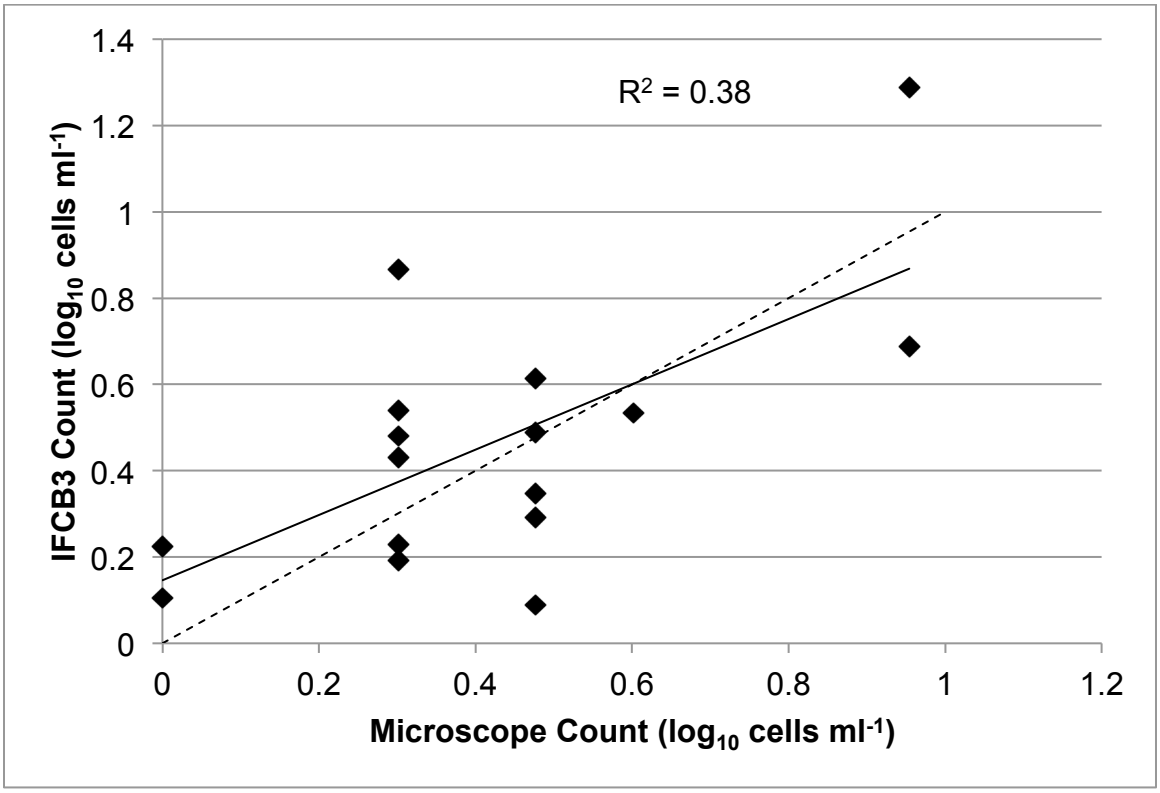

Figure 2.9: Comparison of IFCB and microscope counts of *Myrionecta rubra* (log_{10} cells ml^{-1}). Dashed line indicates a 1:1 relationship. Solid line indicates linear regression. The R^2 of the regression is posted on the graph.

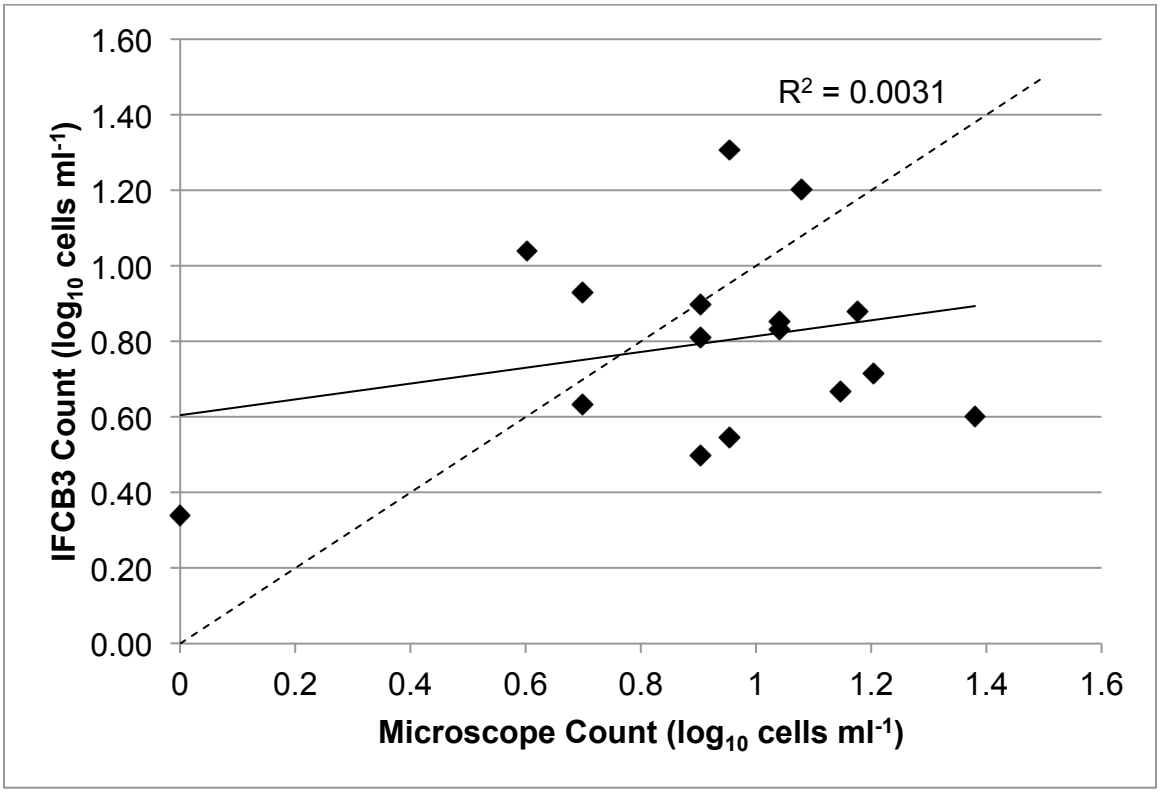

Figure 2.10: Comparison of IFCB and microscope counts of total ciliates (log_{10} cells ml^{-1}). Dashed line indicates a 1:1 relationship. Solid line indicates linear regression. The R^2 of the regression is posted on the graph.

DISCUSSION

The results of these validation experiments indicate that the configuration of the IFCB deployed from 2007-2012 may not suitable for enumerating protozoan grazer populations. The IFCB was developed to observe phytoplankton within the water column and image capture is triggered only on chlorophyll fluorescence. Unless protozoa possess chlorophyll in food vacuoles or sequestered in chloroplasts, they are not imaged (Olson and Sosik 2007). The IFCB images particles ranging from 10 µm to <150 µm in size in a 300 µm by 400 µm field of view. All of the grazers of interest fall within this cell size range and can pass unhindered through the flow cell. The sheath fluid used in the IFCB

ensures that all particles present in the sample pass in focus through the center of the field of view. Microscope and IFCB count comparisons of a range of diatoms and autotrophic dinoflagellates indicate good agreement, especially in those cases where the cells are larger and morphologically distinct; however, as cells decrease in size, IFCB counts increase possibly because smaller cells are harder to distinguish by manual microscopy (Olson and Sosik 2007).

The purpose of this study was to determine if this same instrument could be used as a viable means of enumerating protozoan grazer populations, namely ciliates and heterotrophic dinoflagellates. As indicated by images of fed *G. spirale* and the absence of images of starved *G. spirale*, a particle containing chlorophyll must be present within the grazer to be detected by the IFCB. However, it is surprising that the IFCB detected a higher number of starved *S. stylifer* cells than fed cells. Samples of fed *S. stylifer* were not pre-filtered to exclude the *T. suecica* and could have been too dense for the IFCB to count accurately. The IFCB requires 34-86 ms to process images depending on the size of the imaged cell and cell images could be missed if the cell density of the sample is too high. Dilution experiments revealed that comparison counts of *Dunaliella tertiolecta* and *Ditylum brightwellii* with the IFCB and Coulter EPICS flow cytometer were accurate to concentrations $>10^4$ cells ml^{-1} (Olson and Sosik 2007). Initial concentrations of *T. suecica* in the fed *S. stylifer* treatments were ~5,700 cells ml^{-1} and were diluted by 50 percent before analysis by the IFCB. The maximum *T. suecica* concentration in the analyzed sample would have been ~2,800 cells ml^{-1}. This food concentration combined with the 223 cells ml^{-1} *S. stylifer* calculated from microscope counts would still fall within the cell density limit of $>10^4$ cells ml^{-1} for accurate counts with the IFCB.

When compared to the FlowCAM, IFCB and microscope counts were significantly different except in the case of starved *S. stylifer*. The FlowCAM captures

images of particles ranging in size from 10 µm to 200 µm in a 1023 µm by 767 µm field of view. All of the target grazers fall within this cell size range. The FlowCAM also triggers with a threshold emission of 400 on both chlorophyll fluorescence and light scatter. The Visual Spreadsheet^{TM} software takes into account the percentage of the flow cell imaged and the volume of the sample in calculating final cell concentration. We would expect FlowCAM cell counts to match more closely with microscope counts because it triggers on fluorescence and light scatter allowing for image capture of chlorophyll and non-chlorophyll containing particles. However, the FlowCAM measured grazer concentrations significantly lower than those found by manual microscopy regardless of whether the grazer was fed or starved. One explanation for this mismatch is an underestimate of cells passing outside of the field of view. The FlowCAM does not use sheath fluid so the particles present in the water sample are not constrained to the center of the flow cell. Another explanation is the density of particles in the sample. When running in trigger mode, particle concentration can be underestimated if the original particle density of the sample is too high (Sieracki *et al*. 1998). A second sampling mode on the FlowCAM, auto-image mode, would have been best suited for counting higher density cultures; however, particle fluorescence is not measured in this mode (Sieracki *et al*. 1998, Buskey and Hyatt 2006). Although FlowCAM counts differed from microscope counts, they may provide more accurate grazer counts than the IFCB because FlowCAM counts were consistently higher than those from the IFCB in cultured samples. However, the FlowCAM can highly underestimate those ciliates that exhibit escape responses (e.g. *Myrionecta* sp., *Tontonia* sp.; see Chapter 1).

Cell counts from the sample outflow of the IFCB and FlowCAM to determine how many cells may have been missed in the samples could not be performed. Before reaching the waste container of the FlowCAM, the sample must first pass through the

peristaltic pump, which would damage cells and not allow for accurate counts. Once a sample is analyzed with the IFCB, the sheath is immediately filtered of sample particles, which allows for recycling of sheath fluid and efficient cleaning of the instrument (Olson and Sosik 2007). Thus any outflow from the machine is virtually particle free.

Ciliates are fragile members of the microplanktonic community. Early studies on ciliate preservation and enumeration found that the use of different types of preservation solutions can cause cell losses and cell shrinkage (Choi and Stoecker 1989, Jerome *et al*. 1993, Stoecker *et al*. 1994). The use of 10%-20% acid Lugol's results in higher ciliate counts than the same water samples preserved in 2% buffered formalin; however, higher concentrations of acid Lugol's also results in cell shrinkage, which will cause underestimates of ciliate biomass (Stoecker *et al*. 1994). Buffered formalin causes the least amount of cell shrinkage (Choi and Stoecker 1989); however, cell losses that result from this preservation method will still cause biomass underestimates. Protargol staining is also a preferred preservation method when describing morphological characteristics of ciliates (Lynn and Gilron 1993); however, this method still results in significant cell shrinkage (Jerome *et al*. 1993). Samples analyzed with the FlowCAM and IFCB are live and are not subject to cell shrinkages or losses from preservation; however, the fragility of the ciliates is still observed. As shown in Figure 2.3, *S. stylifer* cells are clearly damaged when analyzed by the IFCB. This damage could occur during sample pre-filtering through the 153-µm Nitex mesh or during sample injection into the sheath fluid and flow cell. This damage will cause underestimates of ciliate abundance in natural water samples because the images will be initially classified as detritus and identification of ciliates this damaged is not possible. There were no damaged *S. stylifer* imaged by the FlowCAM, which could indicate that sample transport through the instrument is not as harmful to ciliates.

Based on the linear regressions in comparing IFCB and microscope counts for ciliates in whole water samples, there is not a predictable error that we can use to extrapolate counts. Although the comparison of *Strombidium/Strobilidium* counts between the IFCB and microscopy did result in a slope that was significantly different than zero, the offset slope was significantly different from one ($p<0.01$, $R^2 = 0.2022$). There was not good agreement between IFCB and microscope *Strombidium/Strobilidium* counts. For the other ciliate categories counted, comparison between the two counting techniques did not result in slopes significantly different from zero or coefficient of determination values higher than 2 percent ($R^2 = -0.071$-0.018). Many of these ciliate categories were "rare" within the water samples, and a comparison of more samples where those ciliates are present would provide a better estimate as to their detection by the IFCB; however, current data would not allow for an accurate extrapolation of ciliate cell concentration from IFCB counts. Heterotrophic protists must be actively feeding in order to be detected by the IFCB. Because of the variability in food abundance, grazer abundance, ingestion and evacuation rates, nutrients, growth rate, and numerous physical water parameters, the number of grazers with ingested particles can differ widely over a short period of time.

The exception to count accuracy appears to be *M. rubra*. This ciliate is hypothesized to sequester an endosymbiont or require the acquisition of nuclei from the chlorophytes it feeds on (Stoecker *et al*. 2009). The IFCB is able to consistently trigger on *M. rubra* cells because of the presence of chlorophyll from either an endosymbiont or sequestered plastids. The linear regression comparing *M. rubra* counts between microscope and IFCB did not significantly differ from a slope of one which would indicate that IFCB counts do not significantly differ from those obtained by traditional

microscopy. This agrees with Campbell *et al*. (2010) who also found good agreement between microscope and IFCB counts of *M. rubra* during a *Dinophysis ovum* bloom.

The IFCB grazer counts are not without merit, however. Although they may not be accurate quantitatively, we are still provided with a record of grazer diversity. In some cases, the resolution is clear enough that we can observe what the grazer has ingested (pers. observ.). A possible future application for these data is determining the portion of the grazer population that is actively feeding. This would require subsequent comparisons with microscope counts as well as ensuring that fragile ciliates are not damaged by the instrument during sampling, but could be valuable time series data in observing food web dynamics over short and long (seasonal) time scales.

Chapter 3: Determining harmful algal bloom species ingestion by a protozoan grazer using epifluorescence and PCR analyses

ABSTRACT

Determining ingestion rate of a harmful algal bloom (HAB) species by potential grazers can provide insight into the role of grazers in harmful algal bloom dynamics. Protozoan grazers may have a potentially higher impact on HAB populations than mesozooplankton grazers because of their faster population growth rates. However, it is unknown to what extent protozoan grazers feed on HABs in nature. The purpose of this study was to test epifluorescent and molecular methods for determining HAB ingestion by protozoan grazers in controlled laboratory grazing experiments, with the goal of testing them under natural bloom conditions. In this study, genus- and species-specific DNA primers for three HAB species – *Karenia brevis*, *Alexandrium monilatum*, and *Gymnodinium catenatum* – were used to determine ingestion of the HAB by the heterotrophic dinoflagellates *Noctiluca scintillans* and *Protoceratium* sp. *K. brevis* primers were also used to analyze heterotrophic dinoflagellates and ciliates collected during a natural *K. brevis* bloom. DNA evidence showed that *Protoceratium* sp. and *N. scintillans* fed on all three HAB species when given sole diets of the HABs or a 50:50 mixture with the control food *Peridinium foliaceum* except in the case of *N. scintillans* fed *A. monilatum*. *K. brevis* DNA was also found in one heterotrophic dinoflagellate and three types of ciliates during the onset of the *K. brevis* bloom. Although the DNA evidence cannot suggest a protozoan grazing control, it did identify protozoan grazers that may be capable of affecting laboratory and natural HAB populations.

INTRODUCTION

Although many studies have focused on mesozooplankton grazing on harmful algal bloom (HAB) species (Calbet *et al*. 2002, Colin and Dam 2002, 2003), protozoan

grazers may be more important in HAB dynamics because of their faster population growth rates that are more comparable to HAB growth rates (Admiraal and Venekamp 1986, Matsuyama *et al*. 1999, Rosetta and McManus 2003). Thus a more specific measurement to determine protozoan feeding on HABs is desirable. The use of epifluorescence microscopy will show whether a photosynthetic cell has been ingested (Pitta *et al*. 2001) and determining the contents of food vacuoles is possible in laboratory studies if the food source is controlled (Bernard and Rassoulzadegan 1990).

Most research on the presence of HAB organisms and associated toxins in grazer gut contents and tissues has employed the use of high performance liquid chromatography (HPLC). HPLC has been used to identify the presence of different photopigments (Millie *et al*. 1993, Mackey *et al*. 1996, Paerl *et al*. 2003) as well as toxin concentrations (Pierce *et al*. 1985, Sullivan *et al*. 1985, Sullivan and Wekell 1987, Robineau *et al*. 1991) within whole water samples and various shellfish, fish, and crustacean guts and tissues. HPLC has also been used to determine copepod and other mesozooplankton grazing behaviors in laboratory and natural settings (Head and Harris 1994, Sellner *et al*. 1994, Buffan-Dubau *et al*. 1996). Echinenone, a pigment specific to cyanobacteria, was used to determine grazing by the cladoceran *Bosmina longispina maritime* on blooms of cyanobacteria (Sellner *et al*. 1994). Chlorin and carotenoid pigments were used to determine grazing by planktonic and harpacticoid copepods on diatoms, green microalgae, cyanobacteria, and purple bacteria (Head and Harris 1994, Buffan-Dubau *et al*. 1996). While HPLC provides a quick analysis that can be performed for large volume water samples, in very few cases are the photopigments species specific (Paerl *et al*. 2003); there are particular photopigments that are associated with dinoflagellates as a group, but do not necessarily indicate the presence of a toxic species. In many cases, the digestive enzymes of grazers can break down certain photopigments,

causing further errors in HPLC pigment analyses (Paerl *et al*. 2003). In the case of toxin analysis through the use of HPLC, many modifications, including pH levels and protein removal from tissue extracts, need to be taken into consideration in order to produce clear toxin peaks (Sullivan *et al*. 1985).

In contrast, DNA and other molecular analyses may provide more specific organism information without pooling samples. Fluorescence labeling using monoclonal antibodies has been used to determine differential feeding of the copepod *Acartia clausi* on toxic and non-toxic strains of the dinoflagellate *Alexandrium minutum* (Barreiro *et al*. 2006). Fluorescent-antibody-labeled bacteria have also been used successfully to determine the level of bacterivory imposed by heterotrophic nanoflagellates (Christoffersen *et al*. 1997). However, use of this antibody technique may not always be efficient or cost effective because cross-reactivity in closely related congeners can create false positives (Ohman 1992) and the development of the antibodies can be costly and time consuming (Symondson 2002).

Polymerase chain reaction (PCR) on a single microalgal cell or cyst can amplify enough DNA to create a visible band on an electrophoresis gel (Patil *et al*. 2005). Quantitative PCR techniques have been developed to study copepod feeding on *Phaeocystis globosa* blooms (Nejstgaard *et al*. 2008); however, DNA can be rapidly degraded by zooplankton during ingestion (Troedsson *et al*. 2009) so assay developments are still ongoing. The development of a species-specific genetic primer for a HAB species of interest would provide stronger evidence of a HAB species being consumed by a potential protozoan grazer. Although molecular analysis could not be used for large volume samples, it would be a very useful tool during grazing experiments to determine whether a protozoan is grazing on a HAB species. If a strong signal is produced during controlled grazing experiments, this assay may be useful for determining grazers of HAB

species in natural assemblages. The analyses performed on those grazers collected during a natural bloom will provide insight on natural grazing behaviors rather than laboratory manipulated food supplies – grazers originally thought to avoid grazing on certain HAB species may actually graze on them during natural bloom conditions.

The purposes of this study were 1) to determine whether epifluorescence microscopy and PCR with genus- or species-specific HAB DNA primers were suitable for determining if a protozoan grazer has ingested a HAB in a laboratory and natural bloom setting by using and 2) to identify grazers capable of feeding on HAB species in laboratory and natural bloom settings. Feeding by two protozoans – *Noctiluca scintillans* and *Protoceratium* sp. – on three HAB species – *Karenia brevis*, *Alexandrium monilatum*, and *Gymnodinium catenatum* – was investigated. All of these microplankton are found in the Gulf of Mexico. *K. brevis*, a red tide dinoflagellate, creates brevetoxins causing neurotoxic shellfish poisoning (NSP; Hallegraeff 1995). This toxin causes massive fish kills as well as respiratory distress in humans (Hallegraeff 1995). A red tide of *K. brevis* from October 2011 through January 2012 also provided field samples of protozoan grazers on which to test the *K. brevis* specific primers. The *Alexandrium* genus contains dinoflagellates that produce the toxin causing paralytic shellfish poisoning (PSP). This toxin also causes high fish mortality and can cause human fatalities in extreme cases (Hallegraeff 1995). However, the local species on the Texas coast, *A. monilatum*, is a chain-forming variety of the *Alexandrium* genus that produces goniodomin A instead of saxitoxin (Hsia *et al*. 2006) and has been linked to fish (Connell and Cross 1950, Howell 1953, Gates and Wilson 1960) and gastropod deaths (Harding *et al*. 2009, May *et al*. 2010). *G. catenatum* is an unarmored, autotrophic dinoflagellate that usually forms chains. Most commonly found on the Pacific coasts of California and Mexico (Taylor *et al*. 1995), *G. catenatum* was recently isolated and cultured from the

Port Aransas ship channel. This is the only known unarmored dinoflagellate to produce PSP (Taylor *et al*. 1995). *N. scintillans* was chosen as a grazer because it feeds on a wide variety of microalgal organisms (Buskey 1995) and is found in coastal waters during the same time period as potential bloom events (see below). *Protoceratium* sp. was also chosen as a grazer because it was isolated from the Port Aransas ship channel in the late summer (Cammie Hyatt, pers. com.) when *K. brevis* blooms are known to occur (Stumpf *et al*. 2003), and preliminary grazing experiments showed that *Protoceratium* sp. cultures could survive when given *K. brevis* as a food source.

MATERIALS AND METHODS

Culture Conditions

A. monilatum (48 µm single cell, 1-5 cell chains; CCMP3105) and *K. brevis* (27-30 µm; CCMP2281) were cultured at 20º C on a 12:12 light:dark cycle in L1 media (Guillard and Hargraves 1993). *G. catenatum* (30-42 µm single cell, 1-5 cell chains) was maintained in F/2 media (Guillard 1975) at 20º C on a 12:12 light:dark cycle. The *G. catenatum* culture was established from a 2-cell chain isolated from a 20-µm mesh net tow (Model 9100 Student Net, Sea-Gear Corporation) taken in the Port Aransas ship channel. Although *A. monilatum* and *G. catenatum* are chain-forming dinoflagellates, cultures contained a majority of single cells plus chains 2-5 cells in length. *K. brevis* cultures were maintained in 500 ml polycarbonate Erlenmeyer flasks while *A. monilatum* and *G. catenatum* cultures were maintained in 50 ml tissue culture flasks. Culture volumes for *A. monilatum* and *G. catenatum* were gradually increased to 500 ml in polycarbonate Erlenmeyer flasks when the two species needed to be cultured in greater numbers for grazing experiments. The control food cultures of *Peridinium foliaceum* were maintained in 1 L polycarbonate bottles of F/2 media at 20º C on a 12:12 light:dark

cycle. Light for all cultures was provided by cool white fluorescent bulbs (12.4 µmol photons m^{-2} s^{-1}). Seawater for all cultures was collected from the UTMSI pier in the Port Aransas ship channel. All HAB and control food cultures were diluted by 50% once per month to prevent culture overcrowding and nutrient depletion.

Protoceratium sp. (35 µm; identification verified by Karen Steidinger, Fish and Wildlife Research Institute) cultures were established from cells isolated from plankton tows using a 20-µm mesh net in the Port Aransas ship channel. These cultures were maintained at 27º C in 50 ml tissue culture flasks of filtered seawater (salinity = 32 psu). To keep grazers and food in suspension, culture flasks were placed atop bottle rollers in sections of PVC pipe rotating at approximately 2 rpm. These rollers were placed under overhead laboratory lighting (6.6 µmol photons m^{-2} s^{-1}) on an 8:16 light:dark cycle during the week and kept in complete darkness over the weekends. Once per week, *Protoceratium* sp. were fed 5 ml aliquots of dense cultures of *P. foliaceum*. *Noctiluca scintillans* (500-1,000 µm) cultures were established from cells isolated from plankton tows using a 20-µm mesh net in the Port Aransas ship channel. These cultures were maintained at 20º C in 1 L polycarbonate bottles in filtered seawater (salinity = 32 psu) on a 12:12 light:dark cycle. Light was provided by cool white fluorescent bulbs (12.4 µmol photons m^{-2} s^{-1}). Once per week, *N. scintillans* cultures were fed approximately 10-20 ml aliquots of dense cultures of *P. foliaceum*. *Protoceratium* sp. and *N. scintillans* cultures were diluted by 50% once per week or month, respectively, to prevent culture overcrowding.

Primer Design and Testing

Genus-specific 5.8S rDNA primers (135 bp amplified length) for *Alexandrium* spp. were taken from Galluzzi *et al*. (2005). This primer set should be sufficient in

determining the ingestion of *A. monilatum* in laboratory experiments and natural assemblages, as other species of *Alexandrium* do not regularly appear locally. Species-specific large subunit (LSU) rDNA primers (237 bp amplified length) for *G. catenatum* were taken from Patil *et al.* (2005). *K. brevis* primers (99 bp amplified length) were developed by comparing LSU rDNA sequences of *K. brevis* (DQ847431) and *K. mikimotoi* (EF469238) in Genbank. *K. brevis* primers were tested on genomic DNA extracted from *K. brevis* and *K. mikimotoi* cultures because the LSU rDNA sequences were very similar to each other. In order to prevent cross-reaction of the *K. brevis* primer with the congener *K. mikimotoi*, a higher annealing temperature of 63 ^{o}C was used.

To test the primers for efficiency and specificity genomic DNA for all three HAB species was obtained by extraction using a DNeasy blood and tissue kit (QIAGEN). A 1.5 ml aliquot of dense cultures of *K. brevis*, *A. monilatum*, and *G. catenatum* were placed in separate microcentrifuge tubes. Tubes were centrifuged for 30 sec at 6000X g (Eppendorf 5414R). The supernatant was removed and DNA from the resulting pellet was extracted using the DNeasy tissue protocol. Genomic DNA also served as positive controls during PCR analysis of grazers isolated from the grazing experiments. Primers were also tested on individual algal cells. A small aliquot from dense cultures of each of the HAB species was preserved with 1% acid Lugol's. Single cells were removed via mouth pipetting with a pulled glass capillary tube and surgical silicon tubing. Each cell was washed three times in 1X PCR buffer and placed in individual PCR tubes with 17 µl 1X PCR buffer. Cells were frozen at -4 ^{o}C until PCR analysis and gel electrophoresis described below.

PCR Time Series

A time series PCR was performed to determine how long after ingestion viable HAB DNA could still be detected. A 50 ml tissue culture flask was filled with filtered

seawater (salinity = 32 psu) and ~100 *N. scintillans* that had been starved overnight (~15 hours). *K. brevis* at a concentration of 250 µg C L^{-1} (290 cells ml^{-1}) was added to the tissue culture flask. Previous studies have shown that positive growth rates for *N. scintillans* and *Protoceratium* sp. occur at food concentrations up to 1 mg C L^{-1} on various phytoplankton diets (Buskey 1995, McDonnell 1998). Cell carbon content was calculated using Strathmann's (1967) equation for non-diatom cells: $logC = -0.46 + 0.866(logV)$, where *C* is the carbon content per cell in pg and *V* is the cell volume in μm^3. Culture density of *K. brevis* was calculated using a 30-grid estimate on a gridded Sedgewick-Rafter counting chamber (1 ml volume) and an aliquot of the culture was added to the tissue culture flask to a final concentration of 250 µg C L^{-1}. The tissue culture flask was placed on a bench top under overhead laboratory lighting (6.6 µmol photons m^{-2} s^{-1}) for 1 hour to allow *N. scintillans* ample time to feed. *N. scintillans* cells with visible food vacuoles after one hour were removed with a pipette and placed in cell wells containing filtered sea water (salinity = 32 psu). Every hour, 3 *N. scintillans* cells were removed from the cell wells, washed 3 times in 1X PCR buffer and placed in individual PCR tubes with 17 µl 1X PCR buffer. Cell removal continued every hour for 8 hours for a total of 24 cells (3 replicate cells for each hour). Cells were frozen at -4 ^{o}C until PCR analysis and gel electrophoresis described below.

Grazing Experimental Protocol

N. scintillans and *Protoceratium* sp. were starved overnight prior to experiment initiation. For the *N. scintillans* experiments, 20 grazers were placed in 50 ml tissue culture flasks with filtered seawater (salinity = 32 psu). Individual *N. scintillans* were isolated from culture with a pipette and added to each flask to a total density of 20 cells per flask. For the *Protoceratium* sp. experiments, 30 grazers were added to each of 6 cell

wells with filtered seawater (salinity = 32 psu). Individual *Protoceratium* sp. were isolated from culture by mouth pipetting with a pulled glass capillary tube and surgical silicon tubing and added to each well to a total density of 30 grazers. Grazing experiments consisted of two food treatments. One treatment included 250 µg C L^{-1} food source of solely the HAB species (*K. brevis* = 290 cells ml^{-1}, *A. monilatum* = 53 cells ml^{-1}, *G. catenatum* = 115 cells ml^{-1}). The other treatment consisted of 50:50 mixtures of the HAB species and control food (*P. foliaceum*) at a 250 µg C L^{-1} total concentration (*K. brevis* = 145 cells ml^{-1}, *A. monilatum* = 27 cells ml^{-1}, *G. catenatum* = 58 cells ml^{-1}, *P. foliaceum* = 138 cells ml^{-1}). Food and carbon concentrations were calculated and added as above. Flasks and cell wells were kept at 20º C illuminated by cool white fluorescent bulbs (12.4 µmol photons m^{-2} s^{-1}) for 1 hour (*N. scintillans*) to 8 hours (*Protoceratium* sp.). The longer feeding time was needed for *Protoceratium* sp. because few cells had food vacuoles after 1 hour.

Ingestion Observation – Direct Epifluorescence Microscopy

After 1 hour, individual *N. scintillans* cells were removed from the treatment flasks and placed in droplets of filtered seawater (salinity = 32 psu) on glass ring slides. *N. scintillans* were kept alive for the following epifluorescence analysis. Their slow swimming motion made analysis less difficult and there was not the risk of damaging the cell with formalin preservation. After 8 hours, the entire cell well contents for the *Protoceratium* sp. experiments were transferred to glass scintillation vials and preserved with 1% buffered formalin. Vials were refrigerated overnight until epifluorescence analysis the following day. A pipette was used to transfer small volumes from the *Protoceratium* sp. grazing vials to glass ring slides. *N. scintillans* and *Protoceratium* sp. were observed for epifluorescence with a compound microscope (Olympus BX60) under

blue excitation. Positive (+) epifluorescence in the form of red emission indicated the presence of chlorophyll inside the grazer. Negative (-) epifluorescence in the form of green emission indicated the absence of chlorophyll inside the grazer. Each cell was noted for the presence or absence of prey items by epifluorescence microscopy and, if possible, visual identification of the food vacuoles. The transparent nature of *N. scintillans* and *Protoceratium* sp. made it possible to visually identify some of the food vacuole contents. Each cell was washed three times with 1X PCR buffer and placed in individual PCR tubes for later DNA analysis.

DNA Analysis

Isolated and washed cells from the epifluorescence observations were analyzed through PCR with primers specific to the HAB offered as food. Cells were broken by vortexing with inert zirconia/silicon beads. PCR mixtures contained one cell in 17 µl of 1X PCR buffer, 0.47 µM of each primer, 0.2 mM dNTPs, 10X buffer, and 1 unit of taq polymerase (Takara) to a total volume of 25 µl. Thermal cycling conditions were: 94 ^{o}C for 5 min then 40 cycles (94 ^{o}C for 45 sec, 63 ^{o}C for 45 sec, 72 ^{o}C for 1 min) then 72 ^{o}C for 7 min (Eppendorf AG Mastercycler epGradient). The 63 ^{o}C annealing step above was used for *K. brevis* and changed to 61 ^{o}C and 52 ^{o}C for *G. catenatum* and *A. monilatum*, respectively. Five µl of each PCR product were loaded onto a 1% agarose electrophoresis gel with blue/orange loading dye (Promega) with added gel red (Biotium). Positive (extracted target HAB species genomic DNA) and negative controls (all PCR reagents minus template DNA) along with a 50 bp DNA standard (Fermentas GeneRuler^{TM}) were included in each gel. Gels were run for 2 hours at 50 volts. Amplified bands were visualized with UV light and photographs taken with an ethidium bromide filtered camera (Fotodyne, Inc.)

Field Testing

From November 2009 through January 2012 zooplankton were collected in the Port Aransas ship channel using a 153 µm, 20 cm diameter mesh bongo net (Research Nets). The net was deployed just below the surface and allowed to stream for 2 minutes. The net was rinsed with additional seawater and the samples preserved with 5% buffered formalin. Upon return to the lab, the sample was concentrated to 100 ml (or 200 ml if sample was dense), stirred to ensure it was well-mixed, and a 1 or 2 ml aliquot was taken using a Hensen Stempel pipet (Wildlife Supply Company). The samples were then enumerated to broad taxonomic categories using a Wild dissecting microscope. Subsamples analyzed for the presence of *N. scintillans* were stained overnight in 0.2% Evans Blue because preservation with formalin caused the cells to wrinkle making them harder to identify.

From October 2011 through January 2012, a bloom of *K. brevis* occurred along the Texas coast. Twice weekly near bottom (~1.5 m from bottom) and surface samples were taken using a Van Dorn bottle sampler in the Port Aransas ship channel. A 50 ml subsample was preserved with 1% acid Lugol's and *K. brevis* and protozoan grazers were enumerated within a Sedgewick-Rafter counting chamber (1 ml volume) using a compound microscope (Olympus BX60). Near bottom subsamples with higher numbers of protozoan grazers at the onset of the bloom (October 2011) were preserved with 1% Lugol's and refrigerated for later PCR analysis. Heterotrophic dinoflagellates and ciliates that were large enough to ingest *K. brevis* (>30 µm oral diameter) were isolated by mouth pipetting (n=24), washed, and analyzed by PCR and gel electrophoresis as described above.

RESULTS

Primer Testing and Time Series

Primer tests resulted in the appropriate fragment bands for individual cells and extracted DNA from cultures of *K. brevis* (99 bp; Figure 3.1A), *A. monilatum* (135 bp; Figure 3.1B), and *G. catenatum* (237 bp; Figure 3.1C). Viable DNA can be analyzed from 1% acid Lugol's preserved single cells provided that the cells are washed correctly. All of the *N. scintillans* cells had visible food vacuoles throughout the 8 hr. experiment after feeding on *K. brevis*; however, amplified bands on the gel became fainter in hours 7 and 8 (Figure 3.2). It is possible to amplify viable *K. brevis* DNA for up to 8 hours after ingestion for *N. scintillans*.

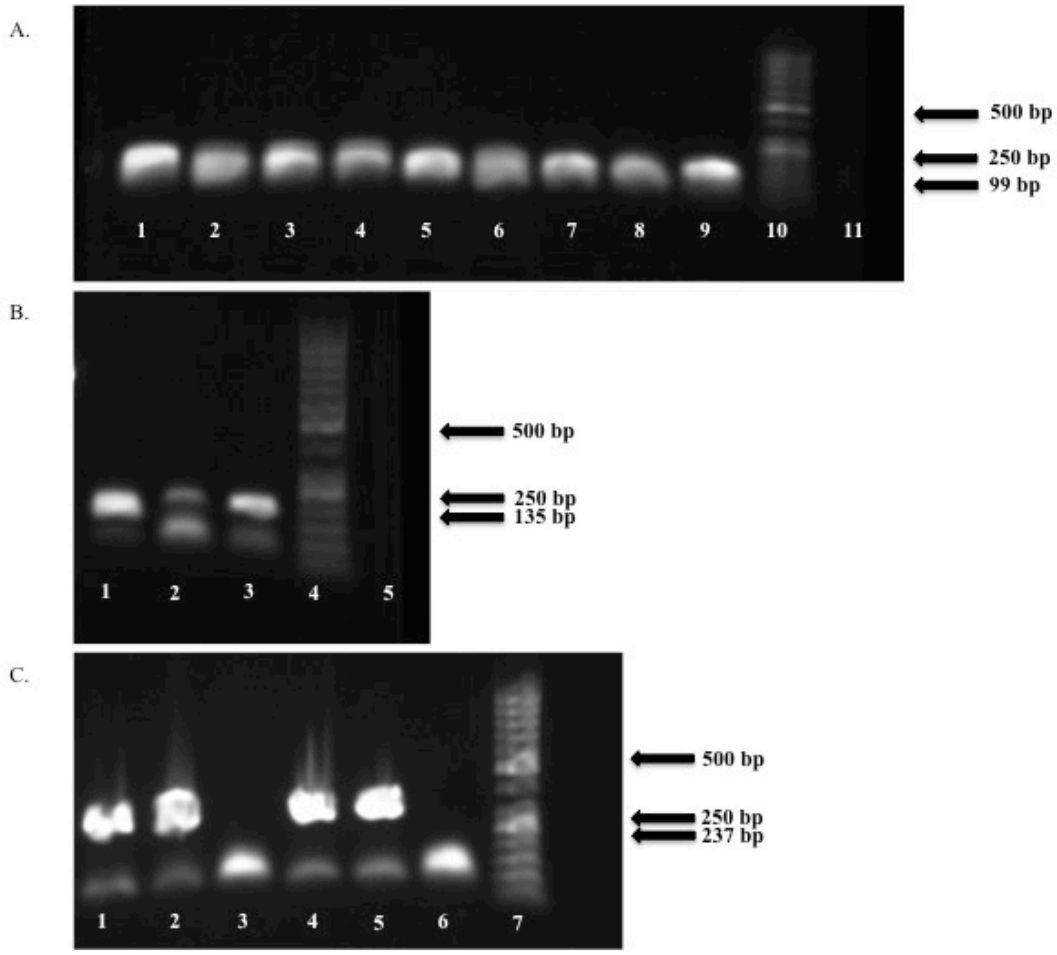

Figure 3.1: Representative gels from primer testing on single cells of *K. brevis* (A), *A. monilatum* (B), and *G. catenatum* (C). A: Lanes 1-8 = *K. brevis* single cells; Lane 9 = *K. brevis* positive control; Lane 10 = DNA ladder; Lane 11 = negative control. B: Lanes 1-2 = *A. monilatum* single cells; Lane 3 = *A. monilatum* positive control; Lane 4 = DNA ladder; Lane 5 = negative control. C: Lanes 1-4 = *G. catenatum* single cells; Lane 5 = *G. catenatum* positive control; Lane 6 = negative control (band resulted from primer dimer); Lane 7 = DNA ladder.

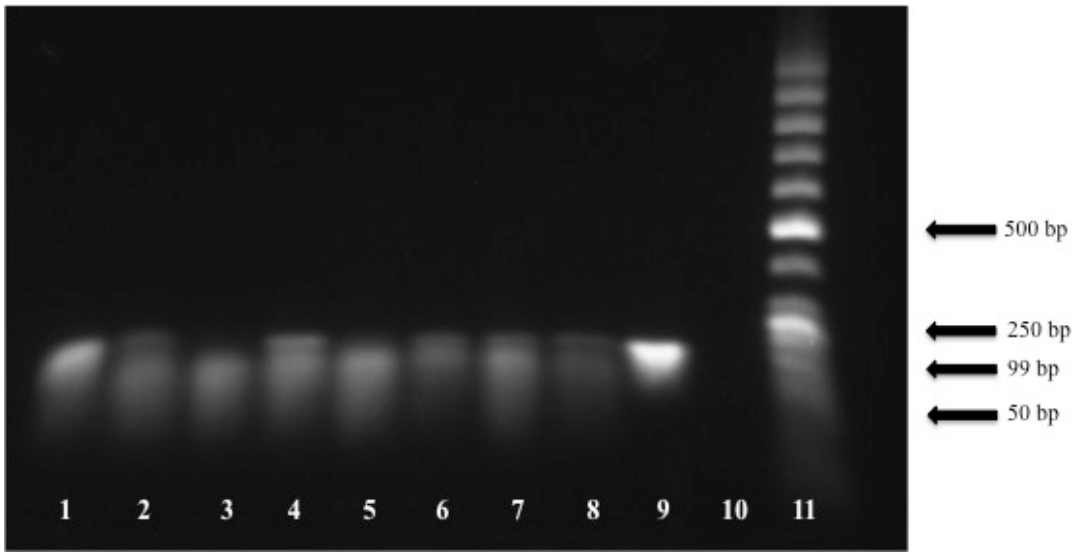

Figure 3.2: Representative gel of the *K. brevis* DNA time series test after ingestion by *N. scintillans*. Lanes 1-8 = Hours 1-8 after ingestion; Lane 9 = *K. brevis* positive control; Lane 10 = negative control; Lane 11 = DNA ladder.

Laboratory Grazing Experiments

N. scintillans fed on *K. brevis* and *G. catenatum* but not on *A. monilatum*. *N. scintillans* fed on *K. brevis* when given as a sole diet and a 50:50 food mixture with *P. foliaceum* (Table 3.1, Figure 3.3A). There were some instances when positive epifluorescence did not result in a positive DNA fragment when *N. scintillans* was fed a sole diet of *K. brevis*. *N. scintillans* was also positive for *K. brevis* DNA in the absence of epifluorescence when fed a sole diet of *K. brevis* or a 50:50 food mixture with *P. foliaceum*. *N. scintillans* also fed on *G. catenatum* when given as a sole diet and a 50:50 food mixture of *P. foliaceum* (Table 3.1, Figure 3.3B). As with analyses of the *K. brevis* diets, positive DNA fragments of *G. catenatum* were obtained from some *N. scintillans* without epifluorescence when fed sole diets of *G. catenatum* and a 50:50 mixture with *P. foliaceum*. There was also an absence of *G. catenatum* DNA fragments in some cells with positive epifluorescence when *N. scintillans* was fed the two different diets of *G.*

catenatum. *N. scintillans* would not feed on sole diets of *A. monilatum* or a 50:50 mixture with *P. foliaceum*. Many *N. scintillans* cells were shriveled and no food vacuoles were formed within 8 hours of the food treatments.

100% *Karenia brevis*			
	Epifluorescence	**DNA (+)**	**% Positive DNA**
Red-Orange (+)	24	16	67
Yellow-Green (-)	16	4	25
50:50 *Karenia brevis:Peridinium foliaceum*			
	Epifluorescence	**DNA (+)**	**% Positive DNA**
Red-Orange (+)	5	5	100
Yellow-Green (-)	3	3	100
100% *Gymnodinium catenatum*			
	Epifluorescence	**DNA (+)**	**% Positive DNA**
Red-Orange (+)	8	7	87.5
Yellow-Green (-)	11	5	45
50:50 *Gymnodinium catenatum:Peridinium foliaceum*			
	Epifluorescence	**DNA (+)**	**% Positive DNA**
Red-Orange (+)	5	2	40
Yellow-Green (-)	2	2	100

Table 3.1: Comparison of epifluorescence and PCR results for *N. scintillans* fed a sole diet of *K. brevis* or *G. catenatum* and 50:50 mixtures with *P. foliaceum*. "Epifluorescence" column contains the number of cells that were negative or positive for epifluorescence. "DNA (+)" column contains the number of cells from each epifluorescence row that tested positive for *K. brevis* or *G. catenatum* DNA. "% Positive DNA" column contains the percentage of cells in each epifluorescence group that tested positive for *K. brevis* or *G. catenatum* DNA.

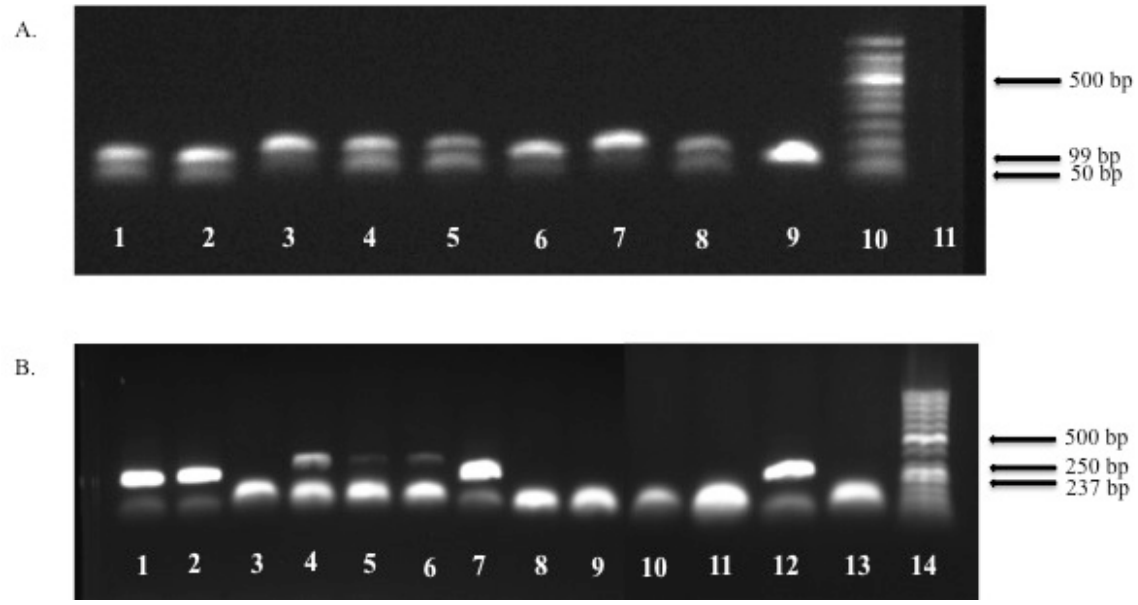

Figure 3.3: Representative gels from *N. scintillans* grazing on *K. brevis* (A) and *G. catenatum* (B). A: Lanes 1-8 = *N. scintillans* tested for *K. brevis* DNA; Lane 9 = *K. brevis* positive control; Lane 10 = DNA ladder; Lane 11 = negative control. B: Lanes 1-11 = *N. scintillans* tested for *G. catenatum* DNA; Lane 12 = *G. catenatum* positive control; Lane 13 = negative control; Lane 14 = DNA ladder.

Protoceratium sp. fed on *K. brevis*, *G. catenatum*, and *A. monilatum* when given as a sole diet or a 50:50 mixture with *P. foliaceum*; however, these results were based on visual examination of food vacuoles (size, color, shape) in *Protoceratium* sp. Positive DNA results were not obtained for any grazing experiments regardless of cell epifluorescence results. *Protoceratium* sp. fed on *K. brevis* when given as a sole diet and a 50:50 food mixture with *P. foliaceum* (Table 3.2; Figure 3.4A). There were some instances when positive epifluorescence did not result in a positive visual identification of *K. brevis* when *Protoceratium* sp. was fed a 50:50 mixture of *K. brevis* and *P. foliaceum*. *Protoceratium* sp. did not have visible food vacuoles when epifluorescence was not present during the *K. brevis* grazing experiments. *Protoceratium* sp. also fed on *G.*

catenatum when given as a sole diet, but none of the *Protoceratium* sp. cells had *G. catenatum* cells present in food vacuoles when fed a 50:50 food mixture with *P. foliaceum* even though there was epifluorescence (Table 3.2; Figure 3.4B). There were no food vacuoles present when epifluorescence was negative during the *G. catenatum* grazing experiments. *G. catenatum* was only found in *Protoceratium* sp. food vacuoles when given as the sole food diet. *Protoceratium* sp. fed on *A. monilatum* when given as a sole diet and as a 50:50 food mixture with *P. foliaceum* (Table 3.2, Figure 3.4C). There was no *A. monilatum* found in *Protoceratium* sp. food vacuoles without epifluorescence. One of the *Protoceratium* sp. positive for epifluorescence when given a 50:50 food mixture with *P. foliaceum* did not contain *A. monilatum* in the food vacuole.

100% *Karenia brevis*			
	Epifluorescence	**HAB (+)**	**% HAB (+)**
Red-Orange (+)	3	3	100
Yellow-Green (-)	5	0	0
50:50 *Karenia brevis:Peridinium foliaceum*			
	Epifluorescence	**HAB (+)**	**% HAB (+)**
Red-Orange (+)	5	2	40
Yellow-Green (-)	3	0	0
100% *Gymnodinium catenatum*			
	Epifluorescence	**HAB (+)**	**% HAB (+)**
Red-Orange (+)	2	2	100
Yellow-Green (-)	6	0	0
50:50 *Gymnodinium catenatum:Peridinium foliaceum*			
	Epifluorescence	**HAB (+)**	**% HAB (+)**
Red-Orange (+)	3	0	0
Yellow-Green (-)	5	0	0
100% *Alexandrium monilatum*			
	Epifluorescence	**HAB (+)**	**% HAB (+)**
Red-Orange (+)	1	1	100
Yellow-Green (-)	7	0	0
50:50 *Alexandrium monilatum:Peridinium foliaceum*			
	Epifluorescence	**HAB (+)**	**% HAB (+)**
Red-Orange (+)	2	1	50
Yellow-Green (-)	6	0	0

Table 3.2: Comparison of epifluorescence and visual inspection of food vacuoles for *Protoceratium* sp. fed a sole diet of *K. brevis, G. catenatum*, or *A. monilatum* or 50:50 mixtures with *P. foliaceum*. "Epifluorescence" column contains the number of cells that were negative or positive for epifluorescence. "HAB (+)" column contains the number of food vacuoles with HAB cell present. "% HAB (+)" column contains the percentage of cells in each epifluorescence group that contained a HAB cell inside a food vacuole.

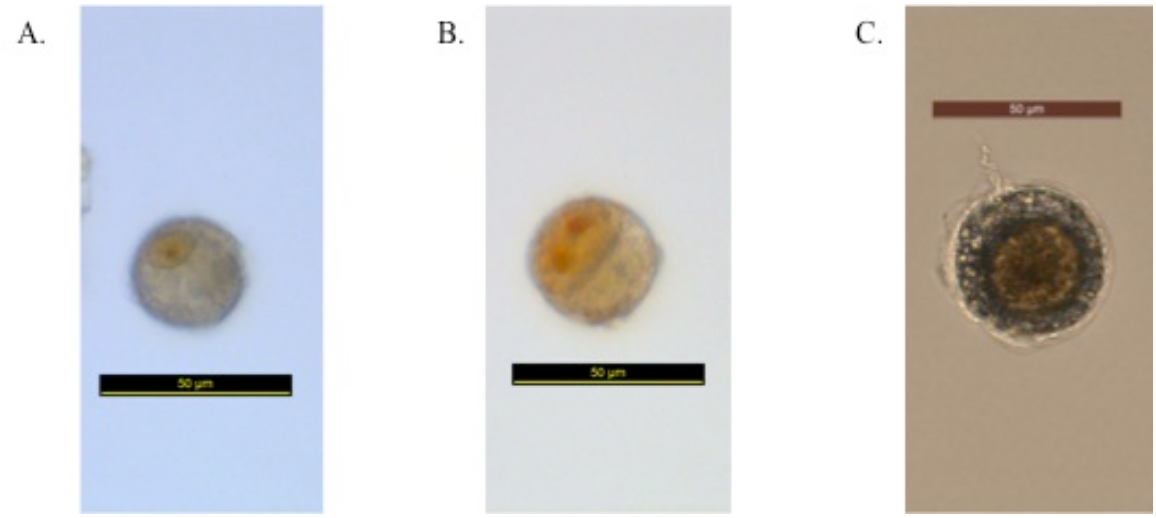

Figure 3.4: (A) 400x light microscope photo of *Protoceratium* sp. after it has ingested a *K. brevis* cell (later stage food vacuole). The cell was taken from an 8-hour grazing experiment where *K. brevis* was given as the sole food source. (B) 400x light microscope photo of *Protoceratium* sp. after it has ingested a *G. catenatum* cell (later stage food vacuole). The cell was taken from an 8 hour grazing experiment where *G. catenatum* was given as the sole food source. (C) 400x light microscope photo of *Protoceratium* sp. after it has ingested an *A. monilatum* cell. The cell was taken from a 96-hour grazing experiment (see Chapter 4) where *A. monilatum* was given as the sole food source. Scale bar = 50 μm. A starved *Protoceratium* sp. cell measures approximately 35 μm.

Bloom samples

N. scintillans was found in ship channel zooplankton tows during the late summer, fall, and winter (Figure 3.5). This is the same time of year *K. brevis* blooms typically occur in the Gulf of Mexico, making *N. scintillans* a potential protozoan grazer on *K. brevis* and other HABs occurring in the summer and winter months. During the 2011-2012 *K. brevis* bloom, depth samples showed a possible inverse relationship between protozoan grazer and *K. brevis* abundances (Figure 3.6). In samples with higher *K. brevis* abundances, there were fewer grazers. It also appeared that protozoan grazer abundances decreased at the onset of the bloom in mid-September 2011 and increased

during bloom decline in December 2011 and January 2012. There were no zooplankton net tows taken at depth so populations of zooplankton grazers could not be compared to protozoan grazer and *K. brevis* abundances. In surface samples, the pattern of protozoan grazer abundance appeared to follow the *K. brevis* abundance (Figure 3.7). Periods with high *K. brevis* abundances generally had higher grazer abundances and vice versa. However, during bloom decline, the protozoan grazer abundance continued to increase. Surface zooplankton samples were not on a fine enough time scale to determine patterns between copepod adults, copepodids and nauplii abundances over the course of the *K. brevis* bloom (Figures 3.8 and 3.9). Copepod nauplii abundances were likely underestimates because a 153-µm mesh net cannot quantitatively sample them accurately. Zooplankton tows were conducted once a month so there were no additional samples from mid-November through mid-December 2011.

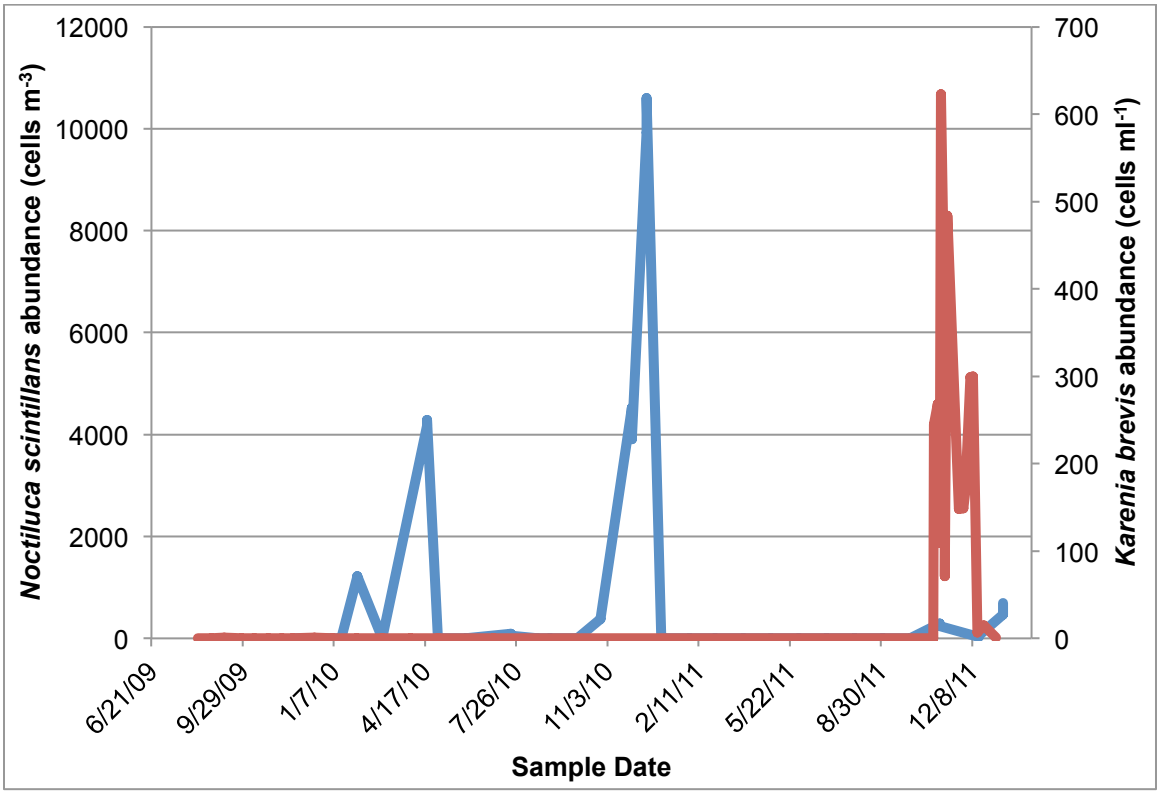

Figure 3.5: *N. scintillans* abundance (cells m^{-3}, blue) and *K. brevis* abundance (cells ml^{-1}, red) in surface zooplankton tows in the Port Aransas ship channel

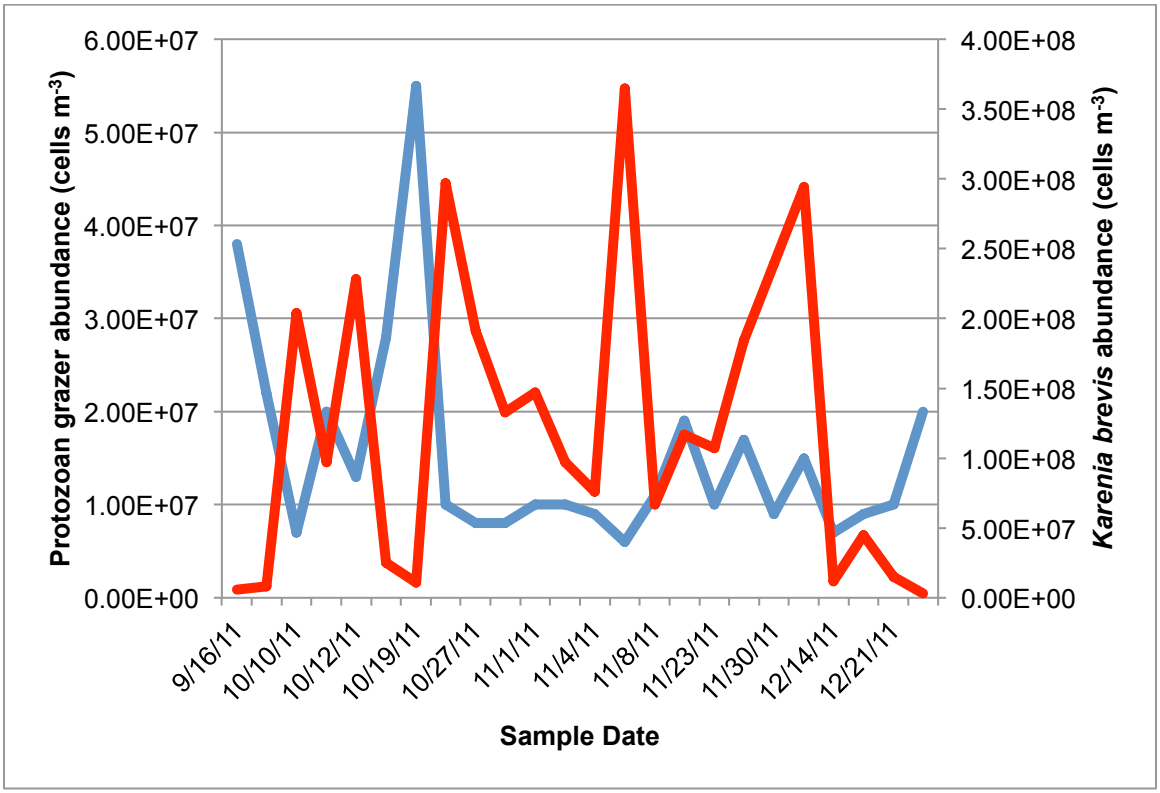

Figure 3.6: Protozoan grazer (blue) and *K. brevis* (red) abundances (cells m^{-3}) at a depth of 1.5 m from the bottom in the Port Aransas ship channel.

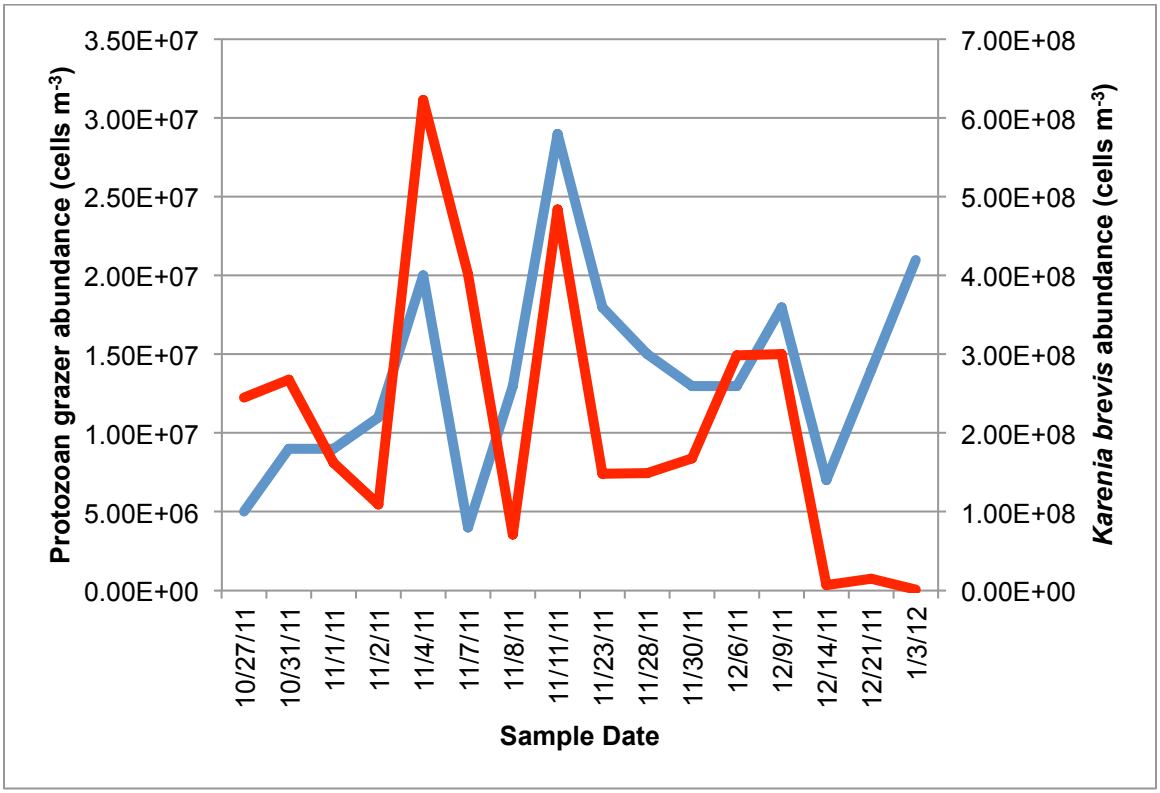

Figure 3.7: Protozoan grazer (blue) and *K. brevis* (red) abundances (cells m^{-3}) at the surface in the Port Aransas ship channel.

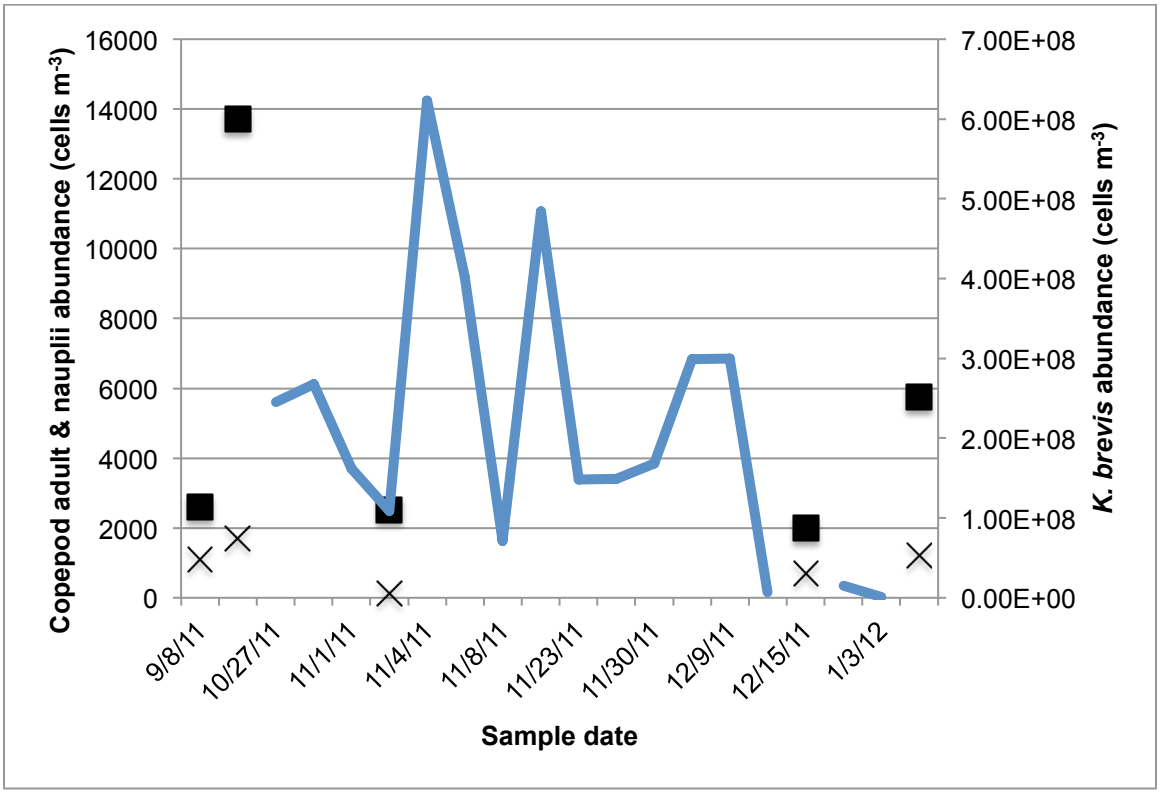

Figure 3.8: Adult copepods and copepodids (squares), copepod nauplii (Xs), and *K. brevis* (blue) abundances (cells m^{-3}) at the surface in the Port Aransas ship channel.

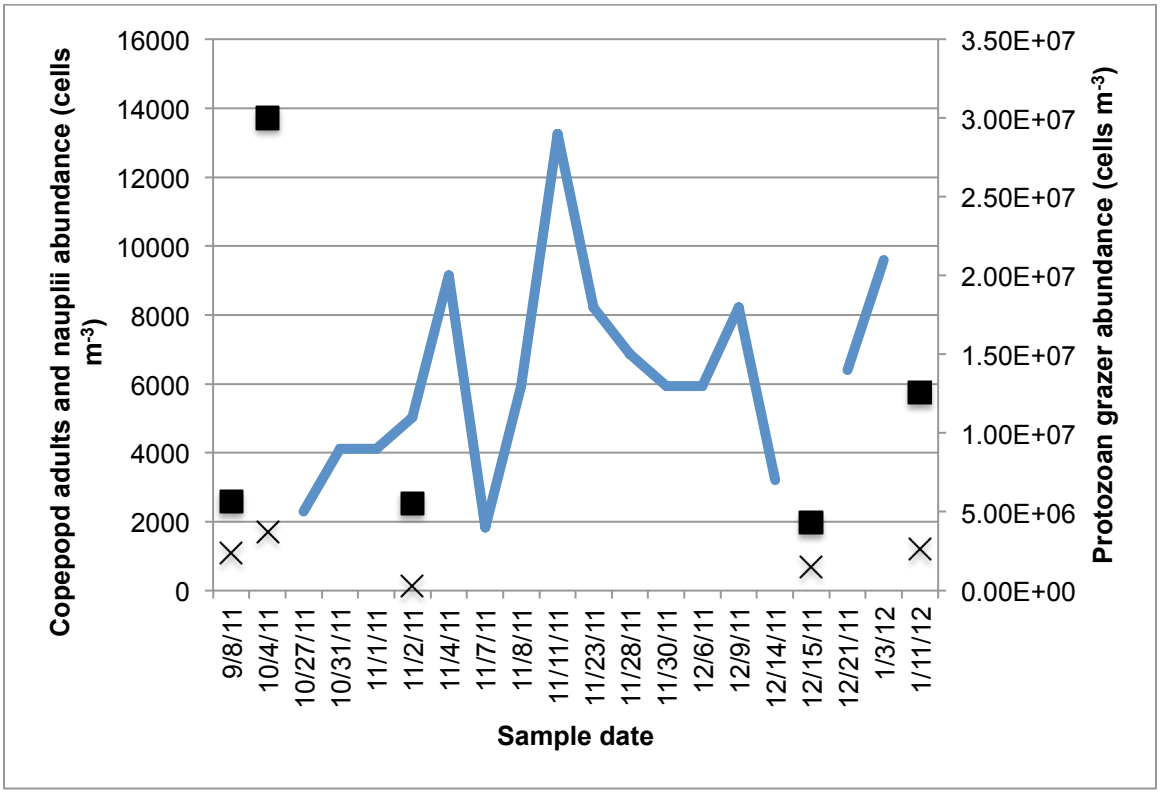

Figure 3.9: Adult copepods and copepodids (squares), copepod nauplii (Xs), and protozoan grazer (blue) abundances (cells m^{-3}) at the surface in the Port Aransas ship channel.

PCR analysis of heterotrophic dinoflagellates and ciliates from ship channel samples taken at depth resulted in some cells that tested positive for the presence of *K. brevis* DNA (Figure 3.12; Table 3.3). Although the representative gel shows an extra band in the negative control sample, the brightness of the bands in lanes 3, 4, and 6 match that of the positive control (lane 9) and were deemed probable positives for the presence of *K. brevis* DNA. A total of 24 cells from October 9-11, 2011 were analyzed because of low abundances of grazers large enough to ingest *K. brevis* and cell losses during mouth pipetting and washing. The heterotrophic dinoflagellate, *Gyrodinium spirale*, and three

ciliates, *Laboea* sp., *Strombidinopsis* sp., and *Tontonia* sp., tested positive for *K. brevis* DNA.

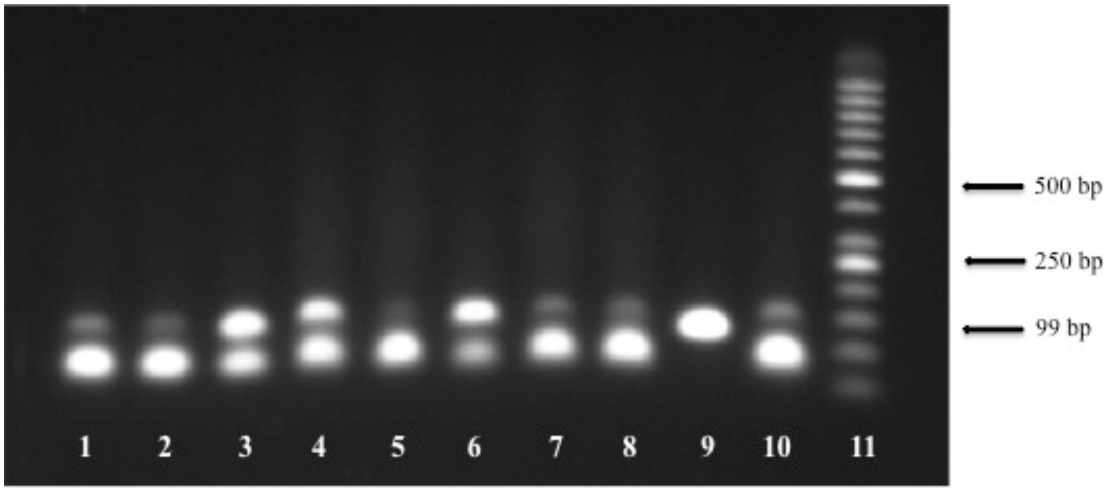

Figure 3.10: Representative gel from analysis of protozoan grazers isolated during the 2011 *K. brevis* bloom. Lanes 1-8 = individual grazers; Lane 9 = *K. brevis* positive control; Lane 10 = negative control; Lane 11 = DNA ladder.

Grazer	Cells Analyzed	DNA (+)
Gyrodinium spirale	7	1
Laboea sp.	1	1
Protoperidinium sp.	1	0
Strombidinopsis sp.	5	2
Strombidium/Strobilidium sp.	6	0
Tontonia sp.	4	1

Table 3.3: Summary of protozoan grazers analyzed for *K. brevis* DNA during the 2011-2012 *K. brevis* bloom. The number of cells analyzed and the number of cells with *K. brevis* DNA are included.

DISCUSSION

The results of this study indicate that PCR analysis can be a useful tool for identifying grazers on HABs from field samples although it may not work for all species of protozoa. DNA evidence indicates that *N. scintillans* will ingest *K. brevis* and *G. catenatum*, but not *A. monilatum*. *N. scintillans* would not form food vacuoles when given sole diets of *A. monilatum* or diets of a 50:50 food mixture of *P. foliaceum* after 8 hours of feeding, and many of the *N. scintillans* cells were senescing within 1 to 8 hours of exposure to *A. monilatum*. *N. scintillans* death without ingestion of *A. monilatum*, could indicate an allelopathic interaction resulting from an extracellular compound excreted by *A. monilatum*. The effects of *A. monilatum* filtrates have not been studied on other protozoan grazers; however, May *et al*. (2010) found that bivalve larval survival was significantly lower when exposed to aliquots of sonicated *A. monilatum* cells. *A. monilatum* filtrate was unable to be tested on *N. scintillans* during this study because of *A. monilatum* culture health decline following the final grazing experiments. The *A. monilatum* culture did not recover. Although there appeared to be a grazing affect of *N. scintillans* on *A. monilatum* during 96-hour grazing experiments (see Chapter 4), these effects may be due to poor *A. monilatum* culture quality. *N. scintillans* abundance was below 1 ml^{-1} within the first 48 hours while the *A. monilatum* population continued to decrease throughout the 96 hours.

There were some cases where positive epifluorescence in *N. scintillans* resulted in negative DNA results and no epifluorescence resulted in a positive DNA signal. Negative DNA amplification paired with positive epifluorescence during experiments where the food was a 50:50 mixture of HAB and *P. foliaceum* could mean that those fluorescent cells were the *P. foliaceum* control food. However, if positive epifluorescence did not result in a positive DNA signal when the grazer was fed a sole diet of the HAB species,

the DNA could have been degraded by digestion. Although *K. brevis* DNA could be detected for up to 8 hours after ingestion by *N. scintillans*, the age and physiological health of the ingested cell will also determine the viability of the DNA. Cells of the diatom *Thalassiosira pseudonana* displayed degraded genomic DNA with age of the culture as well as under iron starved conditions even though the cell appeared to be intact (Bidle and Bender 2008). Grazers that showed no epifluorescence but positive DNA signals could result from chlorophyll that was more degraded than the DNA. Comparisons of DNA fragmentation paired with cell senescence, characterized by differences in cell morphology and fluorescence, in the dinoflagellate *Amphidinium carterae* were inconclusive because in some cases there was no difference in DNA fragmentation between healthy and dead cells (Franklin and Berges 2001).

The failure of HAB DNA amplification in *Protoceratium* sp. may be the result of cell toughness or organism digestion. *Protoceratium* sp. is a highly armored dinoflagellate, and breakage of the cell would be required to release HAB DNA from food vacuoles. Mechanical breakage was required in order to obtain adequate amounts of DNA from cysts of another genus of armored dinoflagellates, *Alexandrium* (Erdner *et al*. 2010). Although vortexing with zirconium/silica beads was used as a means of mechanical breakage, there is the possibility that the *Protoceratium* sp. and food vacuoles remained intact. Trials with boiling *Protoceratium* sp. cells for 2 min also resulted in intact cells, indicating that *Protoceratium* sp. armor is resilient. Another possibility is that *Protoceratium* sp. digest their food at faster rates after ingestion than *N. scintillans*. Grazing experiments with *Protoceratium* sp. had durations of 8 hours in order to find cells with fluorescent food vacuoles. Although a time series study indicated that viable DNA could still be found inside *N. scintillans* food vacuoles, this extended grazing time for *Protoceratium* sp. may have resulted in more degraded DNA. As described above,

degraded DNA can be present inside cells that still appear healthy with regards to morphology and fluorescence.

There appears to be no avoidance of ingesting HABs for *Protoceratium* sp. or *N. scintillans* even when given a mixture with *P. foliaceum*. *K. brevis* and *G. catenatum* DNA was found inside *N. scintillans* cells when they were given as sole diets and mixtures with *P. foliaceum*. Cells from all three HABs were found inside food vacuoles of *Protoceratium* sp. cells when given as sole diets and mixtures with *P. foliaceum* except *G. catenatum* in a 50:50 mixture with *P. foliaceum*. Although some *Protoceratium* sp. cells from the *G. catenatum* mixed food treatment showed epifluorescence, the food vacuoles contained *P. foliaceum* rather than *G. catenatum*. This result may be an artifact of food encounter rate by the grazer rather than food preference. In order to obtain a food concentration of 250 µg C L^{-1} with equal parts *G. catenatum* and *P. foliaceum*, the cell counts were 58 cells ml^{-1} and 138 cells ml^{-1}, respectively. Thus, there is a higher chance of *Protoceratium* sp. encountering a *P. foliaceum* cell before a *G. catenatum* cell.

Protozoan grazers analyzed from a natural bloom indicate that there were some heterotrophic dinoflagellates and ciliates that ingest *K. brevis* in the field. The heterotrophic dinoflagellate, *Gyrodinium spirale*, and three ciliates, *Laboea* sp., *Strombidinopsis* sp., and *Tontonia* sp., appeared to have ingested *K. brevis* during the onset of the bloom. Unlike quantitative DNA analyses on the gut contents of copepods (Nejstgaard *et al*. 2008), DNA analyses on the food vacuoles of protozoan grazers would not be quantitative. Many protozoa ingest one cell at a time as seen with the light microscope image of *Protoceratium* sp. above. These current DNA results also did not indicate any type of "top down" control on *K. brevis* by the protozoan grazers. Although the population pattern from samples collected at depth appeared to indicate increased *K. brevis* abundance with a disappearance of protozoan grazers and a reappearance of

grazers during bloom decline, too few grazers were analyzed for DNA to draw conclusions about the bloom control capability of protozoan grazers. There were also too few zooplankton samples to determine if the protozoan population patterns were due to predation of protozoa by copepods.

This study sets the groundwork for future grazing experiments and field sample analyses. Genus- and species-specific primers can be used to determine the ingestion of a HAB cell by some protozoan grazers. The heterotrophic dinoflagellate and ciliates identified as potential grazers on *K. brevis* should now be cultured and used in laboratory grazing experiments to determine growth and grazing rates on *K. brevis*. Longer term (96 hour) growth experiments have already been completed with the two heterotrophic dinoflagellates – *N. scintillans* and *Protoceratium* sp. – and three HAB species used in these DNA analyses (see Chapter 4). The growth experiments indicated that the HAB as a sole diet produces reduced grazer growth, but *N. scintillans* and *Protoceratium* sp. may be able to serve as potential controls during pre-bloom conditions. During future HAB events, increased zooplankton sampling as well as phytoplankton net tows should be performed. A finer time scale of zooplankton sampling would help determine whether patterns in protozoan grazer abundance are from predation or possible negative effects from the HAB. Phytoplankton net tows would allow for a larger number of protozoan grazers for DNA analyses. Together, these analyses will give more insight into the role of protozoan grazers in harmful algal bloom dynamics.

Chapter 4: Growth of *Protoceratium* sp. and *Noctiluca scintillans* when fed varying diets of three red tide species

ABSTRACT

The increasing occurrence of harmful algal blooms (HABs) has prompted studies aimed at determining biotic and abiotic factors, which may promote bloom initiation, maintenance, and decline. Although many studies have tried to evaluate the effectiveness of "top-down" or "bottom-up" control of HABs, there is evidence to support both mechanisms. Protozoan grazers are likely candidates for "top-down" control of HAB species since they have the potential to increase their populations at growth rates similar to those found for many HAB species. Grazing experiments with the heterotrophic dinoflagellates *Noctiluca scintillans* and *Protoceratium* sp. tested whether grazers can be an effective "top-down" control of HAB species, *Karenia brevis*, *Gymnodinium catenatum*, and *Alexandrium monilatum*. Although, both grazers feed on HAB species, they may be ineffective "top down" controls during established bloom periods. *N. scintillans* and *Protoceratium* sp. experienced negative growth rates when fed sole diets of the HAB species. *K. brevis* showed stimulated growth in the presence of *Protoceratium* sp. However, *Protoceratium* sp. had highest grazing and clearance rates paired with positive average specific growth rates when fed a mixed diet of *A. monilatum* and *P. foliaceum*, which could indicate a potential for "top down" control at lower HAB cell concentrations during bloom initiation.

INTRODUCTION

Many harmful algal blooms (HAB) are characterized by fish, marine mammal, and even human fatalities or illnesses caused by toxin produced by the blooming species (as reviewed in Hallegraeff 1993). However, blooms, which alter food web interactions and cause mass fatalities from dissolved oxygen depletion during algal decay, are also

considered harmful (Horner *et al*. 1997). These blooms can result from "bottom up" regulation, in the form of increased nutrient availability (DeYoe and Suttle 1994, Buskey *et al*. 1998, Doblin *et al*. 1999, Juhl 2005, Vargo *et al*. 2008), or as a release from "top down" regulation caused by decreased grazing on a HAB species (Hansen *et al*. 1993, Demir *et al*. 2008) or a decline in grazer abundance (Buskey *et al*. 1997).

This release from top down regulation can be caused by the physiological effects of various compounds produced by blooming species, suboptimal nutrition for the grazer, or by size mismatch with grazers. Physiologically, biological compounds produced by HAB species can reduce ingestion rates (Huntley *et al*. 1986, Ives 1987, Shaw *et al*. 1995, Shaw *et al*. 1997, Colin and Dam 2002, Colin and Dam 2003), growth rates (Hansen 1989, Hansen 1995, Frangópulos *et al*. 2000, Tang et al. 2001), and fecundity (Gill and Harris 1987, Uye and Takamatsu 1990, Gilbert 1994, Whyte *et al*. 1996, Dutz 1998, Colin and Dam 2002) in grazers, decreasing the ability of protozoan and metazoan grazers to control a bloom. A decrease in ingestion rates on a HAB species may mean that larger populations of grazers are needed to feed on blooming species at rates higher than the growth rate of the bloom. HAB bloom initiation may result from low initial grazer populations that do not serve as an effective control. Decreases in growth rates and fecundity of the grazers mean a decrease in the population of organisms available to feed on the bloom. The gelatinous coatings of some algal cells can provide protection from digestion, allowing grazer fecal pellets to contain and release viable algal cells into the environment (Porter 1973, Porter 1976, Bersano *et al*. 2002). However, blooming species can also reduce grazing mortality by having a low nutrient value for the grazer (Claustre *et al*. 1990, Buskey and Hyatt 1995). *Phaeocystis* sp. was deemed of low nutritional quality for copepods because of low levels of polyunsaturated fatty acids and vitamin C (Claustre *et al*. 1990). The brown tide organism, *Aureoumbra lagunensis* is nutritionally

inadequate to support growth in ciliates, heterotrophic dinoflagellates, and rotifers (Buskey and Hyatt 1995). There may also be a size mismatch between grazer and HAB with the HAB growing to a cell size too large for the grazers' feeding structures (Demir *et al*. 2008). The potentially toxic raphidophyte, *Chattonella* spp., is considerably larger than another toxic raphidophyte, *Heterosigma akashiwo*, and may not be ingested by microzooplankton grazers because of its larger size (Demir et al. 2008). Grazing was detected on the smaller *H. akashiwo* in natural assemblages, but not on the larger *Chattonella* spp. cells.

Although HAB species have many defenses to deter grazing mortality allowing blooms to persist, there are some instances where grazers have successfully controlled or fed on HABs without deleterious effects (Admiraal and Venekamp 1986, Matsuyama et al. 1999, Colin and Dam 2003, Rosetta and McManus 2003). Most of these grazing interactions will be site and species specific, and the effects of grazers on similar HABs occurring at different locations may depend on the grazers present (Turner and Anderson 1983, Teegarden and Cembella 1996). Turner and Anderson (1983) found high grazing impacts of polychaete larvae, *Polydora* sp., and the copepod *Acartia hudsonica*, on the HAB *Alexandrium tamarensis* in Perch Pond, Falmouth, MA. The grazing impact of the polychaete larvae is unique because there have been no other instances of high polychaete larvae abundances during the spring bloom in any other northeastern estuary (Turner and Anderson 1983). The copepods *Acartia tonsa* and *Eurytemora herdmani* exhibit different grazing rates and selectivity when presented with toxic *Alexandrium* spp. and non-toxic *Lingulodinium polyedrum*, indicating that grazing pressure on a bloom of *Alexandrium* spp. would depend on the grazer community composition (Teegarden and Cembella 1996). Protozoan grazers are of particular interest because their growth rates

could match those of HAB species, possibly making them a more effective "top down" control (Admiraal and Venekamp 1986, Strom and Morello 1998).

Three HAB species – *Karenia brevis*, *Gymnodinium catenatum*, and *Alexandrium monilatum* – and two heterotrophic dinoflagellate grazers – *Protoceratium* sp. and *Noctiluca scintillans* – were used for this study. Each of these HAB species is a dinoflagellate found in the Gulf of Mexico. *K. brevis* produces brevetoxins, which cause neurotoxic shellfish poisoning (NSP; Poli *et al*. 2000). *G. catenatum* produces saxitoxin causing paralytic shellfish poisoning (PSP; Oshima *et al*. 1987). *A*. *monilatum* is a congener of the PSP-producing *A. tamarensis*; however it produces a lipophilic toxin called goniodomin A instead of saxitoxin (Hsia *et al*. 2006). *A. monilatum* has been linked to numerous fish (Connell and Cross 1950, Howell 1953, Gates and Wilson 1960), whelk (Harding *et al*. 2009), and larval bivalve deaths (May *et al*. 2010). *Protoceratium* sp. and *N. scintillans* are used as the grazers in this study because short-term grazing experiments have revealed ingestion of the three HABs. Annual population distributions of *Protoceratium* sp. and *N. scintillans* also show that they are present during the time periods of potential HAB events (see Chapter 3) and could be potential grazers on HABs in nature. This study aimed to determine growth, ingestion, or mortality rate changes of protozoan grazers after ingestion of a HAB species. This study investigated whether a particular HAB species was a nutritious food source for a grazer known to ingest the HAB. If *N. scintillans* and *Protoceratium* sp. can feed and grow on *K. brevis*, *A. monilatum*, and *G. catenatum* at rates similar to those on non-HAB species, they may be able to control HABs in nature.

MATERIALS AND METHODS

Culturing Techniques

K. brevis (27-30 µm; CCMP2281) and *A. monilatum* (48 µm; CCMP3105) were cultured in L1 media (Guillard and Hargraves 1993) at 20º C on a 12:12 light:dark cycle. *G. catenatum* (30-42 µm) was isolated from a 20-µm mesh net tow (Model 9100 Student Net, Sea-Gear Corporation) in the Port Aransas ship channel and cultured in F/2 media (Guillard 1975) at 20º C on a 12:12 light:dark cycle. Light was provided by cool white fluorescent bulbs (12.4 µmol photons m^{-2} s^{-1}). *A. monilatum* and *G. catenatum* cultures were maintained in 50 ml tissue culture flasks. *K. brevis* cultures were maintained in 500 ml polycarbonate Erlenmeyer flasks. When the three species needed to be cultured in greater numbers for grazing experiments, cultures were gradually brought up to 500 ml volume in the polycarbonate Erlenmeyer flasks. *Peridinium foliaceum* cultures were maintained in 1 L polycarbonate bottles of F/2 media at 20º C on a 12:12 light:dark cycle. Light was provided by cool white fluorescent bulbs (12.4 µmol photons m^{-2} s^{-1}).

Protoceratium sp. (35 µm; identification verified by Karen Steidinger, Fish and Wildlife Research Institute) was isolated from plankton tows using a 20-µm mesh net in the Port Aransas ship channel, and cultures were maintained in 50 ml tissue culture flasks of filtered seawater (salinity = 32 psu) at room temperature of approximately 27º C. Seawater was collected from the UTMSI pier in the Port Aransas ship channel. Cultures were placed in sections of PVC pipe atop bottle rollers rotating at approximately 2 rpm to keep the cultures suspended. These rollers were located on the laboratory bench top with overhead lighting (6.6 µmol photons m^{-2} s^{-1}) for approximately 8 hours per day. Cultures were in complete darkness over the weekends. *Protoceratium* sp. were fed approximately 5 ml aliquots of dense cultures of *P. foliaceum* once per week. *Noctiluca scintillans* (500-1,000 µm) was isolated from a 20-µm mesh net tow in the Port Aransas ship channel and

maintained in 1 L polycarbonate bottles in 32 psu filtered seawater at 20º C on a 12:12 light:dark cycle. Light was provided by cool white fluorescent bulbs (12.4 µmol photons m^{-2} s^{-1}). *N. scintillans* cultures were fed approximately 10-20 ml aliquots of dense cultures of *P. foliaceum* once per week.

Experimental Protocol

All grazers were starved overnight prior to experiment initiation. Grazers were starved to ensure than any growth or mortality seen through the course of the experiment were the result of experimental food treatments rather than from culture food conditions. Experimental bottles were 250 ml polycarbonate Erlenmeyer flasks filled to a final volume of 250 ml including grazers and food. Seawater medium used for the experimental setup contained F/10 nutrients to ensure that nutrient depletion was not a cause for declines in HAB densities during grazing experiments. Although *K. brevis* and *A. monilatum* were grown on L1 nutrients, the control food *P. foliacium* was grown on F/2 nutrients. All three species of dinoflagellates continued to grow on F/10 nutrients so these nutrients were used throughout the course of the experiments. Grazer and food concentrations were modeled after Fredrickson and Strom (2009) who sustained their grazers on 250 µg C L^{-1} food concentrations during long-term experiments, and food concentrations at 250 µg C L^{-1} (reported below) result in HAB concentrations typical of bloom concentrations. Previous studies have also shown *N. scintillans* and *Protoceratium* sp. to be undersaturated for food at 500 µg C L^{-1} on varying diets of phytoplankton (Buskey 1995, McDonnell 1998). For the *N. scintillans* experiments, 700 grazers were used for each bottle, and 1,500 grazers were used per bottle for the *Protoceratium* sp. experiments. The density of each grazer culture was determined and an aliquot of the culture was added to the experimental bottles to the target concentration of 700 grazers

and 1,500 grazers per bottle for *N. scintillans* and *Protoceratium* sp., respectively. There were 2 treatment groups and 5 control groups for each grazing experiment. One treatment included the grazer and 250 µg C L^{-1} food source of solely the HAB species (*K. brevis* = 290 cells ml^{-1}, *A. monilatum* = 53 cells ml^{-1}, *G. catenatum* = 115 cells ml^{-1}). The other treatment consisted of the grazer and a 50:50 mixture of the HAB species and "good" food (*P. foliaceum*) at a 250 µg C L^{-1} total concentration (*K. brevis* = 145 cells ml^{-1}, *A. monilatum* = 27 cells ml^{-1}, *G. catenatum* = 58 cells ml^{-1}, *P. foliaceum* = 138 cells ml^{-1}). Carbon content per cell was calculated using the Strathmann (1967) equation for non-diatom cells: $logC = -0.46 + 0.866(logV)$; where C is the carbon content per cell in pg and V is the cell volume in μm^3. Controls included: 1) starved grazers; 2) only HAB at a 250 µg C L^{-1} concentration; 3) only *P. foliaceum* at a 250 µg C L^{-1} concentration (275 cells ml^{-1}); 4) HAB plus *P. foliaceum* in a 50:50 mixture at a 250 µg C L^{-1} total concentration; and 5) grazer plus *P. foliaceum* at a 250 µg C L^{-1} concentration. Three replicates were used for each treatment. Bottles were placed in an incubator at 20º C in cool white fluorescent light (12.4 µmol photons m^{-2} s^{-1}) for 96 hours.

Sampling and Enumeration

Every 24 hours, a 10 ml subsample was taken from each bottle and preserved in 1% formalin or acid Lugol's iodine. Acid Lugol's iodine was used to preserve all subsamples except those containing both *Protoceratium* sp. and *P. foliaceum* cells. These two cells look similar when preserved with acid Lugol's iodine, thus preservation with formalin allows for the distinction between photosynthetic and non-photosynthetic cells based on cell color. Before preserving and counting the 10 ml subsamples from the *N. scintillans* experimental bottles, all *N. scintillans* were collected with a pipette and counted from the entire subsample. *N. scintillans* were counted before preservation

because use of preservatives will cause *N. scintillans* to shrivel, making the identification of previously viable cells more difficult. Cells were enumerated for each subsample using a Sedgewick-Rafter counting chamber. The entire Sedgewick-Rafter was counted. Subsample volume was replaced with 10 ml F/10 media to prevent nutrient depletion, and dilution effects were taken into consideration during subsequent subsampling times. Experimental bottle positions were also rotated within the incubator after each subsampling to compensate for any differences in light levels.

Data Analysis

Specific growth rate (μ) for each cell type in each replicate was calculated over the linear slope of the natural log of grazer cell abundance, which would be considered the exponential growth period. Specific growth rate is given as $\mu = \frac{ln\,(\frac{Nt}{N0})}{t}$, where μ is the specific growth rate (d^{-1}), N_t is the grazer cell abundance at the end of the exponential growth period (cells ml^{-1}), N_0 is the initial grazer abundance (cells ml^{-1}), and t is the time (d) of exponential growth. Specific growth rates for the food controls were also calculated in order to determine grazing rates (see below). Although samples were taken every 24 hours for 4 days, N_0 and N_t were not always equal to the first and last days. In some cases, maximum or minimum cell abundances before slope flattening was reached in three days. When grazer specific growth rate data were normally distributed, a one-way ANOVA paired with a parametric Holm-Sidak test or, when data were not normal, non-parametric Kruskal-Wallis test on ranks (SigmaPlot 11.0) was performed on the grazer specific growth rates between each treatment. Grazing rate for each grazer on each food type was calculated using Frost (1972): $N_t = N_0 e^{(\mu - g)t}$. N_t is the food cell abundance at the end of the exponential growth period, N_0 is the initial food cell abundance, μ is the specific growth rate of the food controls, g is the grazing rate (d^{-1}),

and t is the time (d) of exponential growth. Grazer clearance rates were calculated for each food type using the Heinbokel (1978) modification of Frost (1972): $F = \frac{Vg}{\bar{T}}$. F is the clearance rate (ml d^{-1}), V is the volume of the experimental container (250 ml), g is the grazing rate, and $\bar{T}$ is the average grazer abundance (cells ml^{-1}). Heinbokel (1978) calculated average grazer abundance as $\bar{T} = \frac{N_t - N_0}{\ln(N_t) - \ln(N_0)}$ in order to take into consideration grazer abundance changes over the experimental time period. When grazing and clearance rates were normally distributed, a one-way ANOVA paired with a parametric Holm-Sidak test or, when data were not normal, non-parametric Tukey Test on ranks (SigmaPlot 11.0) were performed for each treatment.

RESULTS

Specific growth rates of *Protoceratium* fed a diet of *P. foliaceum* or a 50:50 mixture of *K. brevis* and *P. foliaceum* were significantly higher than those rates when fed a diet of *K. brevis* or starved for 96 hours (Figure 4.1). Specific growth rates on diets of *P. foliaceum* and a 50:50 mixture of *K. brevis* and *P. foliaceum* did not significantly differ from each other (Figure 4.1). Starved *Protoceratium* sp. growth did not significantly differ from that of *Protoceratium* sp. fed a sole diet of *K. brevis* (Figure 4.1). Specific growth rates of *N. scintillans* were significantly higher on diets of *P. foliaceum* and a 50:50 mixture of *K. brevis* and *P. foliaceum* than those for N. scintillans starved for 96 hours or fed a sole diet of *K. brevis* (Figure 4.2). Specific growth rates on diets of *P. foliaceum* and a 50:50 mixture of *K. brevis* and *P. foliaceum* did not significantly differ from each other (Figure 4.2). Starved *N. scintillans* growth did not significantly differ from that of *N. scintillans* fed a sole diet of *K. brevis* (Figure 4.2).

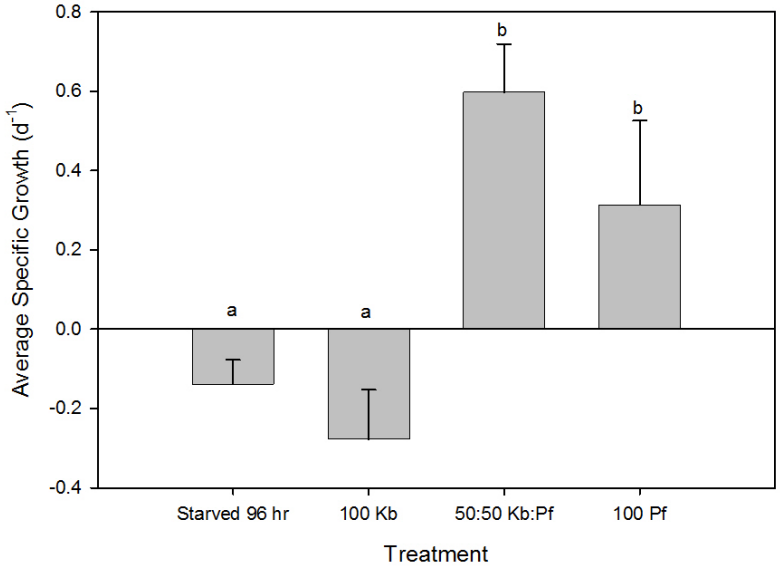

Figure 4.1: Average specific growth rates (d^{-1}) of *Protoceratium* sp. when fed different concentrations of *K. brevis* (Kb) and *P. foliaceum* (Pf). Error bars are standard deviations. Letters above the bars indicate significant differences (ANOVA, $p<0.05$)

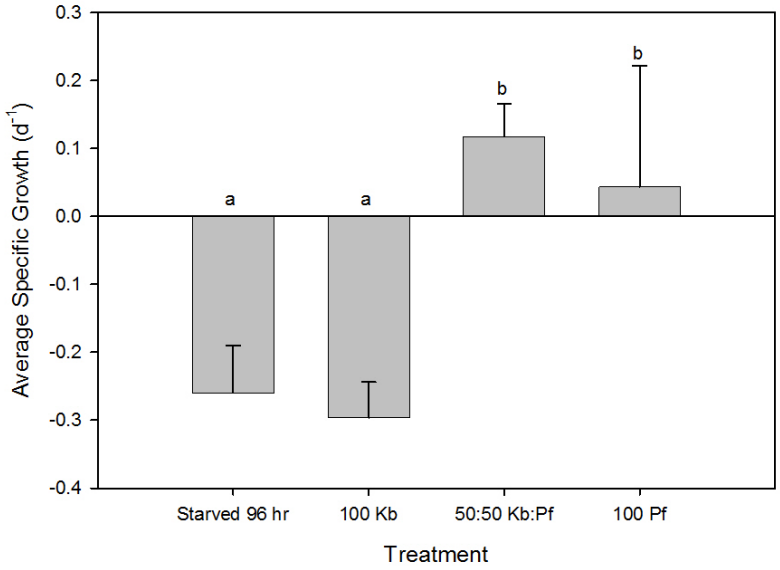

Figure 4.2: Average specific growth rates (d^{-1}) of *N. scintillans* when fed different concentrations of *K. brevis* (Kb) and *P. foliaceum* (Pf). Error bars are standard deviations. Letters above the bars indicate significant differences (ANOVA, $p<0.05$).

Specific growth rates of *Protoceratium* sp. fed a sole diet of *P. foliaceum* were significantly different from those of starved *Protoceratium* sp. but not of those fed a sole diet of *G. catenatum* (Figure 4.3). *Protoceratium* sp. growth rates when fed a 50:50 mixture of *G. catenatum* and *P. foliaceum* were not significantly different from those when *Protoceratium* sp. was starved (Figure 4.3). *Protoceratium* sp. specific growth rates were not normally distributed so a non-parametric Kruskal-Wallis test on ranks with ANOVA was used, and no other comparisons on ranks were made. Specific growth rates of *N. scintillans* were normally distributed for each treatment. Specific growth rates of *N. scintillans* fed a sole diet of *P. foliaceum* were significantly different from those on all other food treatments (Figure 4.4). Growth rates when fed a 50:50 food mixture of *G. catenatum* and *P. foliaceum* were significantly different from those on all other food treatments (Figure 4.4). *Noctiluca scintillans* specific growth rates when fed a sole diet of

G. catenatum were not significantly different than those when *N. scintillans* was starved (Figure 4.4).

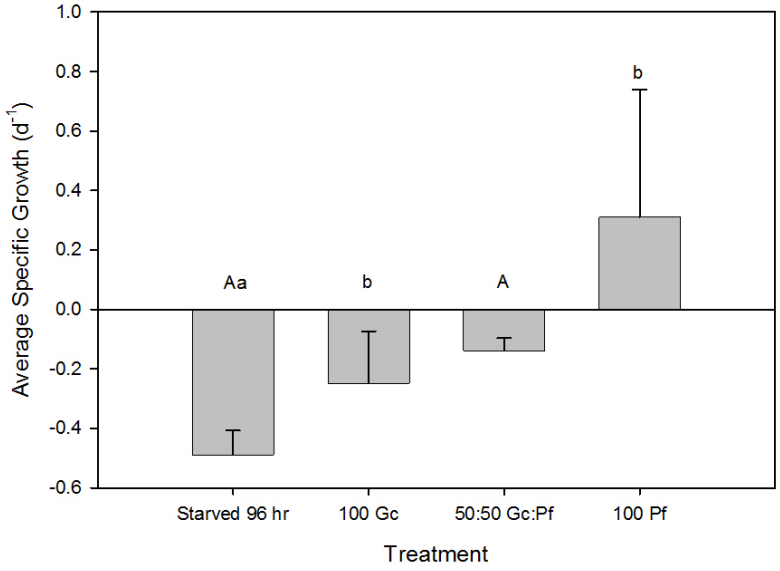

Figure 4.3: Average specific growth rates (d^{-1}) of *Protoceratium* sp. when fed different concentrations of *G. catenatum* (Gc) and *P. foliaceum* (Pf). Error bars are standard deviations. Letters above the bars indicate significant differences (ANOVA, $p<0.05$). Letter case indicates comparisons that were made.

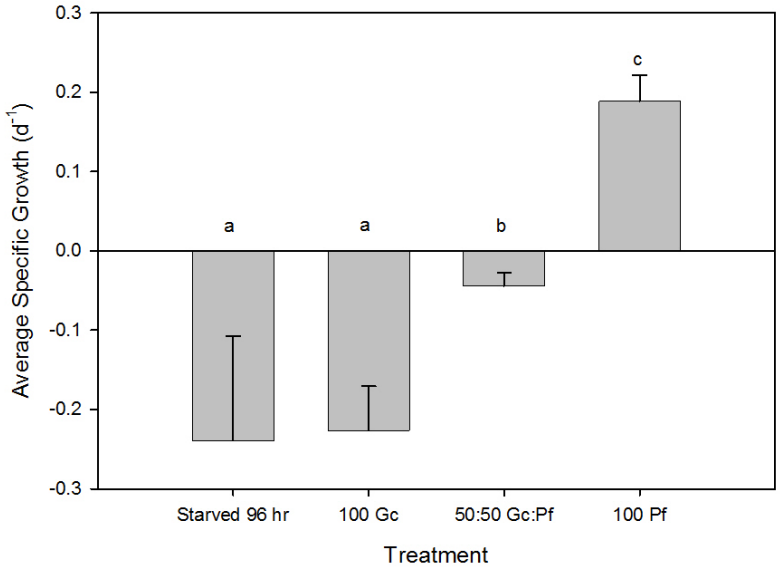

Figure 4.4: Average specific growth rates (d^{-1}) of *N. scintillans* when fed different concentrations of *G. catenatum* (Gc) and *P. foliaceum* (Pf). Error bars are standard deviations. Letters above the bars indicate significant differences (ANOVA, $p<0.05$).

Specific growth rates of starved *Protoceratium* sp. were significantly different from all other *A. monilatum* food treatments (Figure 4.5). *Protoceratium* sp. fed a sole diet of *A. monilatum* had growth rates that were significantly different from all other food treatments (Figure 4.5). Specific growth rates of *Protoceratium* sp. fed a sole diet of *P. foliaceum* were not significantly different from those fed a 50:50 food mixture of *A. monilatum* and *P. foliaceum* (Figure 4.5). *Noctiluca scintillans* specific growth rates failed the normality test so a non-parametric Kruskal-Wallis test on ranks with ANOVA was used. Specific growth rates of *N. scintillans* fed a sole diet of *P. foliaceum* were significantly different from those when fed a sole diet of *A. monilatum* but not of those fed a 50:50 food mixture of *A. monilatum* and *P. foliaceum* (Figure 4.6). Starved *N. scintillans* specific growth rates were not significantly different than those fed a sole diet of *A. monilatum* (Figure 4.6). No other comparisons on ranks were made.

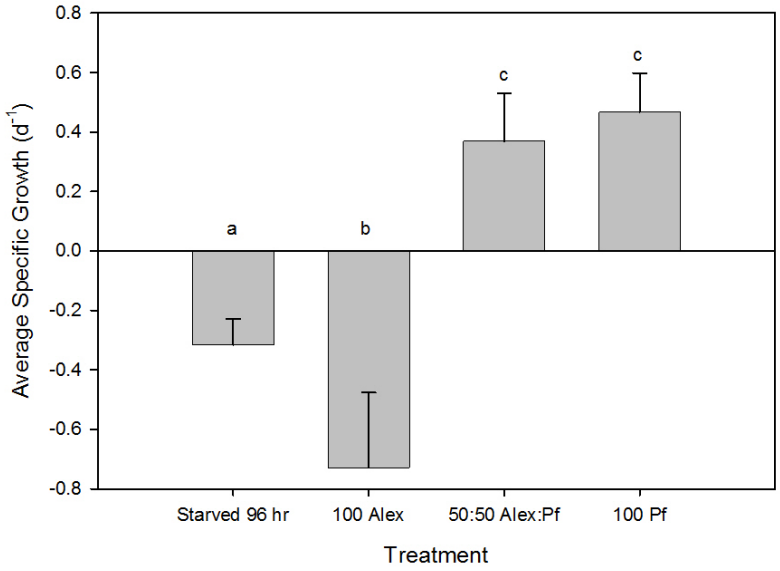

Figure 4.5: Average specific growth rates (d^{-1}) of *Protoceratium* sp. when fed different concentrations of *A. monilatum* (Alex) and *P. foliaceum* (Pf). Error bars are standard deviations. Letters above the bars indicate significant differences (ANOVA, $p<0.05$).

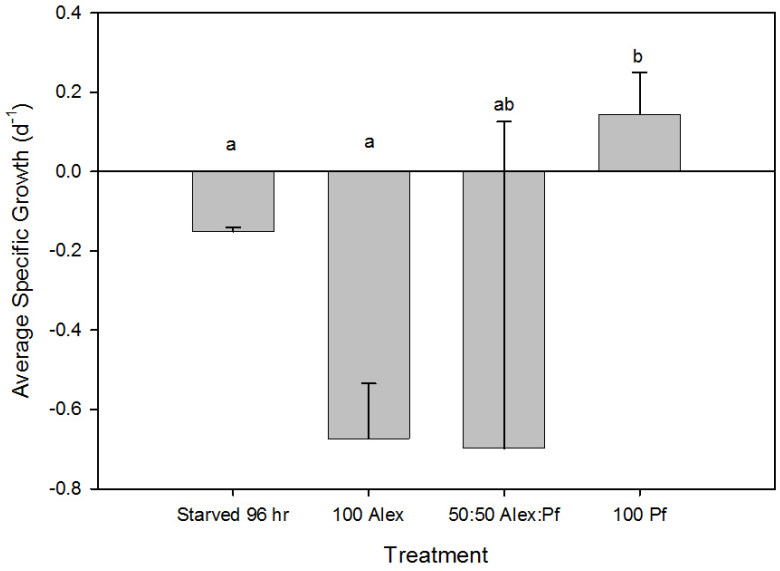

Figure 4.6: Average specific growth rates (d^{-1}) of *N. scintillans* when fed different concentrations of *A. monilatum* (Alex) and *P. foliaceum* (Pf). Error bars are standard deviations. Letters above the bars indicate significant differences (ANOVA, $p<0.05$).

Grazing rates for *N. scintillans* fed differing concentrations of *K. brevis* and *P. foliaceum* were positive but not significantly different from each other (Figure 4.7). Grazing rates appeared highest on *K. brevis* when fed as a 50:50 mixture with *P. foliaceum*. Grazing rates on a sole diet of *P. foliaceum* were higher than on a sole diet of *K. brevis*. Clearance rates for *N. scintillans* fed differing concentrations of *K. brevis* and *P. foliaceum* were also positive but not significantly different from each other (Figure 4.8). Clearance rates appeared highest for *K. brevis* when fed as a 50:50 mixture of *P. foliaceum*, which agreed with the highest grazing rates. Clearance rates were slightly higher for a sole diet of *P. foliaceum* than on a sole diet of *K. brevis*. Clearance and grazing rates of *N. scintillans* on *K. brevis* diets could be misleading, however, because *K. brevis* controls showed mortality throughout the experiment (data not shown).

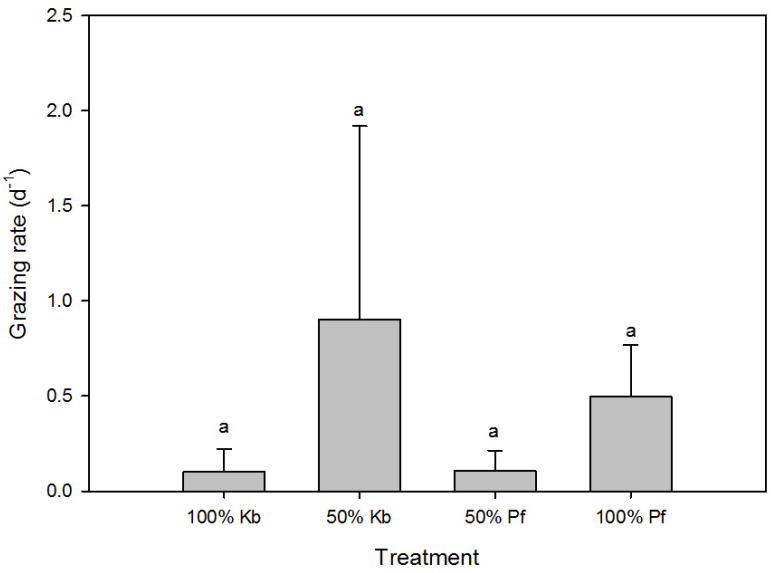

Figure 4.7: Grazing rates for *N. scintillans* on differing concentrations of *K. brevis* (Kb) and *P. foliaceum* (Pf). Bars for 50% Kb and 50% Pf represent grazing rates on each food type when fed as a 50:50 mixture. Grazing rates are represented as means with bars showing the standard deviations. Letters above the bars indicate significant differences (ANOVA, $p<0.05$).

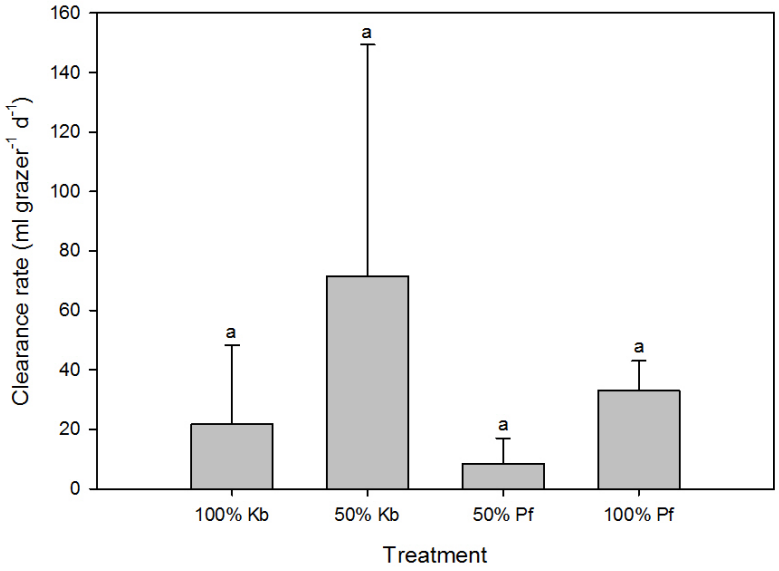

Figure 4.8: Clearance rates for *N. scintillans* on differing concentrations of *K. brevis* (Kb) and *P. foliaceum* (Pf). Bars for 50% Kb and 50% Pf represent clearance rates on each food type when fed as a 50:50 mixture. Clearance rates are represented as means with bars showing the standard deviations. Letters above the bars indicate significant differences (ANOVA, $p<0.05$).

Grazing rates for *Protoceratium* sp. fed a sole diet of *K. brevis* were significantly lower than all other treatments except for those *Protoceratium* sp. fed a sole diet of *P. foliaceum* (Figure 4.9). Negative grazing rates on a sole diet of *K. brevis* indicated that *K. brevis* growth was higher than grazing losses during incubation. Grazing rates on *P. foliaceum* when fed as a 50:50 mixture with *K. brevis* were significantly higher than the other treatments. *Protoceratium* sp. grazing rates on a sole diet of *P. foliaceum* were not significantly different than those on *K. brevis* when it was offered as a sole diet or 50:50 mixture. Clearance rates for *Protoceratium* sp. were not normally distributed so a non-parametric Tukey Test on ranks was performed on the data. *Protoceratium* sp. clearance rates when fed a sole diet of *K. brevis* were significantly lower than clearance rates on *P. foliaceum* when given as a 50:50 food mixture with *K. brevis* (Figure 4.10). The negative

clearance rate on a sole diet of *K. brevis* agreed with the negative grazing rate which indicated that *K. brevis* growth was higher than losses through *Protoceratium* sp. clearing the water of cells. Clearance rates of *Protoceratium* sp. fed a 50:50 mixture of *K. brevis* and *P. foliaceum* were not significantly different for either food cell type. Clearance rates were also not significantly different between those *Protoceratium* sp. fed sole diets of *P. foliaceum* or *K. brevis*. No other comparisons were made.

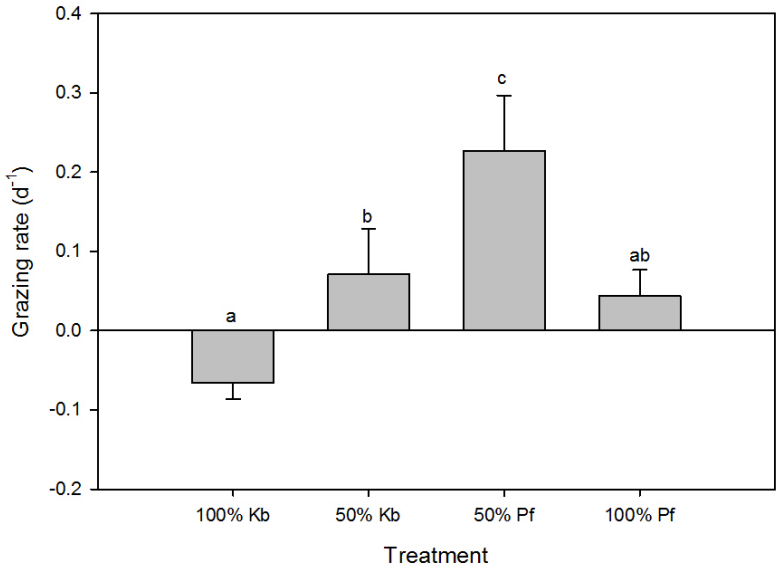

Figure 4.9: Grazing rates for *Protoceratium* sp. on differing concentrations of *K. brevis* (Kb) and *P. foliaceum* (Pf). Bars for 50% Kb and 50% Pf represent grazing rates on each food type when fed as a 50:50 mixture. Grazing rates are represented as means with bars showing the standard deviations. Letters above the bars indicate significant differences (ANOVA, $p<0.05$).

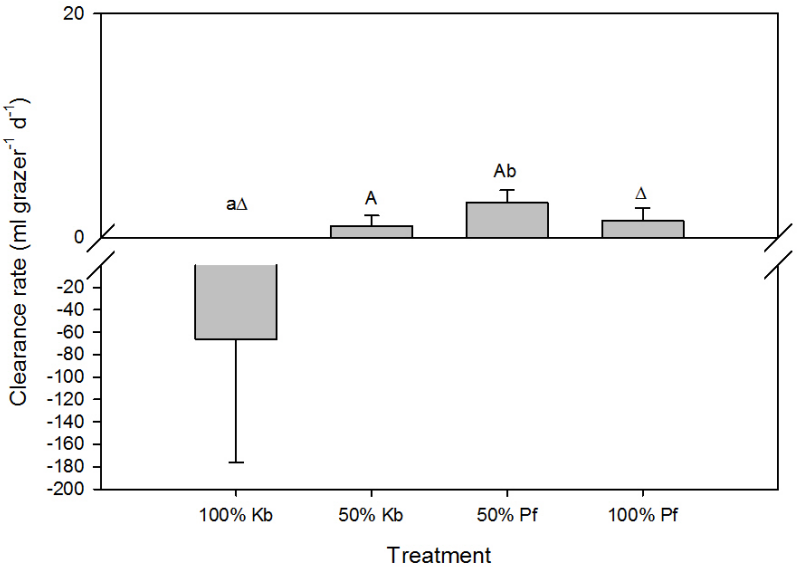

Figure 4.10: Clearance rates for *Protoceratium* sp. on differing concentrations of *K. brevis* (Kb) and *P. foliaceum* (Pf). Bars for 50% Kb and 50% Pf represent clearance rates on each food type when fed as a 50:50 mixture. Clearance rates are represented as means with bars showing the standard deviations. Letters above the bars indicate significant differences (ANOVA, $p<0.05$). Letter case and Greek symbols indicate comparisons that were made.

Grazing rates for *N. scintillans* fed differing concentrations of *G. catenatum* and *P. foliaceum* were positive but not significantly different from each other (Figure 4.11). Grazing rates appeared highest on *G. catenatum* when fed as a 50:50 mixture with *P. foliaceum*. Grazing rates on a sole diet of *P. foliaceum*, a sole diet of *G. catenatum*, and *P. foliaceum* as a 50:50 mixture were similar to each other. Grazing rates for *N. scintillans* were not normally distributed so a non-parametric Tukey Test on ranks was performed on the data. Clearance rates for *N. scintillans* fed differing concentrations of *G. catenatum* and *P. foliaceum* were also positive but not significantly different from each other (Figure 4.12). Clearance rates appeared highest for *G. catenatum* when fed as a 50:50 mixture of *P. foliaceum,* which agreed with the highest grazing rates. Clearance

rates on a sole diet of *P. foliaceum*, a sole diet of *G. catenatum*, and *P. foliaceum* as a 50:50 mixture were similar to each other.

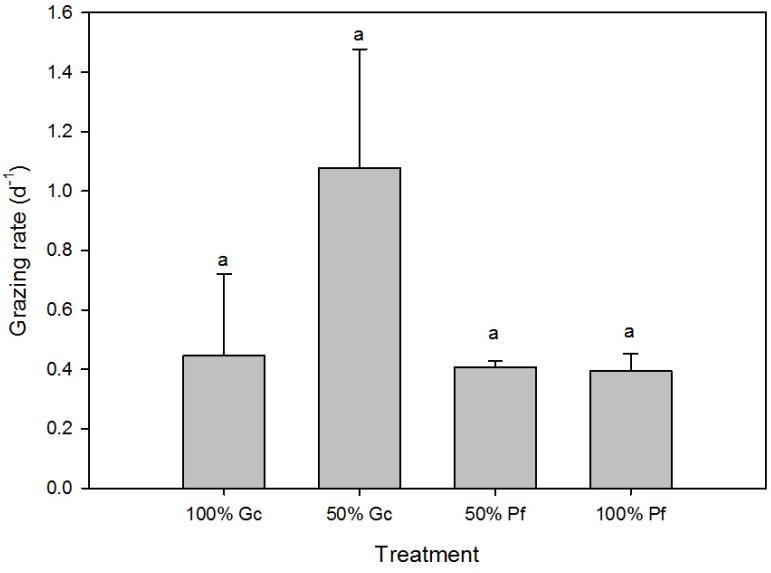

Figure 4.11: Grazing rates for *N. scintillans* on differing concentrations of *G. catenatum* (Gc) and *P. foliaceum* (Pf). Bars for 50% Gc and 50% Pf represent grazing rates on each food type when fed as a 50:50 mixture. Grazing rates are represented as means with bars showing the standard deviations. Letters above the bars indicate significant differences (ANOVA, $p<0.05$).

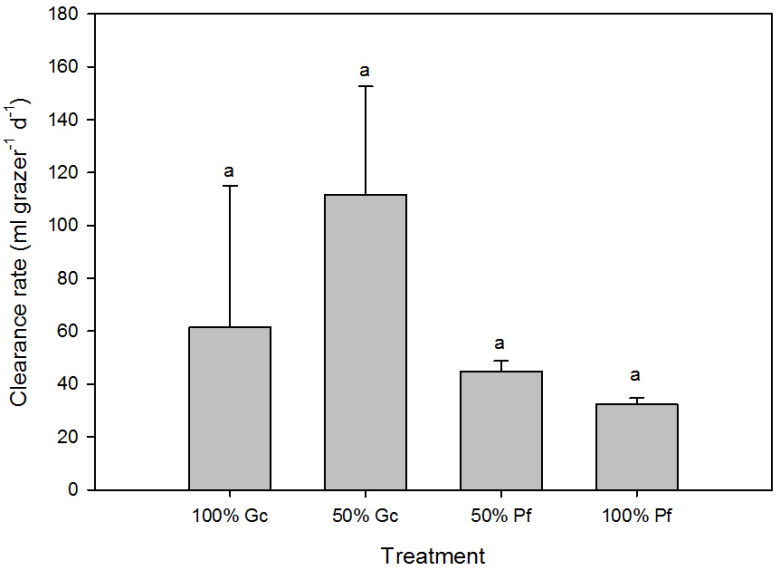

Figure 4.12: Clearance rates for *N. scintillans* on differing concentrations of *G. catenatum* (Gc) and *P. foliaceum* (Pf). Bars for 50% Gc and 50% Pf represent clearance rates on each food type when fed as a 50:50 mixture. Clearance rates are represented as means with bars showing the standard deviations. Letters above the bars indicate significant differences (ANOVA, $p<0.05$).

Grazing rates for *Protoceratium* fed differing concentrations of *G. catenatum* and *P. foliaceum* were positive but not significantly different from each other (Figure 4.13). Grazing rates appeared highest on *G. catenatum* when fed as a sole diet. Grazing rates on a sole diet of *P. foliaceum* and *G. catenatum* in a 50:50 mixture with *P. foliaceum* appeared the lowest of all the food treatments; however, there was large variability in the calculated grazing rates on *G. catenatum* in the food mixture. This variability is likely from mortality rates present in the food mixture controls (data not shown). Clearance rates for *Protoceratium* sp. were not normally distributed so a non-parametric Tukey Test on ranks was performed on the data. There were no significant differences found in clearance rates between each of the food treatments (Figure 4.14). Clearance rates for

Protoceratium sp. appeared highest on *G. catenatum* when given as a 50:50 food mixture with *P. foliaceum*; however, this high clearance rate was probably compounded by the high variability in grazing rates.

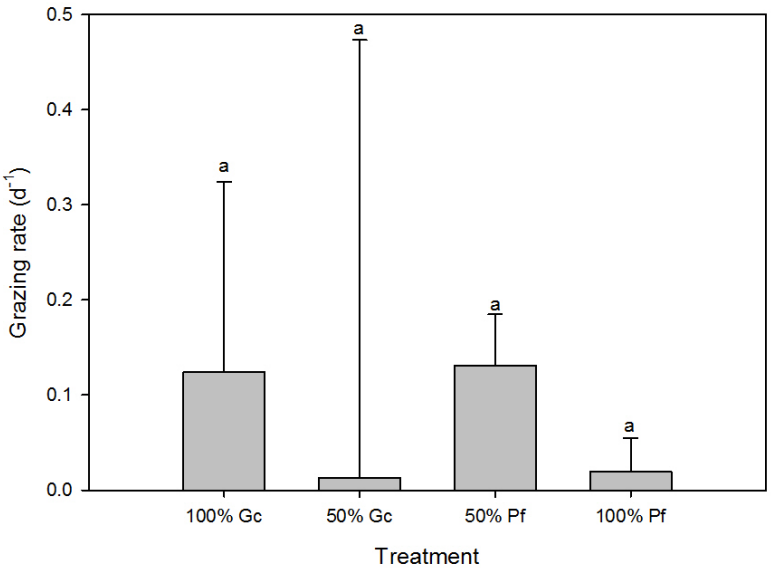

Figure 4.13: Grazing rates for *Protoceratium* sp. on differing concentrations of *G. catenatum* (Gc) and *P. foliaceum* (Pf). Bars for 50% Gc and 50% Pf represent grazing rates on each food type when fed as a 50:50 mixture. Grazing rates are represented as means with bars showing the standard deviations. Letters above the bars indicate significant differences (ANOVA, $p<0.05$).

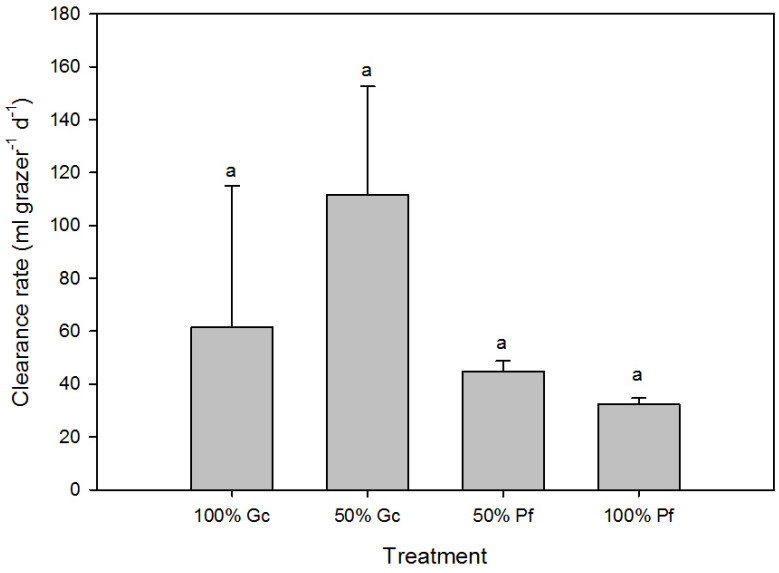

Figure 4.14: Clearance rates for *Protoceratium* sp. on differing concentrations of *G. catenatum* (Gc) and *P. foliaceum* (Pf). Bars for 50% Gc and 50% Pf represent clearance rates on each food type when fed as a 50:50 mixture. Clearance rates are represented as means with bars showing the standard deviations. Letters above the bars indicate significant differences (ANOVA, $p<0.05$).

Grazing rates for *N. scintillans* fed differing concentrations of *A. monilatum* and *P. foliaceum* were positive but not significantly different from each other (Figure 4.15). Grazing rates appeared highest on *A. monilatum* when fed as a 50:50 mixture with *P. foliaceum*. Grazing rates for all other *A. monilatum* food treatments appeared similar to each other. Clearance rates for *N. scintillans* were also positive and not significantly different between the food treatments (Figure 4.16). Clearance rates appeared highest on a diet of *A. monilatum* as a 50:50 mixture with *P. foliaceum*. Lowest clearance rates resulted from a sole diet of *P. foliaceum*. Clearance rates on *P. foliaceum* as a 50:50 food mixture with *A. monilatum* and *A. monilatum* given as a sole diet appeared similar to each other. Although grazing and clearance rates may indicate a grazing control of *N.*

scintillans on *A. monilatum*, *N. scintillans* abundance dropped to near zero in the presence of *A. monilatum* within the first 48 hours while *A. monilatum* abundance continued to decrease throughout the 96 hours (data not shown). *A. monilatum* controls were also declining, thus grazing, clearance, and ingestion rates are an artifact of an unhealthy *A. monilatum* culture.

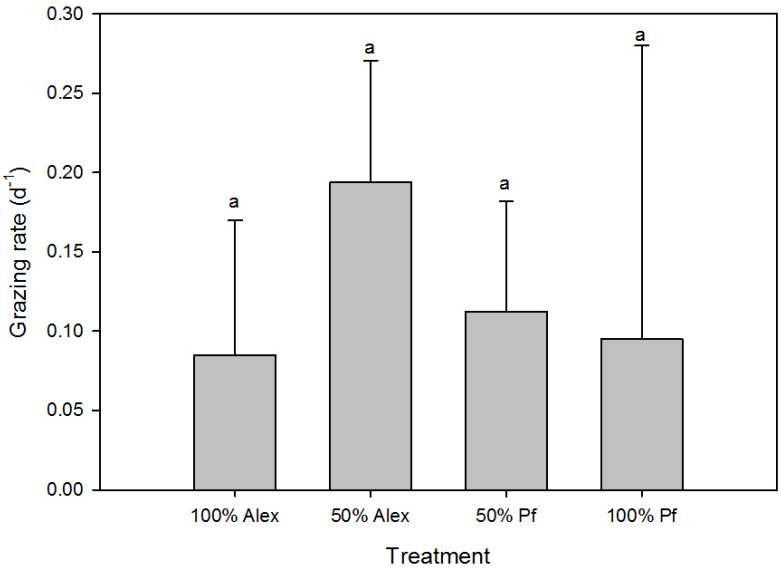

Figure 4.15: Grazing rates for *N. scintillans* on differing concentrations of *A. monilatum* (Alex) and *P. foliaceum* (Pf). Bars for 50% Alex and 50% Pf represent grazing rates on each food type when fed as a 50:50 mixture. Grazing rates are represented as means with bars showing the standard deviations. Letters above the bars indicate significant differences (ANOVA, $p<0.05$).

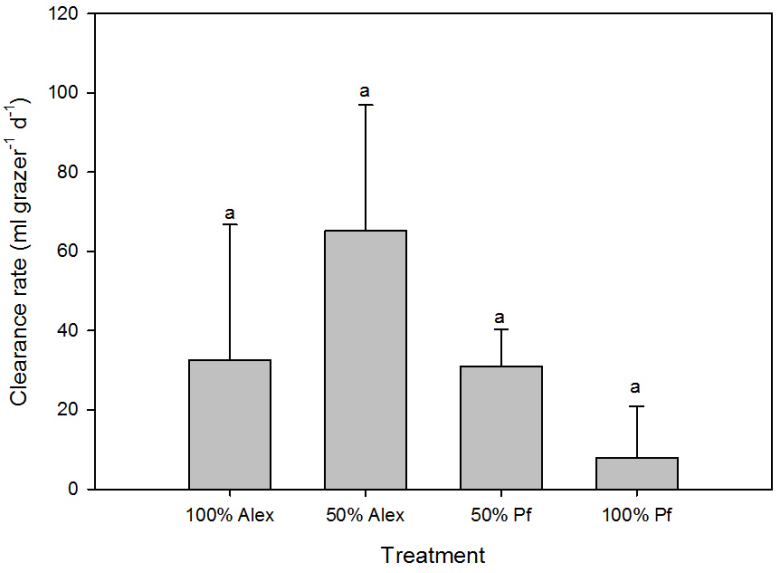

Figure 4.16: Clearance rates for *N. scintillans* on differing concentrations of *A. monilatum* (Alex) and *P. foliaceum* (Pf). Bars for 50% Alex and 50% Pf represent clearance rates on each food type when fed as a 50:50 mixture. Clearance rates are represented as means with bars showing the standard deviations. Letters above the bars indicate significant differences (ANOVA, $p<0.05$).

Grazing rates for *Protoceratium* sp. fed differing concentrations of *A. monilatum* and *P. foliaceum* were not significantly different from each other (Figure 4.17). Grazing rates appeared lowest and negative on *P. foliaceum* when fed as a sole diet, which indicated *P. foliaceum* growth rates higher than grazing losses when compared to controls. Grazing rates on *A. monilatum* as a sole diet and *P. foliaceum* as a food mixture were similar to each other. Grazing rates on *A. monilatum* given in a 50:50 food mixture with *P. foliaceum* appeared the lowest; however these rates were highly variable. Clearance rates for *N. scintillans* were not significantly different between the food treatments (Figure 4.18). A negative clearance rate on a sole diet of *P. foliaceum* agreed with negative grazing rates, which indicated *P. foliaceum* growth faster than

Protoceratium sp. cleared cells from the water. Clearance rates appeared highest on a sole diet of *A. monilatum*. *A. monilatum* cultures appeared physiologically healthy during these grazing experiments with *Protoceratium* sp. (data not shown).

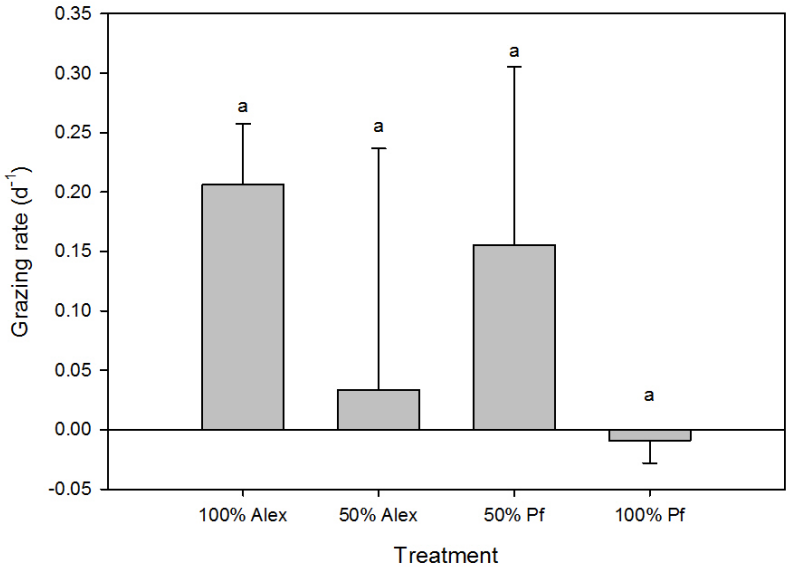

Figure 4.17: Grazing rates for *Protoceratium* sp. on differing concentrations of *A. monilatum* (Alex) and *P. foliaceum* (Pf). Bars for 50% Alex and 50% Pf represent grazing rates on each food type when fed as a 50:50 mixture. Grazing rates are represented as means with bars showing the standard deviations. Letters above the bars indicate significant differences (ANOVA, $p<0.05$).

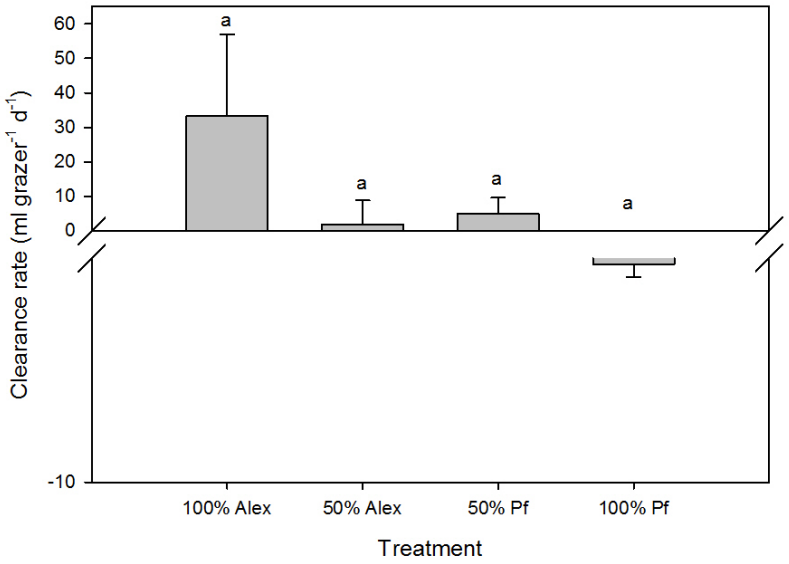

Figure 4.18: Clearance rates for *Protoceratium* sp. on differing concentrations of *A. monilatum* (Alex) and *P. foliaceum* (Pf). Bars for 50% Alex and 50% Pf represent clearance rates on each food type when fed as a 50:50 mixture. Clearance rates are represented as means with bars showing the standard deviations. Letters above the bars indicate significant differences (ANOVA, $p<0.05$).

DISCUSSION

Previous studies provide evidence that protozoan grazers may act as an effective control during bloom initiation rather than during established bloom conditions (Buskey and Hyatt 1995, Jakobsen *et al*. 2001, Buskey 2008). Protozoan grazers may not be capable of controlling established blooms for a couple possible reasons. During blooms or in high-density laboratory cultures, hypoxic events may limit protozoan growth and survival (Buskey 2008). An increase in phytoplankton biomass would lead to an increase in respiration and oxygen demand for both autotrophs and heterotrophs during the dark cycle. An increase in biomass has also caused an increase in pH because of CO_2 drawdown during photosynthesis (Buskey 2008). This increase in pH could also be detrimental to protozoan grazers. Grazing experiments involving protozoa and the brown

tide organism, *Aureoumbra lagunensis*, also showed a possible threshold effect for the effective grazing by protozoa on *A. lagunensis*. Protozoans had the highest growth rates when fed moderate concentrations of *A. lagunensis* (≤1 x 10^5 cells ml^{-1}) with growth decreasing at bloom concentrations (>2.5 x 10^5 cells ml^{-1}; Buskey and Hyatt 1995). The tintinnid ciliate, *Amphorides quadriliniatus*, growth rates also decreased with a food mixture of *A. langunensis* and control food as the proportion of *A. lagunensis* increased (Jakobsen *et al*. 2001). High grazer growth rates at moderate HAB species cell concentration would be indicative of a possible "top down" control during bloom initiation.

Although *Protoceratium* sp. and *Noctiluca scintillans* may feed on HAB species, they may not be capable of effective control during established bloom conditions. Both grazers experienced reduced growth rates with starting food concentrations of 290 cells ml^{-1} for *K. brevis*, 115 cells ml^{-1} for *G. catenatum*, and 53 cells ml^{-1} for *A. monilatum*. Although most grazing and clearance rates were positive in treatments where HABs were present, the HAB populations did not decline to zero with grazer concentrations of 3 ml^{-1} for *N. scintillans* and 6 ml^{-1} for *Protoceratium* sp. If the grazer population disappears while there are still HAB cells present, the bloom could recover and persist. These findings are similar to those from grazing experiments involving the tintinnid ciliate, *Favella ehrenbergii* and the dinoflagellate *Gyrodinium aureolum*. When fed mixed and monocultures of *G. aureolum*, *F. ehrenbergii* experienced reduced growth rates when prey populations were at least 70% *G. aureolum* (Hansen 1995). *G. aureolum* cell concentrations as low as 200 cells ml^{-1} stopped ciliate population growth and rates decreased slowly with time (Hansen 1995).

There were also some instances where grazing and clearance rates indicated that HAB growth was stimulated compared to controls in the presence of grazers. In the

presence of *Protoceratium* sp., *K. brevis* exhibited stimulated growth when compared to controls when given as a sole diet. The positive *K. brevis* growth rate could be indicative of *Protoceratium* sp. cell waste and other exudates stimulating *K. brevis* growth or *Protoceratium* sp. avoidance of *K. brevis* cells allowing the HAB to grow. However, short-term grazing experiments have indicated that *Protoceratium* sp. will ingest *K. brevis* when it is a sole diet or a mixture with *P. foliaceum*. When given in a 50:50 food mixture, *Protoceratium* sp. showed higher grazing and clearance rates on the *P. foliaceum* rather than the *K. brevis* fraction of the diet. This grazing and clearance difference could result from *Protoceratium* selective feeding on *P. foliaceum*, releasing *K. brevis* from nutrient competition and "top down" control.

Although the results of these grazing experiments may indicate the potential of *A. monilatum* bloom control by *N. scintillans* because of high grazing rates on the *A. monilatum* food mixture with *P. foliaceum*, these results can be misleading. *N. scintillans* abundances in experimental bottles containing a sole diet of *A. monilatum* or a 50:50 mixture with *P. foliaceum* dropped to near zero within the first 48 hours of the experiment; however, *A. monilatum* abundance continued to drop throughout the 96 hour experiment. Controls of *A. monilatum* also decreased over the experimental period. What may be seen as high grazing, clearance, and ingestion rates may be an artifact of an unhealthy *A. monilatum* culture. Previous shorter grazing experiments (1-8 hours) indicated that *N. scintillans* would not feed on *A. monilatum* and many were shriveled and dead within 8 hours (see Chapter 3); thus, high grazing rates on *A. monilatum* during these 96-hour grazing experiments were not expected. *A. monilatum* cultures used for the *Protoceratium* sp. grazing experiments were healthy as indicated by *A. monilatum* growth in control bottles (data not shown).

Although there is much evidence to suggest that protozoan and metazoan grazers may not be capable of controlling established blooms, there are some instances where grazers have caused a bloom population to decrease. In the western Yatsushiro Sea off the coast of Kyushu Island, blooms of *G. catenatum* occur (Matsuyama *et al*. 1999). Co-occurring with this species is the heterotrophic dinoflagellate *Polykrikos kofoidii*, which appears to naturally feed on *G. catenatum* (Matsuyama *et al*. 1999). Field and vessel tests revealed that >50% of the *P. kofoidii* population grazed on natural populations of *G. catenatum* and up to eight *G. catenatum* cells were found in *P. kofoidii* food vacuoles (Matsuyama *et al*. 1999). *P. kofoidii* suffers no apparent negative impacts from grazing on *G. catenatum* and provides strong evidence for an ability to control the blooms (Matsuyama *et al.* 1999). In the same way, tintinnid ciliates were able to graze on and cause the decline of a *Phaeocystis pouchetii* bloom in Dutch coastal waters (Admiraal and Venekamp 1986). Toward the end of the bloom, tintinnid populations exceeded those of *P. pouchetii*, showing that the ciliates were able to graze and exceed the growth rate of *P. pouchetii* (Admiraal and Venekamp 1986).

In a similar study, tintinnid ciliates *F. ehrenbergii*, *Eutintinnus pectinis*, and *Metacylis angulata* and non-loricate ciliates *Strombidinopsis* sp. and *Strombidium conicum* were fed two HAB species *Prymnesium parvum* and *Prorocentrum minimum* (Rosetta and McManus 2003). Although the ciliates did experience acute toxicity and mortality at high concentrations of $2x10^4$-$3x10^4$ cells ml^{-1}, they were able to survive and grow well at low concentrations ($5x10^3$–$1x10^4$ cells ml^{-1}) or in mixed cultures with non-toxic species (Rosetta and McManus 2003). As the population of HAB species increases the amount of toxins increases. Because the ciliates are able to graze on the HAB species before bloom conditions, these ciliates may play a role in preventing initiation of *P. parvum* and *P. minimum* blooms (Rosetta and McManus 2003).

These same results are reflected in the grazing experiments of this study. In some cases, the grazers grow as well as and sometimes faster on a 50:50 food mixture as on control food. There is the potential for a "top down" control at lower, pre-bloom cell concentrations. As previously mentioned, *K. brevis* showed stimulated growth compared to controls when in the presence of *Protoceratium* sp. However, *Protoceratium* sp. showed the highest grazing and clearance rates when given sole and mixed diets of *A. monilatum* and *G. catenatum*. *Protoceratium* sp. could serve as an effective "top down" control at lower *A. monilatum* and *G. catenatum* cell concentrations. *N. scintillans* also experienced a positive growth rate when given a 50% food mixture of *K. brevis*. The highest grazing and clearance rates of *N. scintillans* when fed differing concentrations of *K. brevis* and *P. foliaceum* also occurred on the *K. brevis* fraction of the 50:50 food mixtures. While a 50% (145 cells ml^{-1}) concentration of *K. brevis* would still be considered a bloom situation, *N. scintillans* could provide a "top down" control at lower *K. brevis* cell concentrations.

Grazing and clearance rates are difficult to calculate accurately for protozoan grazers. In general heterotrophic dinoflagellates will ingest one cell at a time when given larger food particles (see Chapter 3). A protozoan grazer ingesting one cell at a time out of over 100 cells ml^{-1} would create a small grazing impact unless the grazer concentrations were higher. Grazing and ingestion rates for this experiment were unusually high in comparison to other studies. In a tidal creek in the Duplin River estuary, Sapelo Island, GA, small flagellate (5-15 μm) and ciliate (15-60 μm) clearance rates on <6 μm fluorescently labeled algae (FLA) ranged from $9.6x10^{-5}$ – 0.01992 ml $grazer^{-1}$ d^{-1} and 0.00576 – 0.1992 ml $grazer^{-1}$ d^{-1}, respectively (Sherr *et a*l. 1991). These rates extrapolated over a 4-month period resulted in estimates of 45% water volume and 107% water volume cleared if based on ingestion of 2 μm FLA and larger FLA cells,

respectively. Similarly, nine ciliate species from the Gulf of Finland exhibited clearance rates of 0.0456 – 0.2736 ml grazer^{-1} d^{-1} when given food of their preferred particle size (Kivi and Setälä 1995). The unusually high clearance rates in the current study likely resulted from high sampling variability, low levels of cell ingestion per grazer, and mortality present in some of the food controls.

Although there are few studies that have looked at protozoan grazing and clearance rates on HAB species, copepods appear to have similar responses. Like *N. scintillans* and *Protoceratium* sp. grazing and clearance rates, the copepod *Acartia tonsa* exhibited higher grazing and clearance rates when fed a mixture of *K. brevis* and *P. foliaceum* than a sole diet of *K. brevis* (Breier and Buskey 2006). In contrast to *N. scintillans* and *Protoceratium* sp., bivalves fed sole diets of *A. monilatum* or mixtures with non-toxic algae showed lower clearance and grazing rates than those bivalves fed only non-toxic algae (May *et al*. 2010). *N. scintillans* and *Protoceratium* sp. showed higher grazing and clearance rates when given varying diets of *A. monilatum*, which could indicate a possible "top down" control. Also unlike *N. scintillans* and *Protoceratium* sp., mesozooplankton grazing rates appeared to be depressed by the possible presence of *G. catenatum* during natural incubation experiments (Calbet *et al*. 2002). The results of this study show that the protozoa exhibited highest clearance and grazing rates at stations with the lowest *G. catenatum* abundances (2.0 x 10^6 cells m^{-2}) and lowest grazing rates at stations with highest *G. catenatum* (4.0 x 10^6 – 1.3 x 10^8 cells m^{-2}), which could indicate another possible "top down" control mechanism by protozoa as opposed to mesozooplankton.

There is still much to be discovered concerning food web dynamics between HAB species and protozoan grazers. The next step would involve growth experiments with ciliates and heterotrophic dinoflagellates found to ingest *K. brevis* during a natural bloom

to determine possible grazing pressure. Unfortunately, ciliates were not used for this study because of the failure to establish cultures. However, a recent bloom of *K. brevis* from September 2011 through January 2012 provided more insight on potential grazers of *K. brevis*. Polymerase chain reaction analysis resulted in the detection of *K. brevis* DNA within the heterotrophic dinoflagellate *Gyrodinium spirale* and the ciliates *Strombidinopsis* sp. and *Tontonia* sp. (see results of Chapter 3). Laboratory grazing experiments with these three grazers could help determine the potential grazing impact on *K. brevis*. Being able to calculate and identify these impacts will provide us with more detailed information on HAB dynamics, possibly leading to more precise monitoring and early warning systems and the development of bloom remediation approaches.

References

Admiraal W, Venekamp LAH (1986) Significance of tintinnid grazing during blooms of *Phaeocystis pouchetii* (Haptophyceae) in Dutch coastal waters. Netherlands Journal of Sea Research 20:61-66

Álvarez E, López-Urrutia Á, Nogueira E (2012) Improvement of plankton biovolume estimates derived from image-based automatic sampling devices: application to FlowCAM. Journal of Plankton Research 34:454-469

Anderson P, Sorensen HM (1986) Population dynamics and trophic coupling of pelagic microorganisms in eutrophic coastal waters. Marine Ecology Progress Series 33:99-109

Armstrong NE (1987) The ecology of open-bay bottoms in Texas: a community profile. 85:1-104. Washington, DC, USFWS Biological Report

Barría de Cao MS, Beigt D, Piccolo C (2005) Temporal variability of diversity and biomass of tintinnids (Ciliophora) in a southwestern Atlantic temperate estuary. Journal of Plankton Research 27:1103-1111

Barreiro A, Guisande C, Frangópulos M, González-Fernández A, Muñoz S, Pérez D, Magadán S, Maneiro I, Riveiro I, Iglesias P (2006) Feeding strategies of the copepod *Acartia clausi* on single and mixed diets of toxic and non-toxic strains of the dinoflagellate *Alexandrium minutum*. Marine Ecology Progress Series 316:115-125

Beers JR, Reid FMH, Stewart GL (1982) Seasonal abundance of the microplankton populations of the North Pacific central gyre. Deep Sea Research 29:227-245

Bernard C, Rassoulzadegan F (1990) Bacteria or microflagellates as a major food source for marine ciliates: possible implications for the microzooplankton. Marine Ecology Progress Series 64:147-155

Bersano JGF, Buskey EJ, Villareal TA (2002) Viability of the Texas brown tide alga, *Aureoumbra lagunensis*, in fecal pellets of the copepod *Acartia tonsa*. Plankton Biology and Ecology 49:88-92

Bidle KD, Bender SJ (2008) Iron starvation and culture age activate metacaspases and programmed cell death in the marine diatom *Thalassiosira pseudonana*. Eukaryotic Cell 7:223-236

Bockstahler KR, Coats DW (1993) Grazing of the mixotrophic dinoflagellate *Gymnodinium sanguineum* on ciliate populations of Chesapeake Bay. Marine Biology 116:477-487

Breier CF, Buskey EJ (2006) Effects of the red tide dinoflagellate, *Karenia brevis*, on grazing and fecundity in the copepod *Acartia tonsa*. Journal of Plankton Research 29:115-126

Broglio E, Johansson M, Jonsson PR (2001) Trophic interaction between copepods and ciliates: effects of prey swimming behavior on predation risk. Marine Ecology Progress Series 220:179-186

Buffan-Dubau E, de Wit R, Castel J (1996) Feeding selectivity of the harpacticoid copepod *Canuella perplexa* in benthic muddy environments demonstrated by HPLC analyses of chlorin and carotenoid pigments. Marine Ecology Progress Series 137:71-82

Burkill PH, Mantoura RFC, Llewellyn CA, Owens NJP (1987) Microzooplankton grazing and selectivity of phytoplankton in coastal waters. Marine Biology 93:581-590

Buskey EJ (1993) Annual pattern of micro- and mesozooplankton abundance and biomass in a subtropical estuary. Journal of Plankton Research 15:907-924

Buskey EJ (1995) Growth and bioluminescence of *Noctiluca scintillans* on varying algal diets. Journal of Plankton Research 17:29-40

Buskey EJ (2008) How does eutrophication affect the role of grazers in harmful algal bloom dynamics? Harmful Algae 8:152-157

Buskey EJ, DeYoe H, Jochem FJ, Villareal TA (2003) Effects of mesozooplankton removal and ammonium addition on planktonic trophic structure during a bloom of the Texas 'brown tide': a mesocosm study. Journal of Plankton Research 25:215-228

Buskey EJ, Hyatt CJ (1995) Effects of the Texas (USA) "brown tide" alga on planktonic grazers. Marine Ecology Progress Series 126:285-292

Buskey EJ, Hyatt CJ (2006) Use of the FlowCAM for semi-automated recognition and enumeration of red tide cells (*Karenia brevis*) in natural plankton samples. Harmful Algae 5:685-692

Buskey EJ, Montagna PA, Amos AF, Whitledge TE (1997) Disruption of grazer populations as a contributing factor to the initiation of the Texas brown tide algal bloom. Limnology and Oceanography 42:1215-1222

Buskey EJ, Wysor B, Hyatt C (1998) The role of hypersalinity in the persistence of the Texas "brown tide" in the Laguna Madre. Journal of Plankton Research 20:1553-1565

Butrón A, Iriarte A, Madariaga I (2009) Size-fractionated phytoplankton biomass, primary production, and respiration in the Nervión-Ibaizabal estuary: A comparison with other nearshore coastal and estuarine ecosystems from the Bay of Biscay. Continental Shelf Research 29:1088-1102

Calbet A, Broglio E, Saiz E, Alcaraz M (2002) Low grazing impact of mesozooplankton on the microbial communities of the Alboran Sea: a possible case of the inhibitory

effects of the toxic dinoflagellate *Gymnodinium catenatum*. Aquatic Microbial Ecology 26:235-246

Campbell L, Olson RJ, Sosik HM, Abraham A, Henrichs DW, Hyatt CJ, Buskey EJ (2010) First harmful *Dinophysis* (Dinophyceae, Dinophysiales) bloom in the US is revealed by automated imaging flow cytometry. Journal of Phycology 46:66-75

Chandler C, Knox J, Byrd L (Eds) (1981) Nueces and Mission-Aransas Estuaries: a study of the influence of freshwater inflows. Austin, Texas, Texas Department of Water Resources. LP-108

Christoffersen K, Nybroe O, Jürgens K, Hansen M (1997) Measurement of bacterivory by heterotrophic nanoflagellates using immunofluorescence labeling of ingested cells. Aquatic Microbial Ecology 13:127-134

Choi JW, Stoecker DW (1989) Effects of fixation on cell volume of marine planktonic protozoa. Applied and Environmental Microbiology 55:1761-1765

Claustre H, Poulet SA, Williams R, Marty JC, Coombs S, Ben Mlih F, Hapette AM, Martin-Jezequel V (1990) A biochemical investigation of *Phaeocystis* sp. bloom in the Irish Sea. Journal of the Marine Biological Association of the United Kingdom 70:197-207

Colin SP, Dam HG (2002) Latitudinal differentiation in the effects of the toxic dinoflagellate *Alexandrium* sp. on the feeding and reproduction of populations of the copepod *Acartia hudsonica*. Harmful Algae 1:113-125

Colin SP, Dam HG (2003) Effects of the toxic dinoflagellate *Alexandrium fundyense* on the copepod *Acartia hudsonica*: a test of the mechanisms that reduce ingestion rates. Marine Ecology Progress Series 248:55-65

Connell CH, Cross JB (1950) Mass mortality of fish associated with the protozoan *Gonyaulax* in the Gulf of Mexico. Science 112:359-363

Crawford DW (1992) Metabolic cost of motility in planktonic protists: theoretical considerations on size scaling and swimming speed. Microbial Ecology 24:1-10

Crespo BG, Figueiras FG (2007) A spring poleward current and its influence on microplankton assemblages and harmful dinoflagellates on the western Iberian coast. Harmful Algae 6:686-699

Cushing DH (1959) The seasonal variation in oceanic production as a problem in population dynamics. Journal du Conseil Permanent International Pour l'Exploration de la Mer 24:455-464

Davis CS (1987) Components of the zooplankton production cycles in the temperate ocean. Journal of Marine Research 45:947-983

Demir E, Coyne KJ, Doblin MA, Handy SM, Hutchins DA (2008) Assessment of microzooplankton grazing on *Heterosigma akashiwo* using a species-specific

approach combining quantitative PCR (QPCR) and dilution methods. Microbial Ecology 55:583-594

DeYoe HR, Suttle CA (1994) The inability of Texas "brown tide" alga to use nitrate and the roll of nitrogen in the initiation of a persistent bloom of this organism. Journal of Phycology 30:800-806

Doblin MA, Blackburn SI, Hallegraeff GM (1999) Growth and biomass stimulation of the toxic dinoflagellate *Gymnodinium catenatum* (Graham) by dissolved organic substances. Journal of Experimental Marine Biology and Ecology 236:33-47

Dutz J (1998) Repression of the fecundity of the neritic copepod *Acartia clausi* exposed to the toxic dinoflagellate *Alexandrium lusitanicum*: relationship between feeding and egg production. Marine Ecology Progress Series 175:97-107

Egge JK (1998) Are diatoms poor competitors at low phosphate concentrations? Journal of Marine Systems 16:191-198

Eppley RW, Rogers JN, McCarthy JJ (1969) Half-saturation constants for uptake of nitrate and ammonium by marine phytoplankton. Limnology and Oceanography 14:912-920

Epstein SS, Burkovsky IV, Shiaris MP (1992) Ciliate grazing on bacteria, flagellates, and microalgae in a temperate zone sandy tidal flat: ingestion rates and food niche portioning. Journal of Experimental Marine Biology and Ecology 165:103-123

Erdner DL, Percy L, Keafer B, Lewis J, Anderson DM (2010) A quantitative real-time PCR assay for the identification and enumeration of *Alexandrium* cysts in marine sediments. Deep-Sea Research II 57:279-287

Frangópulos M, Guisande C, Maneiro I, Riveiro I, Franco J (2000) Short-term and long-term effects of the dinoflagellate *Alexandrium minutum* on the copepod *Acartia clausi*. Marine Ecology Progress Series 203:161-169

Franklin DJ, Berges JA (2004) Mortality in cultures of the dinoflagellate *Amphidinium carterae* during culture senescence and darkness. Proceedings of the Royal Society London B 271:2099-2107

Fredrickson KA, Strom SL (2009) The algal osmolyte DMSP as a microzooplankton grazing deterrent in laboratory and field studies. Journal of Plankton Research 31:135-152

Freese LR (1952) Marine diatoms of the Rockport, Texas, bay area. The Texas Journal of Science 4:331-386

Frost BW (1972) Effects of size and concentration of food particles on the feeding behavior of the marine planktonic copepod *Calanus pacificus*. Limnology and Oceanography 17:801-815

Galluzzi L, Penna A, Bertozzini E, Giacobbe MG, Vila M, Garcés E, Prioli S, Magnani M (2005) Development of a qualitative PCR method for *Alexandrium* spp. (Dinophyceae) detection in contaminated mussels (*Mytilus galloprovincialis*). Harmful Algae 4:973-983

Gates JA, Wilson WB (1960) The toxicity of *Gonyaulax monilata* Howell to *Mugil cephalis*. Limnology and Oceanography 5:171-174

Gifford DJ, Dagg MJ (1988) Feeding of the estuarine copepod *Acartia tonsa* Dana: carnivory vs. herbivory in natural microplankton assemblages. Bulletin of Marine Science 43:458-468

Gilbert JJ (1994) Susceptibility of planktonic rotifers to a toxic strain of *Anabaena flos-aquae*. Limnology and Oceanography 39:1286-1297

Gill CW, Harris RP (1987) Behavioural responses of the copepods *Calanus helgolandicus* and *Temora longicornis* to dinoflagellate diets. Journal of the Marine Biological Association of the United Kingdom 67:785-801

Guadayol Ò, Marrasé C, Peters F, Berdalet E, Roldan C, Sabata A (2009) Responses of coastal osmotrophic planktonic communities to simulated events of turbulence and nutrient load throughout a year. Journal of Plankton Research 31:583-600

Guillard RRL (1975) Culture of phytoplankton for feeding marine invertebrates. In: Smith WL, Chanley MH (Eds) Cultures of marine invertebrate animals. Plenum Press, New York, pp. 29-60

Guillard RRL, Hargraves PE (1993) *Stichochrysis immobilis* is a diatom, not a chrysophyte. Phycologia 32:234-236

Hallegraeff GM (1993) A review of harmful algal blooms and their apparent global increase. Phycologia 32:79-99

Hallegraeff GM (1995) Harmful algal blooms: a global overview. In: Hallegraeff GM, Anderson DM, Cembella AD (Eds) Manual on harmful marine microalgae. pp. 1-22. IOC Manuals and Guidelines No. 33. UNESCO: Paris

Hansen FC, Reckermann M, Klein Breteler WCM, Reigman R (1993) *Phaeocystis* blooming enhanced by copepod predation on protozoa: evidence from incubation experiments. Marine Ecology Progress Series 102:51-57

Hansen PJ (1989) The red tide dinoflagellate *Alexandrium tamarense*: effects on behavior and growth of a tintinnid ciliate. Marine Ecology Progress Series 53:105-116

Hansen PJ (1995) Growth and feeding response of a ciliate feeding on the red tide dinoflagellate *Gyrodinium aureolum* in a monoculture and mixture with a non-toxic alga. Marine Ecology Progress Series 121:65-72

Harding JM, Mann R, Moeller P, Hsia MH (2009) Mortality of the veined rapa whelk, *Rapana venosa*, in relation to a bloom of *Alexandrium monilatum* in the York River, United States. Journal of Shellfish Research 28:363-367

Head EJH, Harris LR (1994) Feeding selectivity by copepods grazing on natural mixtures of plankton determined by HPLC analysis of pigments. Marine Ecology Progress Series 110:75-83

Heinbokel JF (1978) Studies on the functional role of tintinnids in the Southern California Bight. I. Grazing and growth rates in laboratory cultures. Marine Biology 47:177-189

Henrichs DW, Sosik HM, Olson RJ, Campbell L (2011) Phylogenetic analysis of *Brachidinium capitatum* (DINOPHYCEAE) from the Gulf of Mexico indicates membership in the Kareniaceae. Journal of Phycology 47:366–374

Hofstetter RP (1965) The Texas Oyster Fishery. Texas Parks and Wildlife Department. Bulletin No. 40

Horner RA, Garrison DL, Plumley FG (1997) Harmful algal blooms and red tide problems on the U.S. west coast. Limnology and Oceanography 42:1076-1088

Howell JF (1953) *Gonyaulax monilata*, sp. nov., the causative dinoflagellate of a red tide on the East Coast of Florida in August-September, 1951. Transactions of the American Microscopical Society 72:153-156

Hsia MH, Morton SL, Smith LL, Beauchesne KR, Huncik KM, Moeller PDR (2006) Production of goniodomin A by the planktonic, chain-forming dinoflagellate *Alexandrium monilatum* (Howell) Balech isolated from the Gulf Coast of the United States. Harmful Algae 5:290-299

Hunt HE, Slack RD (1989) Winter diets of whooping and sandhill cranes in south Texas. The Journal of Wildlife Management 53:1150-1154

Huntley M, Sykes P, Rohan S, Marin V (1986) Chemically-mediated rejection of dinoflagellate prey by the copepods *Calanus pacificus* and *Paracalanus parvus*: mechanism, occurrence and significance. Marine Ecology Progress Series 28:105-120

Ives JD (1987) Possible mechanisms underlying copepod grazing responses to levels of toxicity in red tide dinoflagellates. Journal of Experimental Marine Biology and Ecology 112:131-145

Jakobsen HH (2001) Escape response of planktonic protists to fluid mechanical signals. Marine Ecology Progress Series 214:67-78

Jakobsen HH, Hyatt CJ, Buskey EJ (2001) Growth and grazing on the "Texas brown tide" forming alga *Aureoumbra lagunensis* by the tintinnid *Amphorides quadriliniatus*. Aquatic Microbial Ecology 23:245-252

Jerome CA, Montagnes DJS, Taylor FJR (1993) The effect of the quantitative protargol stain and Lugol's and Bouin's fixatives on cell size: a more accurate estimate of ciliate species biomass. Journal of Eukaryotic Microbiology 40:254-259

Juhl AR (2005) Growth rates and elemental composition of *Alexandrium monilatum*, a red-tide dinoflagellate. Harmful Algae 4:287-295

Kivi K, Setälä O (1995) Simultaneous measurement of food particle selection and clearance rates of planktonic oligotrich ciliates (Ciliophora: Oligotrichina). Marine Ecology Progress Series 119:125-137

Leary SP (1964) The crabs of Texas. Texas Parks and Wildlife Department. Bulletin No. 43

Lynn DH, Gilron GL (1993) Strombidiid ciliates from coastal waters near Kingston Harbour, Jamaica (Ciliophora, Oligotrichia, Strombidiidae). Journal of the Marine Biological Association of the United Kingdom 73:47-65

Mackey M, Mackey D, Higgins H, Wright S (1996) CHEMTAX – a program for estimating class abundances from chemical markers: application to HPLC measurements of phytoplankton. Marine Ecology Progress Series 144:265-283

Matsuyama Y, Miyamoto M, Kotani Y (1999) Grazing impacts of the heterotrophic dinoflagellate *Polykrikos kofoidii* on a bloom of *Gymnodinium catenatum*. Aquatic Microbial Ecology 17:91-98

May SP, Burkholder JM, Shumway SE, Hégaret H, Wikfors GH, Frank D (2010) Effects of the toxic dinoflagellate *Alexandrium monilatum* on survival, grazing and behavioral response of three ecologically important bivalve molluscs. Harmful Algae 9:281-293

McDonnell TA (1998) Growth and feeding behavior of an unclassified heterotrophic dinoflagellate species. Masters Thesis. The University of Texas at Austin. 57 pgs.

McQuoid MR (2005) Influence of salinity on seasonal germination of resting stages and composition of microplankton on the Swedish west coast. Marine Ecology Progress Series 289:151-163

Miller CA, Penry DL, Glibert PM (1995) The impact of trophic interactions on rates of nitrogen regeneration and grazing in Chesapeake Bay. Limnology and Oceanography 40:1005-1011

Millie DF, Paerl HW, Hurley J (1993) Microalgal pigment assessments using high performance liquid chromatography: a synopsis of organismal and ecological applications. Canadian Journal of Fisheries and Aquatic Science 50:2513-2527

Moffett AW (1990) The shrimp fishery in Texas. Texas Parks and Wildlife Department.

Mooney R, McClelland J (in press) Watershed export events and ecosystem responses in the Mission-Aransas National Estuarine Research Reserve, south Texas. Estuaries and Coasts

Mortan RA, McGowen JH (1980) Modern depositional environments of the Texas coast. Austin, TX, Bureau of Economic Geology, The University of Texas, pp. 1-167

National Oceanic and Atmospheric Administration (NOAA) (1993) Salinity characteristics of Gulf of Mexico estuaries. Rockville, MD, Strategic Environmental Assessments Division

Nejstgaard JC, Frischer ME, Simonelli P, Troedsson C, Brakel M, Adiyaman F, Sazhin AF, Artigas LF (2008) Quantitative PCR to estimate copepod feeding. Marine Biology 153:565-577

Ohman MD (1992) Immunochemical recognition of oligotrich ciliates. Marine Biology 114:653-660

Olson RJ, Sosik HM (2007) A submersible imaging-in-flow instrument to analyze nano- and microplankton: Imaging FlowCytobot. Limnology and Oceanography: Methods 5:195-203

Örnólfsdóttir EB, Lumsden SE, Pinckney JL (2004) Nutrient pulsing as a regulator of phytoplankton abundance and community composition in Galveston Bay, Texas. Journal of Experimental Marine Biology and Ecology 303:197-220

Oshima Y, Hasegawa M, Yasumoto T, Hallegraeff G, Blackburn S (1987) Dinoflagellate *Gymnodinium catenatum* as the source of paralytic shellfish toxins in Tasmanian shellfish. Toxicon 25:1105-1111

Paerl HW, Valdes LM, Pinckney JL, Piehler MF, Dyble J, Moisander PH (2003) Phytoplankton photopigments as indicators of estuarine and coastal eutrophication. Bioscience 53:953-964

Park GS, Marshall HG (2000) Estuarine relationships between zooplankton community structure and trophic gradients. Journal of Plankton Research 22:121-135

Patil JG, Gunasekera RM, Deagle BE, Bax NJ, Blackburn SI (2005) Development and evaluation of a PCR based assay for detection of the dinoflagellate, *Gymnodinium catenatum* (Graham) in ballast water and environmental samples. Biological invasions 7:983-994

Pierce RH, Brown RC, Kucklick JR (1985) Analysis of *Ptychodiscus brevis* toxins by reverse phase HPLC. In: Anderson DM, White AW, Baden DG (Eds) Toxic Dinoflagellates. pp. 309-314. Elsevier: New York

Pitta P, Giannakourou A, Christaki U (2001) Planktonic ciliates in the oligotrophic Mediterranean Sea: longitudinal trends of standing stocks, distributions and analysis of food vacuole contents. Aquatic Microbial Ecology 24:297-311

Poli MA, Musser SM, Dickey RW, Eilers PP, Hall S (2000) Neurotoxic shellfish poisoning and brevetoxin metabolites: a case study from Florida. Toxicon 38:981-993

Porter KG (1973) Selective grazing and differential digestion of algae by zooplankton. Nature 233:179-180

Porter KG (1976) Enhancement of algal growth and productivity by grazing zooplankton. Science 192:1332-1334

Reid FMH (1983) Biomass estimation of components of the marine nanoplankton and picoplankton by the Utermöhl settling technique. Journal of Plankton Research 5:235-252

Robineau B, Gagné JA, Fortier L, Cembella AD (1991) Potential impact of a toxic dinoflagellate (*Alexandrium excavatum*) bloom on survival of fish and crustacean larvae. Marine Biology 108:293-301

Rosetta CH, McManus GB (2003) Feeding by ciliates on two harmful algal bloom species, *Prymnesium parvum* and *Prorocentrum minimum*. Harmful Algae 2:109-126

Sanders RW (1987) Tintinnids and other microzooplankton – seasonal distributions and relationships to resources and hydrography in a Maine estuary. Journal of Plankton Research 9:65-77

Sellner KG, Olson MM, Kononen K (1994) Copepod grazing in a summer cyanobacteria bloom in the Gulf of Finland. Hydrobiologia 292/293:249-254

Setälä O, Autio R, Kuosa H (2005) Predator-prey interactions between a planktonic ciliate *Strombidium* sp. (Ciliophora, Oligotrichida) and the dinoflagellate *Pfiesteria piscicida* (Dinamoebiales, Pyrrophyta). Harmful Algae 4:235-247

Shaw BA, Andersen RJ, Harrison PJ (1995) Feeding deterrence properties of apo-fucoxanthinoids from marine diatoms. I. Chemical structures of apo-fucoxanthinoids produced by *Phaeodactylum tricornutum*. Marine Biology 124:467-472

Shaw BA, Anderson RJ, Harrison PJ (1997) Feeding deterrent and toxicity effects of apo-fucoxanthinoids and phycotoxins on a marine copepod (*Tigriopus californicus*). Marine Biology 128:273-280

Sherr EB, Sherr BF, McDaniel J (1991) Clearance rates of <6 μm fluorescently labeled algae (FLA) by estuarine protozoa: potential grazing impact of flagellates and ciliates. Marine Ecology Progress Series 69:81-92

Sieracki CK, Sieracki ME, Yentsch CS (1998) An imaging-in-flow system for automated analysis of marine microplankton. Marine Ecology Progress Series 168:285-296

Simmons EG, Bruer JP (1967) The Texas menhaden fishery. Texas Parks and Wildlife Department. Bulletin No. 45A

Smayda TJ (1997) Harmful algal blooms: their ecophysiology and general relevance to phytoplankton blooms in the sea. Limnology and Oceanography 42:1137-1153

Sosik HM, Olson RJ (2007) Automated taxonomic classification of phytoplankton sampled with imaging-in-flow cytometry. Limnology and Oceanography: Methods 5:204-216

Steidinger KA, Garccés E (2006) Importance of life cycles in the ecology of harmful microalgae. In: Granéli E, Turner JT (Eds) Ecology of Harmful Algae. pp. 37-47. Springer-Verlag: Berlin.

Stoecker DK, Capuzzo JM (1990) Predation of protozoa: its importance to zooplankton. Journal of Plankton Research 12:891-908

Stoecker DK, Gifford DJ, Putt M (1994) Preservation of marine planktonic ciliates: losses and cell shrinkage during fixation. Marine Ecology Progress Series 110:293-299

Stoecker DK, Johnson MD, de Vargas C, Not F (2009) Acquired phototrophy in aquatic protists. Aquatic Microbial Ecology 57:279-310

Strathmann RR (1967) Estimating the organic carbon content of phytoplankton from cell volume or plasma volume. Limnology and Oceanography 12:411-418

Strom SL, Morello TA (1998) Comparative growth rates and yields of ciliates and heterotrophic dinoflagellates. Journal of Plankton Research 20:571-584

Stumpf RP, Culver ME, Tester PA, Tomlinson M, Kirkpatrick GJ, Pederson BA, Truby E, Ransibrahmanakul V, Soracco M (2003) Monitoring *Karenia brevis* blooms in the Gulf of Mexico using satellite ocean color imagery and other data. Harmful Algae 2:147-160

Sullivan JJ, Jonas-Davies J, Kentala LL (1985) The determination of PSP toxins by HPLC and autoanalyzer. In: Anderson DM, White AW, Baden DG (Eds) Toxic Dinoflagellates. pp. 275-280. Elsevier: New York

Sullivan JJ, Wekell MM (1987) The application of high performance liquid chromatography in a paralytic shellfish poisoning monitoring program. In: Kramer DE, Liston J (Eds) Seafood quality determination. pp. 357-372. Elsevier: Amsterdam

Symondson WOC (2002) Molecular identification of prey in predator diets. Molecular Ecology 11:627-641

Tang KW, Jakobsen HH, Visser AW (2001) *Phaeocystis globosa* (Prymnesiophyceae) and the planktonic food web: feeding, growth, and trophic interactions among grazers. Limnology and Oceanography 46:1860-1870

Taylor FJR, Fukuyo Y, Larsen J (1995) Taxonomy of harmful dinoflagellates. In: Hallegraeff GM, Anderson DM, Cembella AD (Eds) Manual on harmful marine microalgae. pp. 283-317. IOC Manuals and Guidelines No. 33. UNESCO: Paris

Teegarden GJ, Cembella AD (1996) Grazing of toxic dinoflagellates, *Alexandrium* spp., by adult copepods of coastal Maine: Implications for the fate of paralytic shellfish toxins in marine food webs. Journal of Experimental Marine Biology and Ecology 196:145-176

Troedsson C, Simonelli P, Nägele V, Nejstgaard JC, Frischer ME (2009) Quantification of copepod gut content by differential length amplification quantitative PCR (dla-qPCR). Marine Biology 156:253-259

Turner JT, Anderson DM (1983) Zooplankton grazing during dinoflagellate blooms in a Cape Cod embayment, with observations of predation upon tintinnids by copepods. Marine Ecology 4:359-374

Turner JT, Tester PA (1997) Toxic marine phytoplankton, zooplankton grazers, and pelagic food webs. Limnology and Oceanography 42:1203-1214

Uye S, Takamatsu K (1990) Feeding interactions between planktonic copepods and red-tide flagellates from Japanese coastal waters. Marine Ecology Progress Series 59:97-107

Van Dolah FM (2000) Marine algal toxins: origins, health effects, and their increased occurrence. Environmental Health Perspectives 108:133-141

Vargo GA, Heil CA, Fanning KA, Dixon LK, Neely MB, Lester K, Ault D, Murasko S, Havens J, Walsh J, Bell S (2008) Nutrient availability in support of *Karenia brevis* blooms on the central West Florida Shelf: What keeps *Karenia* blooming? Continental Shelf Research 28:73-98

Verity PG (1987) Abundance, community composition, size distribution, and production rates of tintinnids in Narragansett Bay, Rhode Island. Estuarine, Coastal and Shelf Science 24:671-690

Viličic D, Terzic S, Ahel M, Buric Z, Jasprica N, Caric M, Mihalic KC, Olujic (2008) Phytoplankton abundance and pigment biomarkers in the oligotrophic, eastern Adriatic estuary. Environmental Monitoring and Assessment 142:199-218

Ward GH (1997) Processes and trends of circulation within the Corpus Christi Bay national estuary program. Corpus Christi, TX, CCBNEP-21

Welschmeyer NA (1994) Fluorometric analysis of chlorophyll *a* in the presence of chlorophyll *b* and other pheopigments. Limnology and Oceanography 39:1985-1992

Whyte JNC, Townsend LD, Ginther NG (1996) Fecundity, toxin and trophic levels of the rotifer *Brachionus plicatilis* fed *Pseudonitzschia pungens* f. *multiseries*. In:

Harmful and Toxic Algal Blooms, pp. 401–404. (Yasumoto T, Oshima Y, Fukuyo Y, Eds.). Paris: Intergovernmental Oceanographic Commission of UNESCO

Zimmerman RJ (1983) Selection of vegetated habitat by brown shrimp, *Penaeus aztecus*, in a Galveston Bay salt marsh. Fishery Bulletin 82:325-336

Vita

Jena Renee Campbell is a 2007 graduate of Wittenberg University in Springfield, Ohio. She graduated with honors with her Bachelor of Science in Biology with a minor in Marine Science. In 2008 she joined the doctoral program at The University of Texas at Austin Marine Science Institute under the supervision of Dr. Edward Buskey. She advanced to Ph.D. candidacy in the summer of 2009. Her research interests include zooplankton and microplankton population dynamics, harmful algal bloom dynamics, and molecular analyses as tools for describing community dynamics. Jena has been the recipient of a 3-year NOAA National Estuarine Research Reserve Graduated Research Fellowship, the Walter B. Jones Memorial Award for Excellence in Graduate Marine and Coastal Studies, and the University of Texas Marine Science Institute E.J. Lund Endowed Fellowship.

Permanent address (or email): 1200 North Magnolia, Apt. 45, Rockport, Texas 78382

jena.campbell23@gmail.com

This dissertation was typed by Jena Renee Campbell.